CONTROLLED SYNTHESIS OF TOPOLOGICALLY TEMPLATED CATENANE AND KNOTTY POLYMER

A Dissertation

Presented to

the Faculty of the Department of Chemistry

University of Houston

In Partial Fulfillment

of the Requirements for the Degree

Doctor of Philosophy

By

Ajaykumar Bunha

May 2013

CONTROLLED SYNTHESIS OF TOPOLOGICALLY TEMPLATED CATENANE AND KNOTTY POLYMER

Ajaykumar Bunha

APPROVED:

Dr. Randolph P. Thummel, Chairman

Dr. Rigoberto C. Advincula

Dr. Ognjen S. Miljanic

Dr. Roman S. Czernuszewicz

Dr. Megan L. Robertson

Dr. Dan E. Wells, Dean

College of Natural Sciences and Mathematics

ACKNOWLEDGMENTS

I am grateful to all of those with whom I have had the pleasure to work with during my entire time in graduate school.

To my committee members, Dr. Thummel, Dr. Miljanic, Dr. Czernuszewicz, and Dr. Robertson, for their encouraging words, thoughtful criticism, time and attention.

To Dr. Rigoberto Advincula, who gave me the opportunity to learn and for his guidance.

To the past member of the Advincula group Rams, Guoqian, Cel, Jane, Roderick, Nicel, Ed, Allan, Katie, Subbu, Deepali, and Kim for their support; to the present members Joey, Pengfei, Kat, Al, and Brylee for participating in my learning experience.

To my parents and other family members for all their guidances.

To my dear wife Megha for her love, support, and patience.

CONTROLLED SYNTHESIS OF TOPOLOGICALLY TEMPLATED CATENANE AND KNOTTY POLYMER

An Abstract of a Dissertation

Presented to

the Faculty of the Department of Chemistry

University of Houston

In Partial Fulfillment

of the Requirements for the Degree

Doctor of Philosophy

By

Ajaykumar Bunha

May 2013

ABSTRACT

The topologically interesting structure of polymer catenanes and knotty polymers are of high interest for their unique chemical and physical properties. However, the practical applications of these materials have not been explored well due to synthetic obstacles in obtaining high yields. Chapter 1 reviews template directed synthesis of low molecular weight catenanes and the trefoil knot. In addition, recent advances in synthesis of topologically similar cyclic polymer *via* end-to-end cyclization of linear analogue or ring-expansion polymerization from cyclic catalyst/initiator are also discussed. Chapter 2 demonstrates a novel route for the synthesis of polymer catenanes using supramolecularly templated Atom Transfer Radical Polymerization (ATRP) initiator for polymerization and subsequent closing of the resulting four-armed type polymer template by Atom Transfer Radical Coupling (ATRC). Direct visualization of the interlocked topology of polymer catenane was achieved by Atomic Force Microscopy (AFM) imaging technique. Chapter 3 reports an important extension of the above mentioned methodology to obtain a catenated block copolymer. The four-armed type homopolymer template was used as macroinitiator to polymerize another monomer by ATRP. The resulting block copolymer template was subjected to template-closing *via* slightly modified ATRC method. Chapter 4 demonstrates another novel approach to synthesize polymer catenanes by first grafting a preformed alkyne-functionalized linear polymer to an azide-functionalized supramolecular template, followed by ATRC of the resulting polymer template. Detailed analysis of AFM image reveals important information about the side products of ATRC

such as inter-molecular coupling and other isomer formation. Chapter 5 reports on a preliminary study of thermally initiated ring-expansion Reversible Addition Fragmentation Chain Transfer (RAFT) polymerization from cyclic RAFT initiator. A novel dixanthate type cyclic RAFT initiator was synthesized and used in a thermally initiated free radical polymerization of N-vinylcarbazole. The cyclic topology of the resulting polyvinylcarbazole was confirmed by Gel Permeation Chromatography (GPC) and AFM analysis. Chapter 6 demonstrates for the first time the synthesis of trefoil knot polymer (knotty polymer) *via* grafting of an alkyne-functionalized polymer to azide-functionalized double helical type supramolecular template. A well-defined knotty polymer was then obtained by closing the polymer template *via* ATRC method. Finally in Chapter 7, conclusions, perspectives, and future work on these topics are discussed.

TABLE OF CONTENTS

LIST OF FIGURES

LIST OF SCHEMES

LIST OF ABBREVIATIONS

CAN	Acetonitrile
AFM	Atomic force microscopy
AIBN	Azobisisobutyronitrile
ATRC	Atom transfer radical coupling
ATRP	Atom transfer radical polymerization
BPP34C10	bisparaphenylene-34-crown-10
Br	Bromine
Co	Cobalt
CRP	Controlled radical polymerization
CTA	Chain transfer agent
Cu	Copper
CuAAC	Copper(I)-catalyzed alkyne-azide cycloaddition
Da	Dalton
DCC	Dicyclohexylcarbodiimide
DCM	Dichloromethane
DLS	Dynamic light scattering
DMAP	Dimethylaminopyridine
DMF	Dimethylformamide
DMSO	Dimethyl sulfoxide
DNA	Deoxyribonucleic acid
Dpp	diphenylphenanthroline

Fe	Iron
FT-IR	Fourier transform infrared spectroscopy
GPC	Gel permeation chromatography
HMTETA	1,1,4,7,10,10-hexamethyltriethylenetetraamine
IV	Intrinsic viscosity
LMCT	Ligand-to-metal charge transfer
MA	Methylacrylate
MALDI-TOF	Matrix-asisted laser desorption/ionization-time of flight
Me_6TREN	Tris[2-(dimethylamino)ethyl]amine
MLCT	Metal-to-ligand charge transfer
MMA	Methyl methacrylate
M_n	Number-average molecular weight
M_p	Peak-average molecular weight
M_w	Weight-average molecular weight
MWCO	Molecular weight cut off
N_2	Nitrogen gas
Ni	Nickel
NMP	Nitroxide mediated polymerization
NMR	Nuclear magnetic resonance
NVK	N-vinylcarbazole
PDI	Polydispersity index
PMDETA	N,N,N′,N″,N″-Pentamethyldiethylenetriamine

PPh_3	Triphenylphosphine
PS	Polystyrene
PS-b-PMMA	Polystyrebe-block-polymethylmethacrylate
PVK	Polyvinylcarbazole
RAFT	Reversible addition fragmentation chain transfer
RALS	Right-angle light scattering
RCM	Ring-closing metathesis
REMP	Ring-expansion metathesis polymerization
R_h	Hydrodynamic radius
RI	Refractive index
Ru	Ruthenium
R_v	Retention volume
SFRP	Stable free radical polymerization
THF	Tetrahydrofuran
UV-Vis	Ultraviolet-visible
Zn	Zinc

Chapter 1: Introduction

Tailored control of polymer architectures or microstructures has been of interest to polymer chemists since it was first understood that physical properties of a polymer are inherently dependent on its structure.[1] Various types of polymer architectures such as linear polymers, polymer brushes, star polymers, ladder polymers, dendrimers, hyperbranched polymers, and network polymers have been explored to understand how covalent architecture specifically affects their observed macroscopic properties.[2-4] Among these architectures, cyclic polymers are unique in structures because of their lack of chain ends. In addition, cyclic polymers exhibit distinct static and dynamic properties such as smaller hydrodynamic volumes, lower viscosities, and higher glass transition temperatures as compared to linear polymers of the same molecular weight.[5-14] Moreover, polymers with orderly entangled cyclic topology such as a catenane and trefoil knot have been of interest in modern polymer physics, notably in the fields of rheology, adhesion, crystallinity, surface and interfaces, block copolymers, and viscoelasticity.[15-20] Although, recent advances in living radical polymerization and click chemistry enable the efficient synthesis of cyclic polymers, synthesis of polymer catenanes and knotty polymers remains a challenge.[21] This chapter highlights templated routes to obtain orderly entangled architectures *via* supramolecular assemblies. Advances in the synthesis of well-defined cyclic polymers, which was considered as model approaches for this dissertation work, are also discussed. The specific objectives of this dissertation are then presented at the end of this chapter.

1.1. Synthesis of Catenanes and Knots *via* Supramolecular Assembly

The study of orderly molecular entanglements offers unique challenges in the most subtle and demanding aspects of stereochemistry, regiochemistry, and mechanistic control. As inspired by the Knot Theory, various supramolecular templates have been designed to enable reaction pathways leading to the formation of complex macromolecular architectures.

1.1.1. Knot theory

Mathematical knot theory is the formal discipline dealing with knots and links, derived from the early work of chemists in the middle of the 19th century.[22] Mathematicians define a 'knot' as a cord that is intertwined with itself, with its loose ends joined so that it cannot become untangled. As per this definition, a macrocycle can be described as a rudimentary knot, or the 'unknot'. If two or more knots are interlocked with each other, the result is called a 'link'. Catenanes are links composed of at least two unknots. From here on [n]catenanes means catenanes with *n* unknots. Recently, Epple has recorded a fascinating history of topology in the 19th century by a beautiful reproduction of a tabulation of over 150 knots from one of Tait's trailblazing papers.[23-24] Different knots and links can be distinguished by the Alexander–Briggs notation.[25-26] The descriptor x_z^y represents a knot (or link), where x is the minimum number of nodes, or crossing points of any projection of the knot or link, y is the number of components (in a knot, $y = 1$ and is usually not displayed in the Alexander–Briggs notation), and z is the order of the knot among its peers with the same number of nodes and component. In

detail, z is the number of handles that must be added when embedding the knot or link on a sphere, such that no crossings are observed.

In addition, knots can also be classified as prime (or simple) knots or composite knots similar to that of integer numbers. A composite knot can be formed from prime knot by taking two nontrivial knots, cutting them, and joining the ends. In the reverse process, a composite knot is decomposed into its factor knots. On the other end, a prime knot cannot be further decomposed, in the same manner as a prime number cannot be divided by numbers other than one and itself.[27] Aside from the simplest knots, it is also extremely difficult to distinguish whether a knot is a prime knot or a composite knot. **Figure 1.1** displays all prime knots with seven or less crossings, and some of their interesting links together with their Alexander–Briggs notation. Some trivial names applied to the interlocked species are based on both artistic and chemical contexts. Although knot theory remains a well-studied branch of mathematics to this day, it has also gained scientific interest after the so-called Michelson Morley experiment reported in 1887.[28-29] Today, knot theory is inextricably linked to particle physics, to DNA replication and recombination, and to other areas of statistical mechanics.

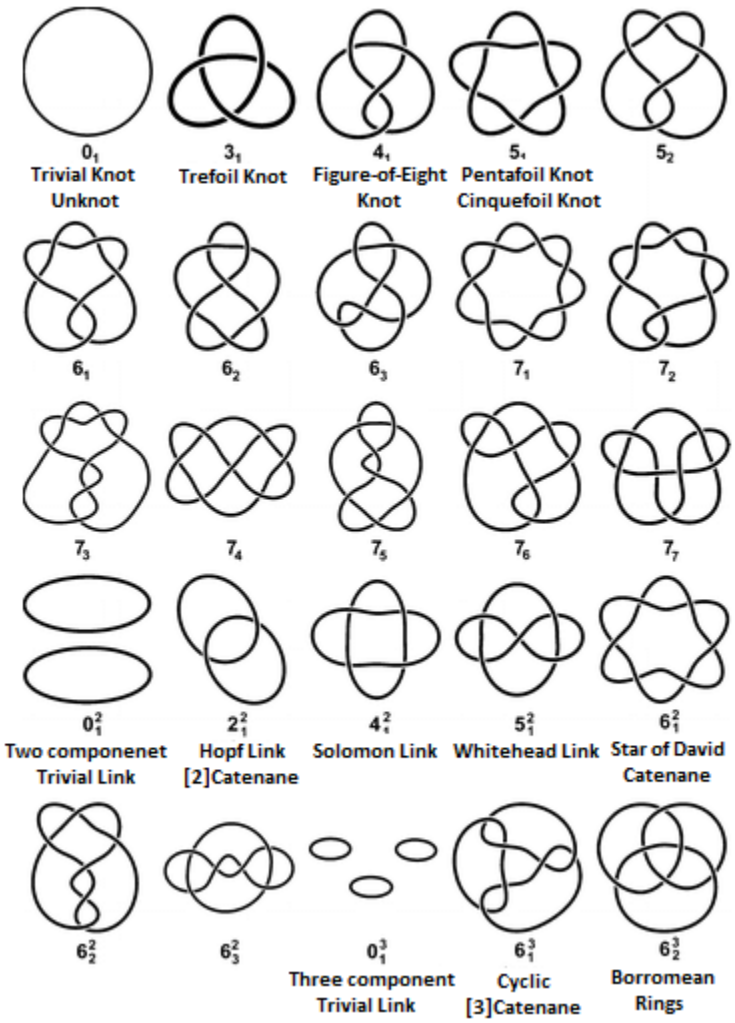

Figure 1.1. Schematic tabulation of simple knots and links, accompanied by their trivial names and descriptors using the Alexander–Briggs notation.[25]

1.1.2 Naturally occurring molecular knots

Aside from the mathematical discussion of knots and links, they are also particularly relevant in the field of biology. The discovery of the first naturally occurring catenated DNA in 1967 marked the beginnings of "Biochemical Topology" as defined by Wasserman and Cozarelli.[30-33] Soon after, trefoil knot DNAs in both single-stranded and

double-stranded form were discovered.[34-35] Subsequently, a wealth of highly complex knotted DNA architectures, including composite knots, were discovered and imaged by electron microscopy **(Figure 1.2)**.[36] The effective separation of these entities was made possible by gel electrophoresis, which takes advantage of the differences in compactness of knots as they become more complex.[37]

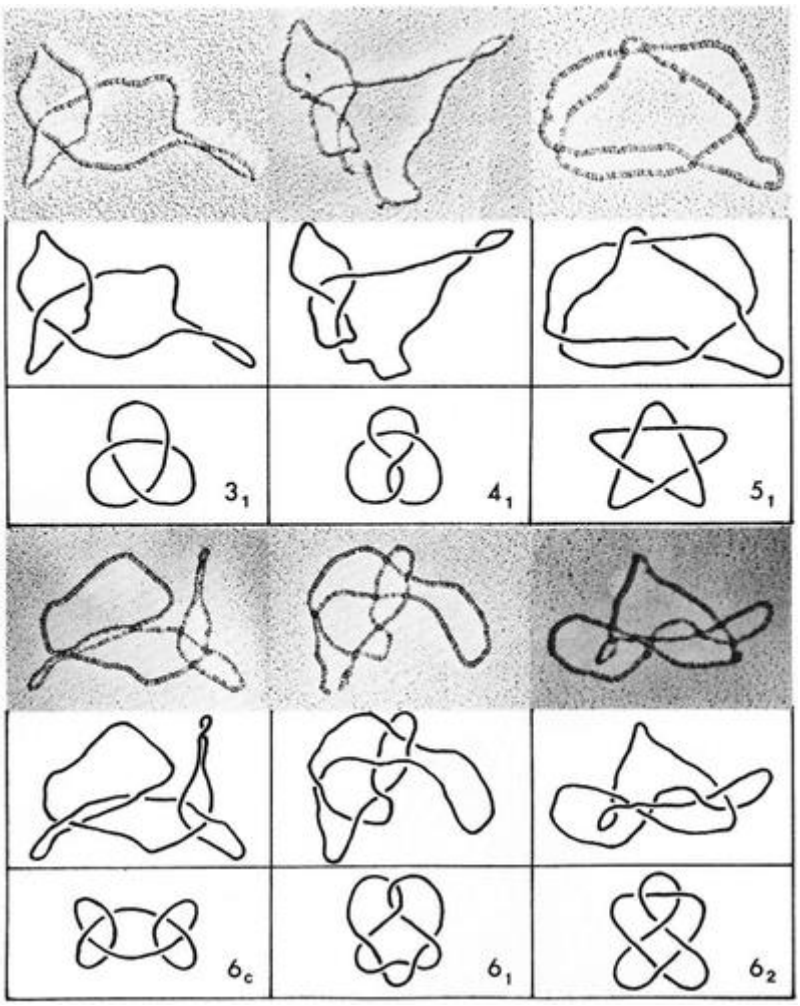

Figure 1.2. Electron micrographs of knotted DNA, prepared by the action of DNA topoisomerases, at 80 000× magnification.[36] Retraced representations of the DNA are shown below the micrograph along with idealized diagrams of the knot and their descriptors using the Alexander–Briggs notation. Copyright 1985 American Society for Biochemistry and Molecular Biology.

The detailed study of these DNA architectures revealed that the faulty versions of enzymes (DNA topoisomerases) are responsible for the formation of these topological constructs.[38] It has also been found in many forms of cancer.[39-40] These enzymes are responsible for knotting DNA's, but not in a controlled manner; as a result many species are generated, rather than one specific target.

1.1.3. Chemical template for forming catenanes and knots

The presence of knotted structures in naturally occurring biological systems has inspired chemists to design synthetic pathways for mechanically interlocked catenanes and trefoil knot compounds. A number of approaches have been used to form interlocked structures, which favor the formation of interlocked products over unwanted non-interlocked macrocycles, oligomers, and polymers. The most widely used method is the template-directed synthesis, where a template helps to build a turn into the emerging structure. Over the last two decades, various types of chemical templates have been utilized as discussed in detail in the following sections.

Metal-ion template approach:

The most efficient template is the metal-ion complex since the metal ion constitutes a multifunctional center about which molecular turns (ligands) of various kinds are readily oriented. This approach has provided accessible pathways to topologically complex interlocked molecules that would be unobtainable by classical synthetic methods. The potential of metal-ion templates for the production of interlocked structures were first widely recognized through their success in the preparation of

catenanes. There are mainly two routes to catenane formation: ring-turn approach and two-turn approach, as shown in **Scheme 1.1**.

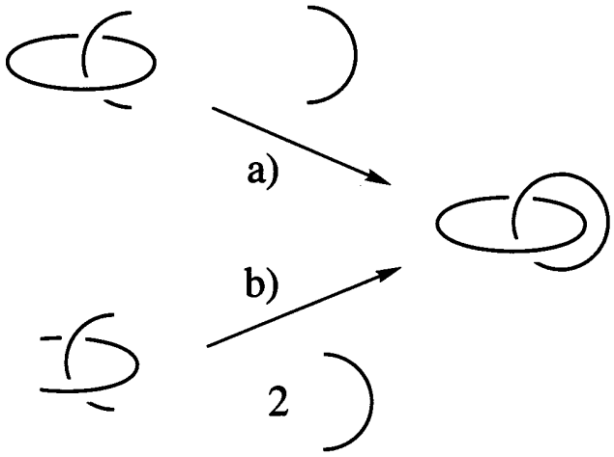

Scheme 1.1. Strategies for template catenane formation: (a) the ring-turn approach, (b) the two-turn approach.

The *ring-turn approach*, a cyclic precursor is initially formed by simple macrocyclization reaction of a turn and a difunctional reactant. In next step, complexation of this macrocycle with a metal-ion and another equivalent of the turn gives the threaded template, also called as a pseudorotaxane. The second ring can then be closed by other difunctional reactant to produce the [2]catenanes.[41] In case of two-turn approach, complexation of two turns with a metal-ion gives a template composed of a single cross-over, followed by cyclization of both turns using difunctional reagents yields the [2]catenanes. The same pseudorotaxane is a likely intermediate. This method requires fewer steps, yet often leads to lower yields due to higher possibility of side reactions.[42]

Among various type of metal-ion template, the classic Sauvage group strategy of complexing two phenanthroline ligand to Cu(I) ($Cu(I)(dpp)_2$) has been a widely utilized technique in the synthesis of many types of mechanically interlocked molecules **(Figure**

1.3). The two ligands are held in orthogonally by the tetrahedral coordination preference of the metal-ion.

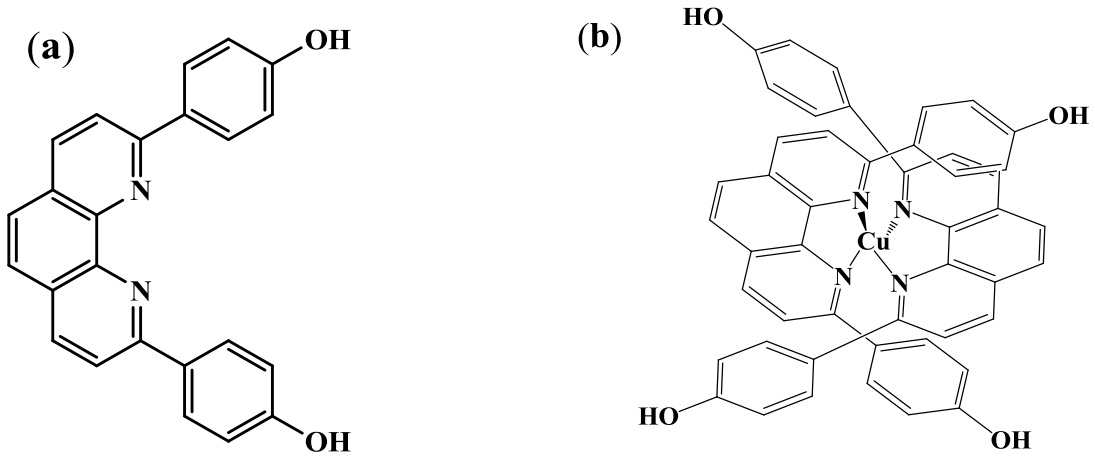

Figure 1.3. (a) Sauvage's molecular turn, (b) the resulting two-turn complex of Cu(I).

In the first reported template synthesis of [2]catenanes using pentaethylene glycol dihalides as bifunctional ring closing reagents, the two-turn approach gave only 27% of the product, while the ring-turn approach yielded 42%.[41-42] Recently, the Sauvage group has demonstrated further improvement in yield of [2]catenanes by using the Grubbs' ring-closing metathesis (RCM) reaction and moving the ring closure reaction to a much greater distance for the metal-anchored cross-over.[43] From this and other examples, it is apparent that the efficiency of catenane formation can be improved by carefully choosing and locating the terminal functional groups in interlocking turns so that no additional linking agent are required to complete the ring. The advantage of this methodology derives largely from the reduced competition between the formation of intra-molecular and inter-molecular linkages. Another advantage includes a lower possibility of forming side products since the number of reacting groups is fewer.

The $Cu(I)(dpp)_2$ motif has also been explored to make higher order interlocked compounds by assembling helicates with multiple $Cu(I)(dpp)_2$ motifs (each $Cu(I)(dpp)_2$ unit corresponds to a cross-over point) and cyclizing the end-groups. Depending upon the number of cross-over points in the helicates, single or multiply entwined catenanes and knots can be generated as shown in **Figure 1.4**.[44]

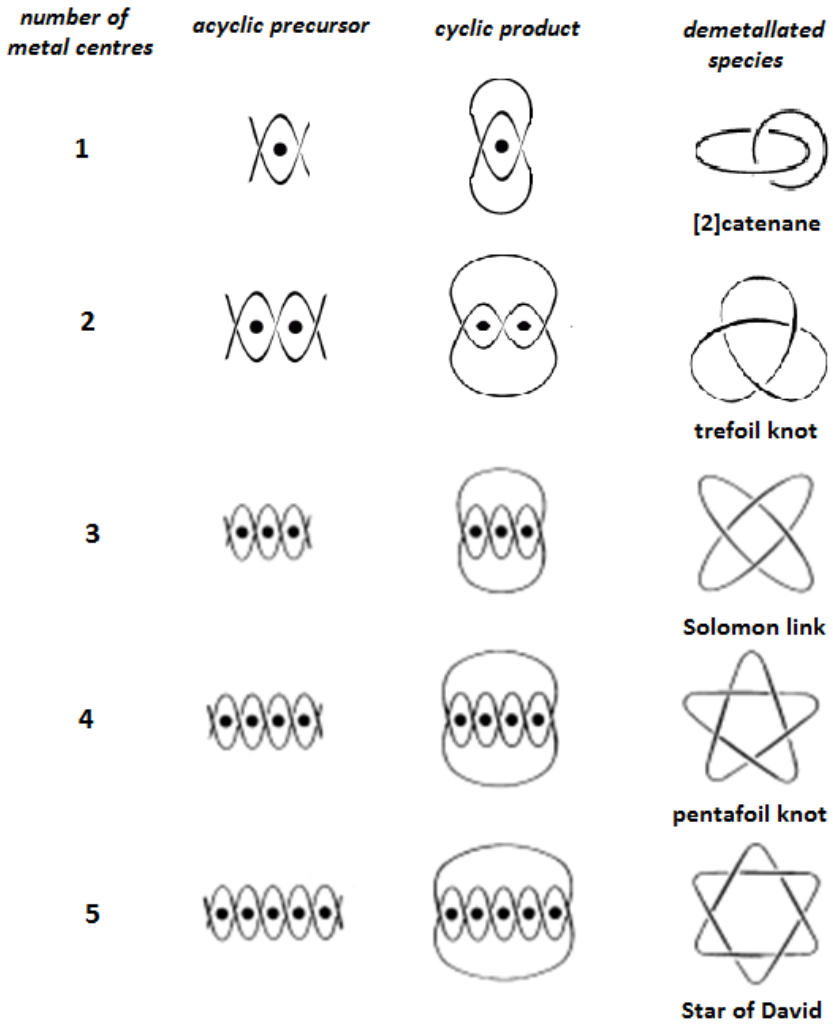

Figure 1.4. Sauvage's strategy for forming catenanes and knots by linking the end groups of linear metal ion helicates with various numbers of turns.

Sauvage demonstrated for the first time the synthesis of a molecular trefoil knot by linking two dpp ligand turns together with a methylene group, which produces a pair of linked turns. Complexation of such a ligand/conjugate with Cu(I) gives a desired double helical complex and a mixture of products as a result of combinations of two ligands with two Cu(I) ions **(Scheme 1.2)**.[45] The pair of didentate turns constituting a single ligand is twisted orthogonally (with respect to each other) at the linkage between the two Cu(I) ions. A pair of polyglycol chains creates new links between each ligand in the double helical complex and the other. Removal of the metal-ion gives a trefoil knot (3% yields) and a large macrocycle having the same linkages as made up of two molecules of the double-turn and two molecules of the bridging unit. However, the trefoil knot is topologically very different from the simple macrocycle because these two

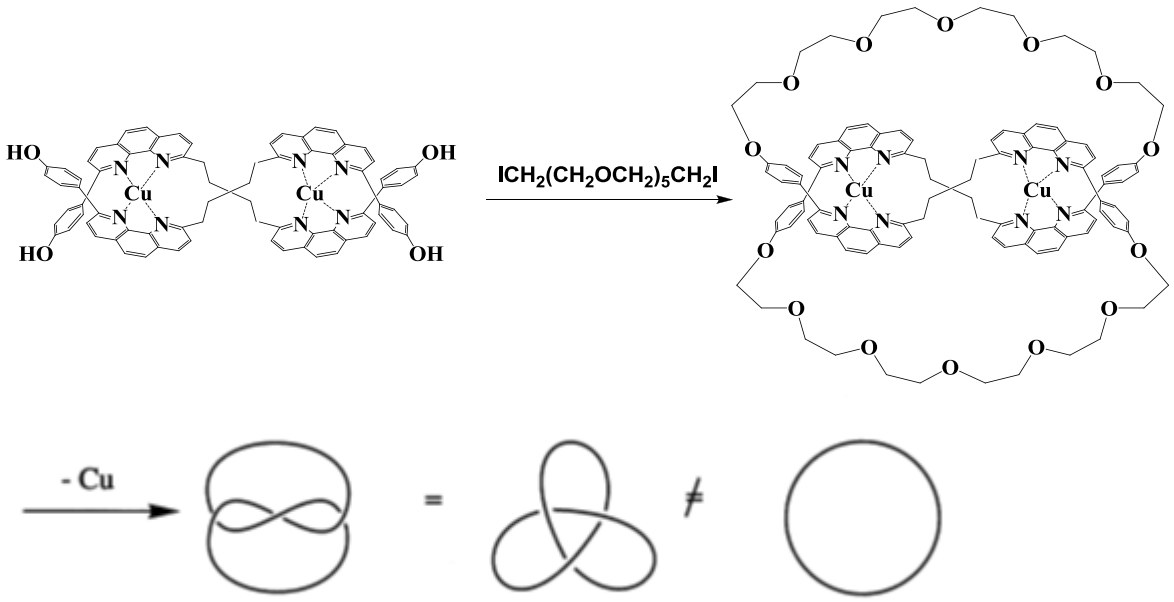

Scheme 1.2. Synthesis of the first trefoil knot using a two-anchor helical template.

topological isomers cannot be interconverted without breaking at least one chemical bond. Further improvement in the yield of the trefoil knot was achieved by replacing the flexible methylene bridging unit in pair of turns with a rigid *m*-phenylene group.[44] This improvement resulted from a quantitative formation of the double helical precursor complex, instead of a mixture of complexes. In addition, this favorable yield has made further studies possible, including separation of the enantiomers of this chiral knot.[46]

Other than Sauvage's phenanthroline system, octahedral metal ion templates have also been used for synthesis of catenane and knot, but those systems have not yet been fully exploited. For example, successful synthesis of [2]catenanes have been demonstrated by utilizing an octahedral complex of Ru(II) with a 5,5'-disubstituted terpyridine ligand as the turn. **(Figure 1.5a)**.[47] The geometry and rigidity of both aforementioned systems; (1) the two tridentate chelates around an octahedral metal ion and (2) the orthogonal chelation of two bidentate ligands around tetrahedral Cu(I) are almost similar. However, the overlapping of ligands around the metal center are less with the terpyridine system, hence, it resulted only to an 11% yield of the [2]catenanes upon cyclization with hexaethylene glycol diiodide. A trefoil knot was also obtained in 20% yield by following the same strategy as mentioned earlier using a precursor helicate made of the octahedral complex of terpyridine ligands and Fe(II) ions and closing the turn by RCM.[48]

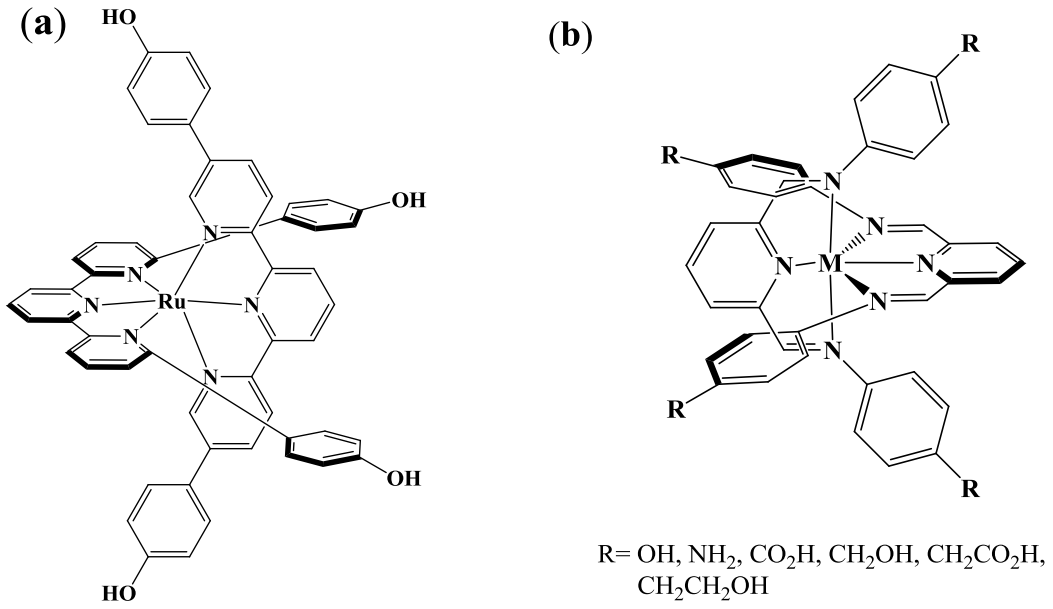

Figure 1.5. (a) Sauvage's Ru-terpyridine octahedral complex, (b) Vance's Schiff-base octahedral complex.

A new family of potential molecular templates based on octahedral transition metal complexes of Schiff base ligands has been explored by Vance and co-worker.[49] A distinct advantage of these systems is their ease of synthesis; a simple one-pot reaction of 2,6-dicarbonyl pyridines and *para*-substituted anilines gives tridentate Schiff base ligands in high-yield. A variety of terminal functional groups of the ligand can be obtained by simply varying the aniline derivatives, without altering the basic structure of the template complex. As shown in **Figure 1.5b**, complexes with different end-functional group have been prepared and characterized by crystallography. However, more work has to be accomplished to optimize the use of this system for synthesis of rotaxanes and catenanes. In addition, it is also difficult to extend this approach for synthesis of trefoil knot and higher order interlocked structures.

In efforts to demonstrate other possible ways of synthesizing the trefoil knot, Hunter and co-workers have formed an open-knotted structure assembled around an octahedral metal center **(Scheme 1.3)**.[50] A multidentate ligand containing three bipyridyl units entwines itself around an octahedral Zn(II) template to generate an open knot conformation. The reversibility of the folding process was tested by addition of chloride ions, which regenerated the free ligand, and subsequent addition of silver salts (precipitating the chloride ion as AgCl) reassembles the open knot complex. In a recent report, successful closing of open knot was demonstrated by either a bis-esterification reaction of the two terminal alcohols or by ring closing metathesis (RCM) of allyl intermediate.[51] The trefoil knot with remarkably good yield was obtained by optimizing the length of linker, followed by removal of the Zn(II) from template using Li_2S.

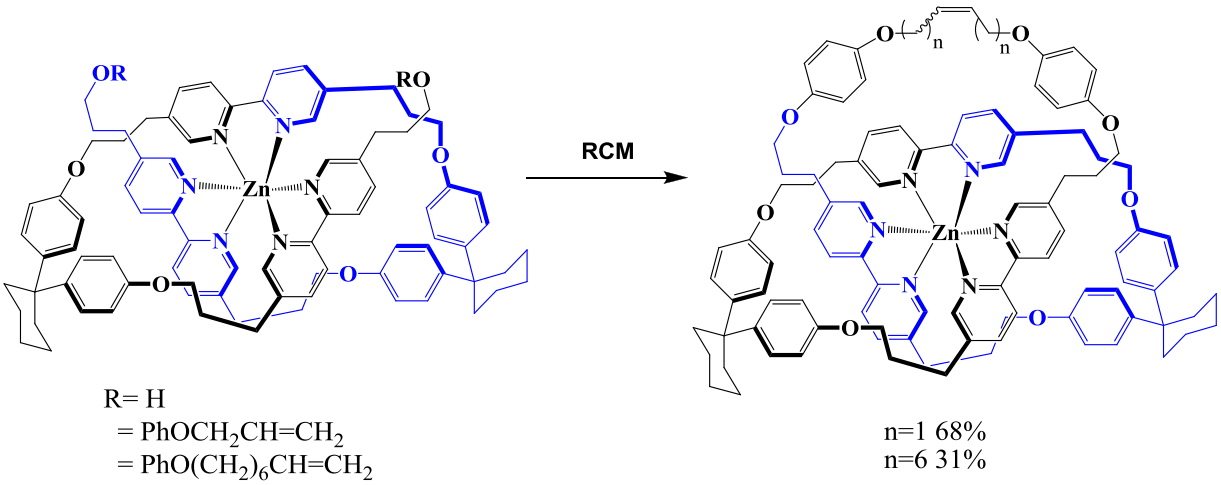

Scheme 1.3. Hunter's open-knot derivatives and cyclization by RCM to produce trefoil knot.

Non metal-ion/hydrogen bonding templates:

Hydrogen bonding complexes are almost as diverse as the metal ion complex, but the interactions are much weaker than covalent bonds, even those in many metal complexes. The strong complex can be formed by incorporating multiple hydrogen bonding sites in a template. In 1992, the first serendipitous discovery of a hydrogen bonding template was reported by Hunter.[52] As shown in **Scheme 1.4**, the macrocyclization reaction of diamide template with *iso*-phthaloyl chloride at high dilution gave the unexpected [2]catenanes in 34% yield. Other H-bond template such as Busch/Stoddart secondary ammonium ion crown ether templates have also been widely explored for rotaxane synthesis.[53-54]

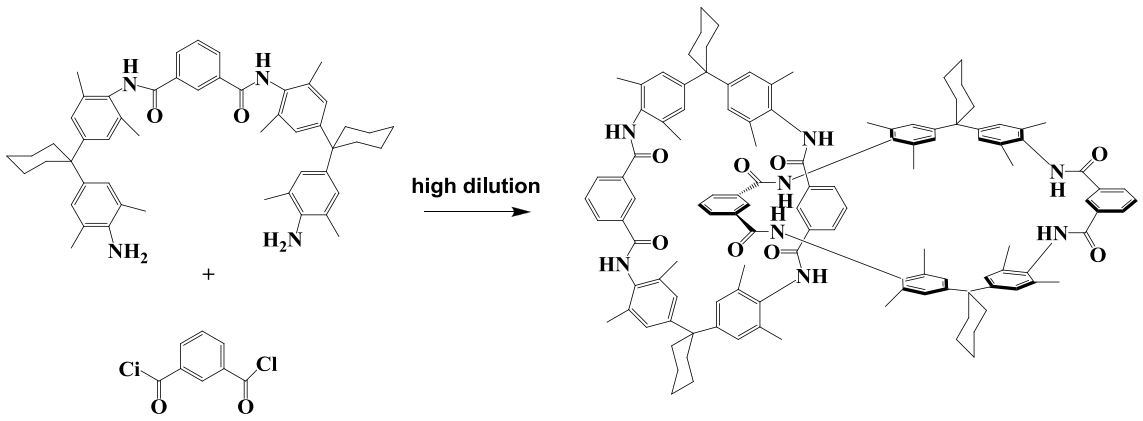

Scheme 1.4. The synthesis of Hunter's first amide [2]catenane.

Another area of synthesis of interlocked architectures using non-metal ion template was developed by Stoddart and his co-workers. The so called Stoddart's template also known as π-donor/acceptor templates, composed of electron rich aromatic ether moieties and paraquat-containing moieties.[55] In contrast to Sauvage's chemistry

where the metal-ion always serves as the anchor and the ligand is always the turn, the π–π templates is the designation of its common parts, the anchor and the turn. The combination of interactions within templates such as π - π stacking, ion–dipole attractions and unusual, but undeniable, hydrogen bonding interactions makes it nearly an ideal system for the template synthesis of interlocked molecules. An excellent example of Stoddart's work is shown in **Scheme 1.5** representing his discovery of a turn, accompanying the interesting anchor technology. The [2]catenane was obtained in a remarkable 70% yield upon complexation of phenylene-linked bis-paraquat, followed by reaction with *p*-xylene dibromide.

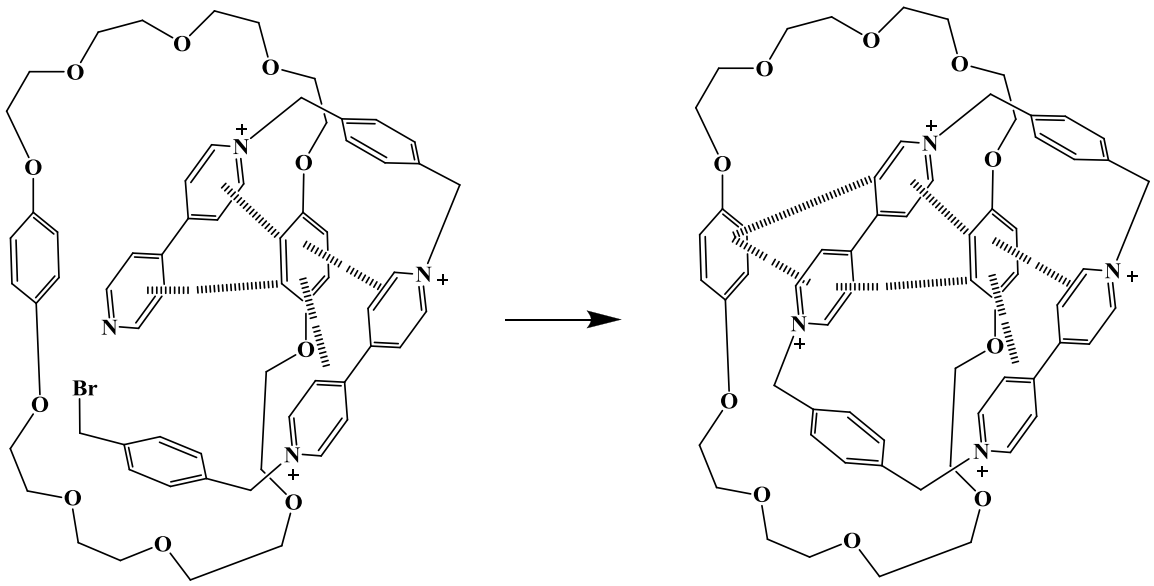

Scheme 1.5. The π–π templates synthesis of Stoddart's prototypical [2]catenane.

1.2. Controlled Radical Polymerization Method

Currently, there are three main types of "living"/controlled radical polymerization (CRP) method. Atom transfer radical polymerization (ATRP),[56] reversible addition fragmentation chain transfer polymerization (RAFT),[57] and, stable free radical polymerization (SFRP),[58] which includes nitroxyl mediated polymerization (NMP).[59] With the discovery of CRP techniques and click chemistry, a great variety of complex macromolecular architectures became available under non-demanding reaction conditions.

1.2.1. Atom transfer radical polymerization

Atom Transfer Radical Polymerization is among the most effective and most widely used methods of controlled radical polymerization. The mechanism of polymerization involves the transfer of a halogen atom from the polymer to a metal catalyst yielding an active chain end (a radical), hence the term Atom Transfer Radical Polymerization (ATRP). As shown in **Scheme 1.6**, the reaction takes place through a reversible redox reaction involving the transition metal catalyst (Mt), which is oxidized as the polymer is converted from the dormant state (PX) to the active species (P·) through the transfer of the halogen (X). A multidentate ligand (L) helps the metal catalyst to dissolve in various organic solvent and also assists in binding the halogen. The deactivation reaction is kinetically favored in the equilibrium (kd »ka), which means only a small concentration of active radical species present at a given time. Ideally, this eliminates the possibility of termination between two activated polymer chain ends; however in practice termination does occur.

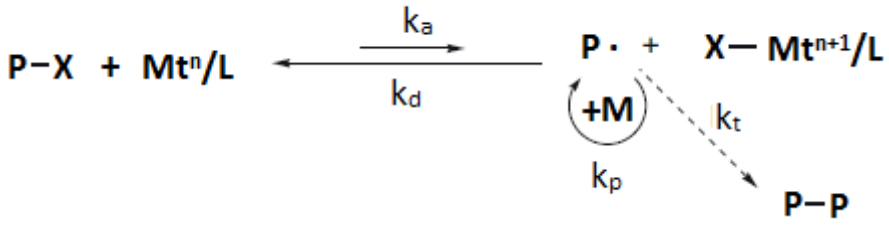

Scheme 1.6. Mechanism of atom transfer radical polymerization.

A typical ATRP system consists of an initiator, a metal halide (at low oxidation state) complexed with ligand(s), and a monomer. Various catalysts have been developed based on Cu(I),[60] Ni(II),[61] Ru(II),[62] and Fe(II)[63]elements, but Cu(I) and Ru(II) systems have been mostly studied. Generally, bipyridine or multidentate amine ligands are used for copper-based catalysts and PPh_3 ligands are used for other metal catalysts. The catalyst activity and control of the polymer molecular weight greatly depends on the type of ligand used (i.e. electronic, steric, and solubility characters). In addition, the structure of the initiator must match with the structure of the propagating species of the monomer for effective polymerization.

1.2.2. Reversible addition fragmentation chain transfer polymerization

RAFT polymerization has proven to be a versatile tool due its unique advantages such as less sensitivity to oxygen, proceeds at lower temperatures than ATRP and NMP, and is compatible with a wider range of monomers, such as acrylate, methacrylate, and styrenic monomers. RAFT polymerization was pioneered by a team of scientists in Australia, and has been explored extensively for many applications.[64] In RAFT polymerization a thiocarbonylthio group-containing compound, with a general structure

of Z-C(=S)S-R, is added to an otherwise conventional free radical polymerization in order to control the polymerization. These controlling agents are also called chain transfer agent (CTA) or RAFT agents. As shown in **Scheme 1.7**, first, a radical initiator

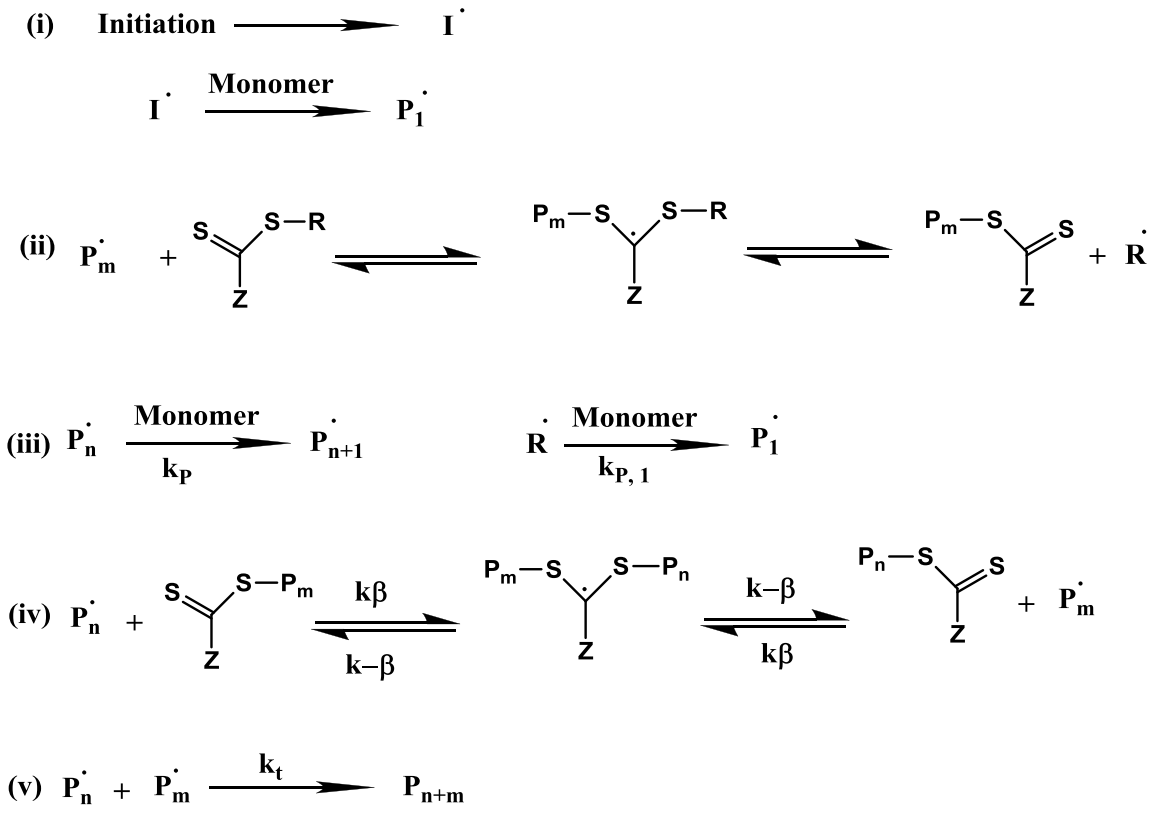

Scheme 1.7. Proposed general mechanism of RAFT polymerizations showing the steps of initiation (I), propagation (II), pre-equilibrium (III), reinitiation, main-equilibrium (IV) and termination (V).

decomposes to radicals which initiate the polymerization. In a next step, a propagating radical then adds to the thiocarbonyl group of the CTA (1) molecule and forms an intermediate radical (2) (also called "dormant" species). Eventually the intermediate radical undergoes a β-scission reaction in either direction to yield original radical or creating a new propagating radical from the leaving group (R group) and polymeric

RAFT agent (3). After the initial phase equilibrium is established between the propagating radicals and the intermediate radical species, the rate coefficients become independent of the chain length. During the main equilibrium process, a rapid interchange of growing polymer chain occurs through polymeric chain transfer agent (4). Ideally the radicals are shared equally, causing chains to have equal opportunities for growth and thus narrow molecular weight distribution. However, the polymerization being of a radical nature, side reactions like chain transfer, recombination and disproportionation cannot fully be suppressed. Still, RAFT polymerizations show a linear growth of the molecular weight with respect to conversion and yield polymers with narrow polydispersity.

1.2.3. Click chemistry

In 2001, Sharpless proposed the concept of "click" chemistry, which is undeniably one of the most noticeable synthetic trends in the research area of chemistry and material science of this new century.[65] The term "click" refers to simple, efficient, energetically favored, specific and versatile chemical transformations, which lead to a single reaction product.

Among all currently identified click reactions, the Huisgen 1,3-dipolar cycloaddition of azides and alkynes is known for being closest to an ideal click reaction. The uncatalyzed version of cycloadditions of azides and alkynes require long reaction times, high temperatures and result in the formation of two products, 1,4- and 1,5-regioisomers.[66] The groups of Sharpless and Meldal separately discovered the Cu(I)-catalyzed variation of this reaction, which allows very fast and efficient formation of

exclusively 1,4-triazoles at mild reaction conditions **(Scheme 1.8)**. This breakthrough led to a remarkable exploration of Huisgen cycloadditions in synthetic chemistry. In particular, research focuses its widespread application in all fields of polymer chemistry and biochemistry over the last few years.[67]

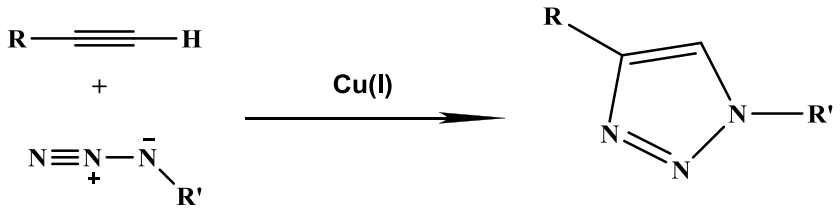

Scheme 1.8. Cu(I) catalyzed Huisgen 1,3-dipolar cycloaddition of azides and alkynes.

Living free radical polymerization and click pericyclic reactions are independently known for having many similar advantages such as reaction under mild conditions and tolerance of a range of functionalities. Recently, research groups have begun combining these click reactions with different polymerization techniques to synthesize new polymeric materials, which was otherwise inaccessible *via* traditional polymerization methods. Moreover, azide–alkyne chemistry has found large potential for a variety of biological applications, such as chemoselective platform for the functionalization or ligation of biomaterials, modified stationary phases for bioseparation, site-specific modified proteins or viruses, drug or gene delivery carriers, protein or oligonucleotide microarrays, and functionalized cell surfaces.[68]

1.3. Advances in Synthesis of Cyclic Polymers

In the field of synthetic polymer chemistry, the form of macromolecules has long been restricted to a linear or a randomly branched topology. In the last decade, however, the developments of intriguing synthetic protocols, based on living polymerization as well as on self-assembly processes have enabled access to a variety of precisely controlled, branched, and moreover cyclic topological polymers.[69] In particular, a number of approaches has recently been reported to produce a variety of single-cyclic (ring) and multi-cyclic polymers of well-defined chemical structures and functionalities.[70] These developments, has not only created unprecedented opportunities to bring new insights in the frontier of basic polymer chemistry and physics, but also enable the study of unusual properties and functions of polymer materials based on their topologies.[71]

Synthetic strategies for the formation of cyclic polymers can be divided into two main categories: (1) ring-closure techniques **(Figure 1.6a)** and (2) ring-expansion techniques **(Figure 1.6b)**. The ring-closure method involves the cyclization of a linear polymer *via* end-group coupling, while the ring-expansion technique involves the insertion and propogation of monomer units into cyclic initiator or catalyst. The synthetic aspects of both approach is discussed in detail below.

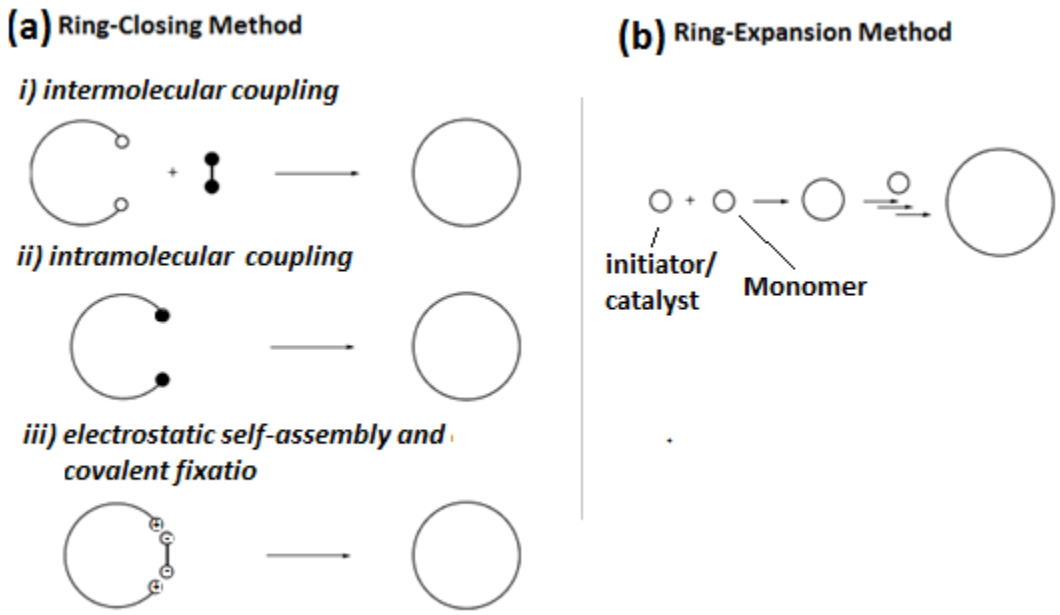

Figure 1.6. General methods of synthesis of cyclic polymers.

1.3.1. Ring-closing approach

The most appropriate method used for the synthesis of cyclic polymers of controlled size and narrow polydispersity are based on the end-to-end chain coupling of difunctional linear chains in highly dilute reaction conditions. The cyclization yield of end-group linking can be expressed by eqn. (1), where C is the actual concentration and C_{equal} stands for the concentration at which the probability for the intra- and inter-molecular reactions to occur is the same [eqn. (2)].[10]

$$\text{Cyclization yield} = C_{equal} / (C_{equal} + C) \qquad (1)$$

$$C_{equal} = [3 / (2 \pi \langle r^2 \rangle)]^{3/2} M / N_A \qquad (2)$$

where $\langle r^2 \rangle$ is the mean square end-to-end distance of the linear precursor, N_A is the Avogadro number, and M is the molar mass.

According to the eqn. 1, the intra-molecular cyclization is favored over inter-molecular coupling when the polymer concentration is low ($C < 10^{-5}$ M). This requirement of very dilute solution condition is a severe limitation to the production of reasonable amounts of macrocycles. This approach becomes even more impractical for the synthesis of high molecular weight cyclic polymers as it requires an even more diluted medium than the cyclization of oligomers. However, the use of living polymerization techniques (e.g. anionic or RAFT polymerization) for the preparation of the linear precursors allows more control over the molar mass and end group functionality. Thus, different strategies have been investigated to improve the efficiency of end-to-end closure.

As an example of an earlier method for the synthesis of cyclic polymers, Cassasa and co-worker has demonstrated the ring-closure reaction of α, ω-polymer dianions by using a bifunctional coupling agent **(Figure 1.6a (i))**.[72] A variety of cyclic polymers with a range of different molecular weights have been synthesized by this route. However, the yield of cyclization was often low (< 50%) due to the competition between intra- and inter-molecular coupling.

An alternative approach, which overcomes the complications of the bimolecular coupling reaction, involves the direct coupling reaction between two identical polymer end-groups in homodifunctional polymers **(Figure 1.6a (i))**. In this unimolecular case, dilution of the linear precursors not only represses the oligomerization, but also favors the rate of intra-molecular coupling since the reactive groups are tethered to one another. One early example of an efficient homocoupling cyclization reaction was demonstrated by

Tezuka and Komiya using ring closing metathesis of allyl end-functionalized polymers.[73] As a result, significant improvement in the yield of cyclization was reported by this approach.

Another strategy to minimize linear by-products utilizes the principle of pre-organization of cyclic precursors bearing specific ionic end-functions *via* electrostatic non-covalent interactions. This approach was thoroughly investigated by Tezuka and coworkers for a broad diversity of cyclic polymers **(Figure 1.6c (iii))**.[74] However, this approach is limited to produce only low molecular weight polymer (below 5 kDa).

1.3.2. Ring-expansion approach

The unique advantage of this technique is that high dilution is not required to yield cyclic polymers, and thus makes it amenable to synthesis on a larger scale. Bielawaski *et al*. demonstrated ring-expansion metathesis polymerization (REMP) using cyclic ruthenium catalyst as shown in **Scheme 1.9**.[75] In this coordinated polymerization, the cyclooctene monomer coordinates onto the ruthenium center before insertion into the cyclic carbene ring which grows of one monomer unit.

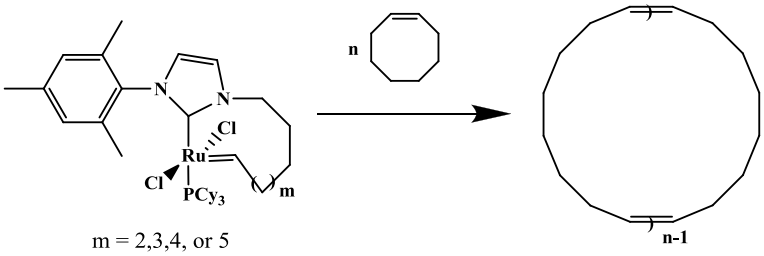

Scheme 1.9. Synthesis of macrocyclic poly(octane) by REMP.

This unique strategy gives nearly 100% cyclic polymers, yet is limited by the incompatibility of catalyst with other functional monomer.

Ring-expansion by RAFT polymerizations using cyclic initiator involves a reversible homolytic bond cleavage, polymerization, and radical recombination. This approach is particularly attractive because of the large number of monomers that can be polymerized by CRP and the preparation of functionalized cyclic polymers is achievable. Pan and co-workers have demonstrated the synthesis of cyclic polymers using a modified RAFT polymerization.[76] Methyl acrylate was polymerized by its insertion into the cyclic dithioester initiator using ^{60}Co γ-rays induce polymerization **(Scheme 1.10)**. The temperature was kept low enough (–30^{o}C) to reduce the diffusion rate and to prevent the inter-molecular chain transfer of active radicals. As a versatile living radical nature of RAFT polymerization, ABA type cyclic block co-polymers were obtained via the polymerization of N-isopropylacrylamide using poly(methylacrylate) as the macroinitiator under the same experimental conditions.

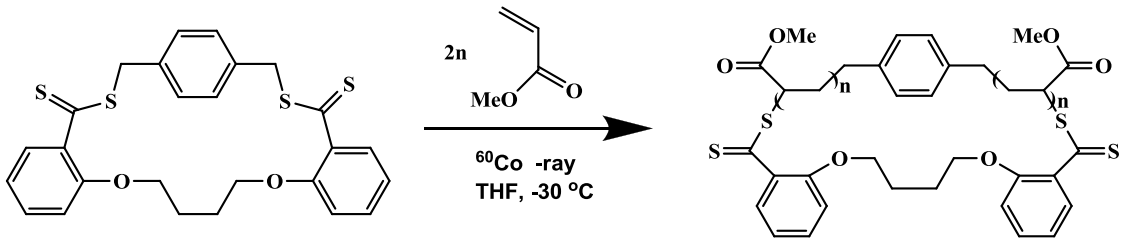

Scheme 1.10. Ring-expansion of a cyclic dithioester initiator to produce cyclic poly(methyl acrylate).

Another efficient way to make cyclic polymer was demonstrated by Kricheldorf and Lee *via* ring-opening polymerization of lactones and lactides using a series of cyclic tin

dialkoxide initiator **(Scheme 1.11)**.[77] The mechanism involves the insertion of monomer into tin–oxygen bond to produce ring-expanded macrocycles. As a result of a coordination-insertion polymerization, no linear oligomer or polymer is formed at any stage of the process. However, the hydrolytically labile tin-oxide bond in the cyclic polymer backbone limits its further application or characterizations. A number of groups have developed techniques for removal of the tin catalyst while retaining the cyclic topology. In a representative example shown in **Scheme 1.11**, slightly excess of 1,3-dithian-2-one was used as a terminating agent. The coordination of sulfur with tin forms the cyclic 2-stanna-1,3-dithiane and selectively eliminates from the cyclic polymer backbone.

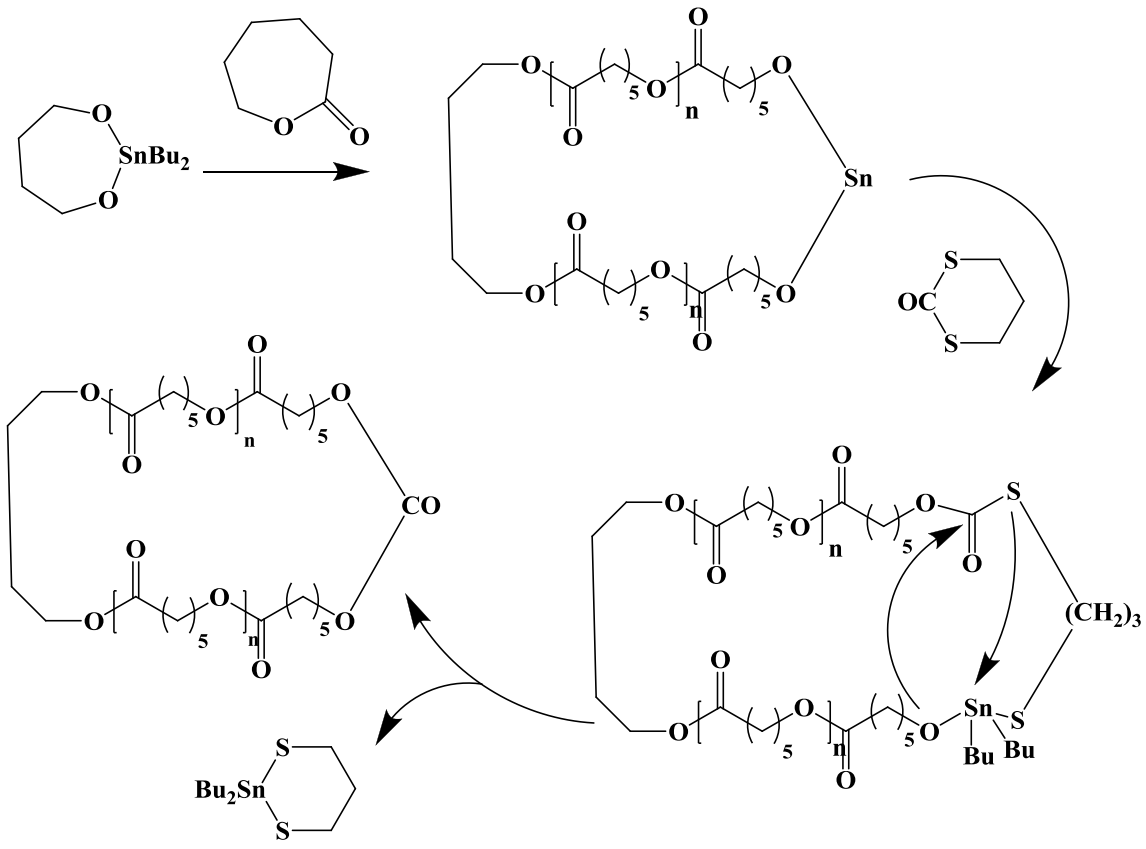

Scheme 1.11. Synthesis of cyclic polyester from cyclic tin initiator.

1.4. Literature Methods for Synthesis of Polymer Catenanes

Even though the successful synthesis of various mechanically interlocked molecules was made possible by the template-directed approach, obtaining such orderly entangled topology in high molecular weight (MW) polymer remains a synthetic challenge. For example, a polymer catenane consists of one cyclic polymer threading through another cyclic polymer. The synthetic method proposed or used toward polymer catenane commonly includes threading and cyclization steps **(Scheme 1.12)**; In this case, a linear polymer threads through a cyclic polymer ring, after which a cyclization is carried out on the resulting pseudo rotaxane to produce the polymer catenanes. However, a long and flexible polymer chain tends to form a randomly coiled, thus contracted conformation, and the threading by another polymer chain appears ineffective, particularly in dilution.[78] In addition, the purification of polymer catenane is always difficult due to the complexity of crude products, which may contain the desired catenated, cyclic and linear polymers. Therefore, the reported yield of isolated polymer catenanes is very low, only less than 1%.[79]

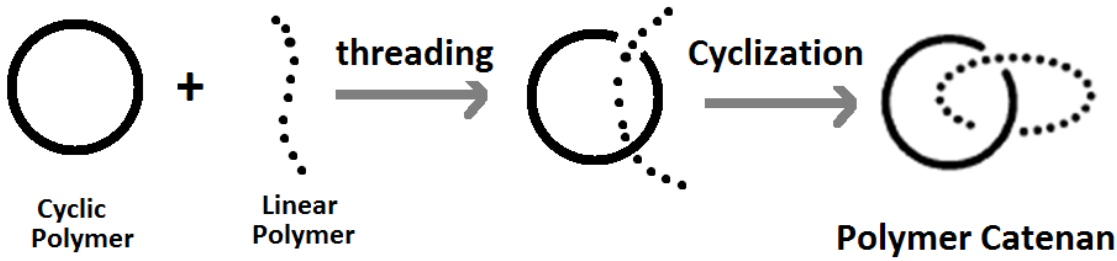

Scheme 1.12. General route for synthesis of polymer catenane.

Another attempt for the synthesis of high MW polymer catenanes have been demonstrated by Tezuka and co-worker *via* cooperative electrostatic/ hydrogen-bonding

self-assembly and covalent fixation **(Scheme 1.13)**.[80] First, a cyclic poly(tetrahydrofuran) (poly(THF)) was prepared by covalent conversion reaction of a preorganized assembly having an isophthaloyl benzylic amide group at the center position and having N-phenylpyrrolidinium salt end groups carrying a biphenyldicarboxylate counteranion.

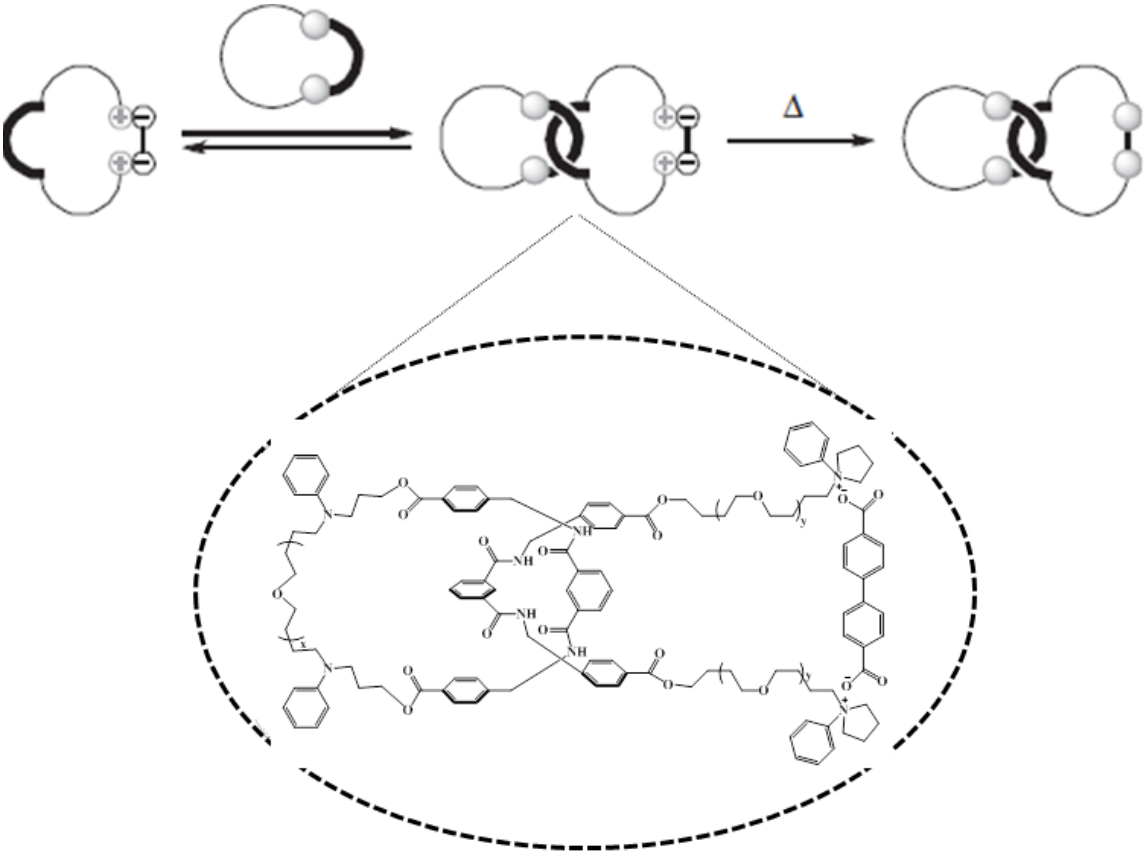

Scheme 1.13. Synthesis of a polymer catenane through a cooperative electrostatic/ hydrogen-bonding self-assembly and covalent fixation.

In next step, another pre-formed cyclic poly(THF) having the hydrogen-bonding unit was mixed and allowed to thread through a cyclic poly(THF). A polymer catenane comprised of the two different cyclic poly(THF) components was obtained in relatively good yield (7%) as a results of directive threading approach.

Recently, our group has demonstrated the efficient synthesis of polymer catenane using supramolecular templated tin initiator and ring-opening polymerization of caprolactam (**Scheme 1.14**).[81]

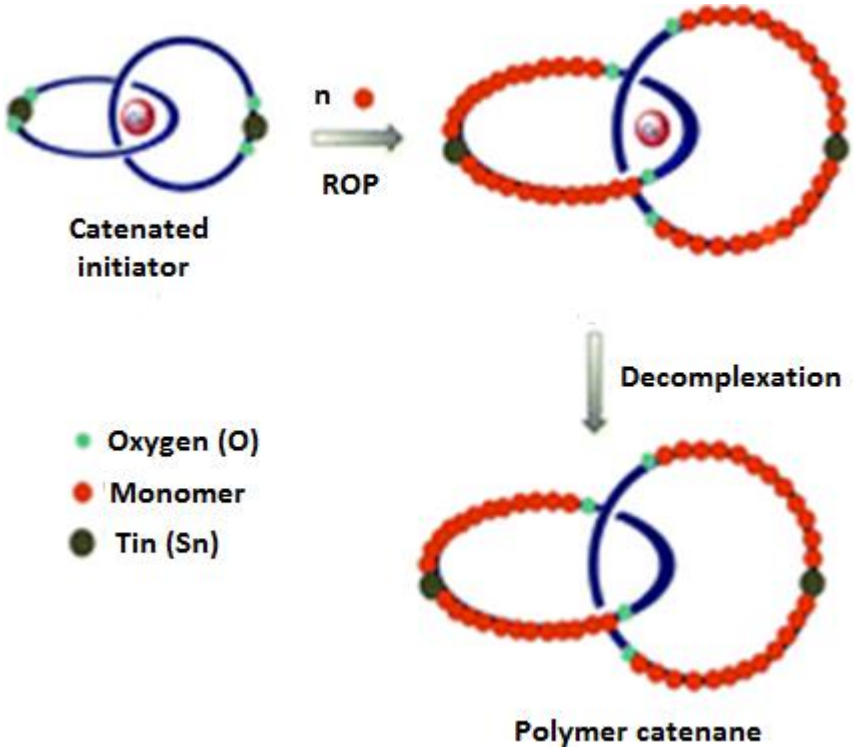

Scheme 1.14. Synthesis route for polymer catenane using catenated tin initiator.

A catenane initiator was synthesized by the ring-closure reaction of hydroxyl functionalized phenanthroline copper(I) complex and dibutyldimethoxytin. In next step, ring-opening polymerization of caprolactam monomer was carried out under kinetically driven conditions. Since the polymerization progressed through insertion of monomer to tin-oxide bond of catenated initiator, high molecular weight polymer catenane was obtained in 73% yield.

1.5. Chapter Outlines and Objectives

The main objective of this dissertation is to pursue the investigation of templated routes for the synthesis of interlocked macromolecular architectures and orderly entanglements. The specific objectives are as follows: (1) design and synthesis of supramolecularly templated initiators and utility for controlled radical polymerization, (2) investigate the efficiency of the initiator template to control the polymerization of vinyl monomers and to test the stability of the template under polymerization conditions, (3) demonstrate a simpler route to close the polymer template in order to obtain the mechanically interlocked polymer topology, (4) explore other possible methods of template directed synthesis, such as grafting of preformed polymer to supramolecular template followed by intra-molecular template-closing reaction, and (5) conduct preliminary studies to obtain high purity interlocked polymer architecture *via* an efficient ring-expansion RAFT polymerization approach.

Chapter 2 demonstrates the synthesis of polymer catenanes *via* controlled radical polymerization from ATRP initiators templated on Sauvage's phenanthroline Cu(I) complex and subsequent template-closing of resulted four-armed type polymer by Atom Transfer Radical Coupling (ATRC). In addition to other characterization method, direct visualization of polymer catenane was demonstrated by AFM imaging technique.

Chapter 3 reports on an important extension of above methodology to obtain a catenated block copolymer. The four-armed type homopolymer template as mentioned above was used as macroinitiator to polymerize another monomer by ATRP. The

resulting block copolymer template was subjected to template-closing *via* slightly modified ATRC method.

Chapter 4 demonstrates another novel approach to synthesize polymer catenanes *via* grafting a preformed alkyne-functionalized linear polymer to azide-functionalized phenanthroline Cu(I) template, followed by ATRC of resulting polymer template. Detailed analysis of the AFM images reveals important information about side product of ATRC such as inter-molecular coupling and other isomer formation.

Chapter 5 reports on a preliminary study of ring-expansion RAFT polymerization using cyclic initiator. A novel cyclic RAFT initiator was synthesized and used for thermally initiated free radical polymerization of N-vinyl carbazole. The cyclic topology of resulted polyvinylcarbazole was confirmed by GPC and AFM analysis.

Chapter 6 reports for the first time, synthesis of a trefoil knot polymer (knotty polymer) *via* grafting an alkyne-functionalized polymer to azide-functionalized Sauvage's diCu(I) double helical phenanthroline template. A well-defined knotty polymer was obtained by closing the template *via* ATRC method.

Finally, Chapter 7 summarizes the important results of the projects mentioned in Chapter 2 thru 6 and provides a global conclusion of the dissertation including future research work.

1.6. References

1. Nasongkla, N.; Chen, B.; Macaraeg, N.; Fox, M. E.; Frechet, J. M. J.; Szoka, F. C. *J. Am. Chem. Soc.* **2009,** *131*, 3842–3843.
2. Bosman, A. W.; Vestberg, R.; Heumann, A.; Frechet, J. M. J.; Hawker, C. J. *J. Am. Chem. Soc.* **2003,** *125*, 715–728.
3. Schluter, A. D.; Rabe, J. P. *Angew. Chem., Int. Ed.* **2000**, *39*, 864–883.
4. Pyun, J.; Kowalewski, T.; Matyjaszewski, K. *Macromol. Rapid Commun.* **2003**, *24*, 1043–1059.
5. Tezuka, Y.; Oike, H. *J. Am. Chem. Soc.* **2001**, *123*, 11570–11576.
6. Tomalia, D. A.; Frechet, J. M. J. *J. Polym. Sci., Part A: Polym. Chem.* **2002**, *40*, 2719–2728.
7. Kasehagen, L. J.; Macosko, C. W. *J. Rheol*. **1998**, *42*, 1303–1327.
8. Kapnistos, M.; Semenov, A. N.; Vlassopoulos, D.; Roovers, J. *J. Chem. Phys.* **1999**, *111*, 1753–1759.
9. Roovers, J. *J. Polym. Sci. Polym. Phys. Ed*. **1985**, *23*, 1117.
10. Roovers, J. In *Cyclic Polymers*, 2nd ed.; Semlyen, J. A., Ed.; Kluwer Academic Publishers: Dordrecht, 2000; pp 347–384.
11. McKenna, G. B.; Hostetter, B. J.; Hadjichristidis, N.; Fetters, L. J.; Plazek, D. J. *Macromolecules* **1989**, *22*, 1834–1852.
12. Subramanian, G.; Shanbhag, S. *Phys. Rev. E* **2008**, *77*, 11801–11809.
13. Hur, K.; Winkler, R. G.; Yoon, D. Y. *Macromolecules* **2006**, *39*, 3975–3977.
14. Kapnistos, M.; Lang, M.; Vlassopoulos, D.; Pyckhout-Hintzen, W.; Richter, D.; Cho, D.; Chang, T.; Rubinstein, M. *Nature Mater*. **2008**, *7*, 997–1002.

15. E. Wasserman, *J. Am. Chem. Soc.* **1960**, *82*, 4433.

16. Busch, D. H.; Stephenson, N. A. *Chem. Rev*. **1990**, *100*, 119–154.

17. Walba, D. M.; *Tetrahedron* **1985**, *41*, 3161.

18. Sauvage, J. -P. *Chem.–Eur. J*. **2005**, *11*, 4374–4386.

19. Sarbu, T.; Lin, K. Y.; Spanswick, J.; Gil, R. R.; Siegwart, D. J.; Matyjaszewski, K. *Macromolecules* **2004**, *37*, 9694–9700.

20. Rique-Lurbet, L.; Schappacher, M.; Deffieux, A. *Macromolecules* **1994**, *27*, 6318.

21. Laurent, B. A.; Grayson, S. M. *Chem. Soc. Rev.*, **2009**, *38*, 2202–2213.

22. (a) Tait, P. G. *Proc. R. Soc. Edinbur*gh **1875–1878**, *9*, 289. (b) Tait, P. G. *Proc. R. Soc. Edinburgh* **1875–1878**, *9*, 306. (c) Tait, P. G. *Proc. R. Soc. Edinburgh* **1875–1878**, *9*, 321. (d) Tait, P. G. *Proc. R. Soc. Edinburgh* **1875–1878**, *9*, 363. (e) Tait, P. G. *Proc. R. Soc. Edinburgh* **1875–1878**, *9*, 391. (f) Tait, P. G. *Proc. R. Soc. Edinburgh* **1875–1878**, *9*, 403.

23. Epple, M. *Arch. Hist. Exact Sci*. **1998**, *52*, 297.

24. Tait, P. G. *Trans.-R. Soc. Edinburgh* **1884**, *32*, 327.

25. Alexander, J. W.; Briggs, G. B. *Ann. Math*. **1926**–**1927**, *28*, 562.

26. Scharein, R. G. Department of Computer Science, University of British Columbia: Vancouver, Canada, 1995–2004; see: http://www. pims.maths.ca/knotplot.

27. Adams, C. C. *The Knot Book*; Freeman: New York, 1994.

28. Michelson, A. A.; Morley, E. W. *Am. J. Sci.* **1887**, *34*, 333.

29. Rolfsen, D. *Knots and Links*; Publish or Perish: Berkeley, 1976.

30. Clayton, D. A.; Vinograd, J. *Nature* **1967**, *216*, 652.

31. Hudson, B.; Vinograd, J. *Nature* **1967**, *216*, 647.

32. Radloff, R.; Bauer, W.; Vinograd, J. *Proc. Natl. Acad. Sci. U.S.A.***1967**, *57*, 1514.

33. Wasserman, S. A.; Cozzarelli, N. R. *Science* **1986**, *232*, 951.

34. Liu, L. F.; Depew, R. E.; Wang, J. C. *J. Mol. Biol*. **1976**, *106*, 439.

35. Liu, L. F.; Liu, C. C.; Alberts, B. M. *Cell* **1980**, *19*, 697.

36. Dean, F. B.; Stasiak, A.; Koller, T.; Cozzarelli, N. R. *J. Biol. Chem.* **1985**, *260*, 4975.

37. Stasiak, A.; Katritch, V.; Bednar, J.; Michoud, D.; Dubochet, J. *Nature* **1996**, *384*, 122.

38. (a) Gellert, M. *Annu. Rev. Biochem*. **1981**, *50*, 879. (b) Vosberg, H. P. *Curr. Top. Microbiol.* **1985**, *114*, 19. (c) Wang, J. C. *Annu. Rev. Biochem*. **1985**, *54*, 665. (d) Chen, A. Y.; Liu, L. F. *Annu. Rev. Pharmacol. Toxicol*. **1994**, *34*, 191. (e) Wang, J. C. *Annu. Rev. Biochem.* **1996**, *65*, 635. (f) Champoux, J. *J. Annu. Rev. Biochem*. **2001**, *70*, 369. (g) Wang, J. C. *Nat. Rev. Mol. Cell Biol*. **2002**, *3*, 430.

39. Fortune, J. M.; Osheroff, N. *Progress in Nucleic Acid Research and Molecular Biology*; Academic Press Inc.: San Diego, CA, 2000; Vol. 64, p 221.

40. Li, T. K.; Liu, L. F. *Annu. Rev. Pharmacol. Toxicol*. **2001**, *41*, 53.

41. Dietrich-Buchecker, C.O.; Sauvage, J.-P. *Tetrahedron Lett*. **1983**, *24*, 5095.

42. Dietrich-Buchecker, C.O.; Sauvage, J.-P. *J. Am. Chem. Soc*. **1984,** *106*, 3043.

43. Mohr, B.; Weck, M.; Sauvage, J.-P.; Grubbs, R.H. *Angew. Chem. Int. Ed. Engl*. **1997,** *36*, 1308.

44. Dietrich-Buchecker, C. O.; Colasson, B.; Jouvenot, D.; Sauvage, J.-P. *Chem. Eur. J.* **2005**, *11*, 4374–4386.

45. Dietrich-Buchecker, C.O.; Sauvage, J.-P. *Angew. Chem. Int. Ed. Engl*. **1989,** *28*, 189.

46. Rapenne, G.; Dietrich-Buchecker, C. O.; Sauvage, J.-P. *J. Am. Chem. Soc.* **1996,** *118*, 10932.

47. Ward, M.; Sauvage, J.-P. *Inorg. Chem*. **1991,** *30*, 3869.

48. Rapenne, G.; Dietrich- Buchecker, C.; Sauvage. J.-P. *J. Am. Chem. Soc*. **1999**, *121*, 994–1001.

49. Vance, A.L.; Alcock, N.W.; Heppert, J.A.; Busch, D.H. *Inorg. Chem.* **1998,** *37*, 6912.

50. Adams, H.; Ashworth, E.; Breault, G. A.; Guo, J.; Hunter, C. A.; Mayers, P. C. *Nature* **2001**, *411*, 763.

51. (a) J. Guo, P. C. Mayers, G. A. Breault, C. A. Hunter, *Nat. Chem*. **2010**, *2*, 218 – 222. (b) Fenlon, E. E. *Nat. Chem*. **2010**, *2*, 156 – 157.

52. (a) Hunter, C.A. *J. Am. Chem. Soc*. **1992,** *114*, 5303. (b) Adams, H.; Carver, F.J.; Hunter, C.A. *J. Chem. Soc. Chem. Commun*. **1995**, 809.

53. Thompson, M.C.; Busch, D.H. *J. Am. Chem. Soc*. **1964**, *86*, 3651.

54. Amabilino, D.B.; Stoddart, J.F. *Chem. Rev*. **1995,** *95*, 2725.

55. Ashton, P.R.; Goodnow, T.T.; Kaifer, A.E.; Reddington, M.V.; Slawin, A.M.Z.; Spencer, N.; Stoddart, J.F.; Vicent, C.; Williams, D.J. *Angew. Chem. Int. Ed. Engl*. **1989,** *28*, 1396.

56. Greszta, D.; Mardare, D.; Matyjaszewski, K. *Macromolecules* **1994**, *27*, 638–44.

57. Moad, G.; Rizzardo, E.; Thang, S. H. *Aust. J. Chem.* **2005**, *58*, 379–410.

58. Georges M. K.; Veregin, R. P. N.; Kazmaier P. M.; Hamer G. K. *Macromolecules* **1993**, *26*, 2987–2988.

59. Hawker C. J.; Bosman A. W.; Harth, E. *Chem. Rev.* **2001,** *101*, 3661–3688.

60. Lena, F. di.; Matyjaszewski, K. *Prog. Polym. Sci.* **2010**, *35*, 959–1021.

61. Busico, V.; Cipullo, R. *Prog. Polym. Sci.* **2001**, *26*, 443 –533.

62. Camerano, J. A.; Rodrigues, A.-S.; Rominger, F.; Wadepohl, H.; Gade, L. H. *J. Organomet. Chem.* **2011**, *696*, 1425–1431.

63. Abu-Surrah, A.; Ibrahim, K. A.; Abdalla, M. Y.; Issa, A. A. *J.Polym. Res*. **2011**, *18*, 59–66.

64. (a) Barner-Kowollik, C.; Davis, T. P.; Heuts, J. P. A.; Stenzel, M. H.; Vana, P.; Whittaker, M. *J. Polym. Sci. Part A: Poly. Chem.* **2003**, *41*, 365. (b) Cacioli, P.; Hawthorne, D. G.; Laslett, R. L.; Rizzardo, E.; H., S. D. *J. Macromol. Sci. Chem.* **1986**, *23*, 839. (c) Delduc, P.; Tailhan, C.; Zard, S. Z. *J. Chem. Soc. Chem. Commun.* **1988**, 308. (d) Hutson, L.; Krstina, J.; Moad, C. L.; Moad, G.; Morrow, G. R.; Postma, A.; Rizzardo, E.; Thang, S. H. *Macromolecules* **2004**, *37*, 4441. (e) Quémener, D.; Hellaye, M. L.; Bissett, C.; Davis, T. P.; Barner-Kowollik, C.; Stenzel, M. H. *J. Poly. Sci. Part A: Poly. Chem.* **2008**, *46*, 155.

65. Kolb, H. C.; Finn, M. G.; Sharpless, K. B. *Angew. Chem., Int. Ed.* **2001**, *40*, 2004.

66. (a) Huisgen, R. *Angew. Chem. Int. Ed. Engl*. **1963**, *2*, 565. (b) Huisgen, R. *Angew. Chem. Int. Ed. Engl*. **1963**, *2*, 633.

67. (a) Collman, J. P.; Devaraj, N. K.; Chidsey, C. E. D. *Langmuir* **2004**, *20*, 1051. (b) Díaz, D. D.; Punna, S.; Holzer, P.; McPherson, A. K.; Sharpless, K. B.; Fokin, V. V.; Finn, M. G. *J. Polym. Sci. Part A: Poly. Chem.* **2004**, *42*, 4392. (c) Helms, B.; Mynar, J. L.; Hawker, C. J.; Fréchet, J. M. J. *J. Am. Chem. Soc.* **2004**, *126*, 15020. (d) Lutz, J.-F.; Börner, H. G.; Weichenhan, K. *Macro. Rapid Comm.* **2005**, *26*, 514. (19) Wu, P.; Feldman, A. K.; Nugent, A. K.; Hawker, C. J.; Scheel, A.; Voit, B.; Pyun, J.; Fréchet, J. M. J.; Sharpless, K. B.; Fokin, V. V. *Angew. Chem.* **2004**, *116*, 4018.

68. (a) Deiters, A.; Cropp, T. A.; Summerer, D.; Mukherji, M.; Schultz, P. G. *Bioorg. & Med. Chem. Lett.* **2004**, *14*, 5743 Link, A. J.; Vink, M. K. S.; Tirrell, D. A. *J. Am. Chem. Soc* **2004**, *126*, 10598. (24) Punna, S.; Kaltgrad, E.; Finn, M. G. *Bioconju. Chem.* **2005**, *16*, 1536. (25) Seo, T. S.; Li, Z.; Ruparel, H.; Ju, J. *J. Org. Chem.* **2002**, *68*, 609.

69. (a) Hadjichristidis, N.; Iatrou, H.; Pitsikalis, M.; Mays, J. *Prog. Polym. Sci,* **2006,** *31*, 1068–1132; (b) K. Endo, *Adv. Polym. Sci*. **2008**, *217*, 121–184.

70. (a) Adachi, K.; Tezuka, Y. *J. Synth. Org. Chem. Jpn.* **2009**, *67,* 1136–1143. (b) Tezuka, Y. *Chem. Rec*. **2005**, *5*, 17–26. (c) Grayson, S. M. *Nat. Chem*. **2009**, *1*, 178–179. (d) Grayson, S. M. *Chem. Soc. Rev*. **2009**, *38,* 2202–2213. (e) Perrier, S. *Nat. Chem*. **2011**, *3*, 194–196.

71. (a) McLeish, T. *Science*, **2002**, *297*, 2005–2006. (b) McLeish, T. *Nat. Mater*. **2008**, *7*, 933–935. (c) Fox, M. E.; Szoka, F.; Frechet, J. M. J. *Acc. Chem. Res*. **2009**, *42*, 1141–1151. (d) Kricheldorf, H. R. *J. Polym. Sci., Part A: Polym. Chem*. **2010**, *48*, 251–284.

72. Casassa, E. F. *J. Poly. Sci. Part A: General Papers* **1965**, *3*, 605.

73. Hiyashi, S.; Adachi, K.; Tezuka, Y. *Chem. Lett.* **2007**, *36*, 982.

74. Tezuka, Y.; Oike, H. *J. Am. Chem. Soc.* **2001**, *123*, 11570.

75. (a) Bielawski, C. W.; Benitez, D.; Grubbs, R. H. *Science*, **2002**, *297*, 2041. (b) Bielawski, C. W.; Benitez, D.; R. H. Grubbs. *J. Am. Chem. Soc*., **2003**, *125*, 8424.

76. He, T.; Zheng, G.; Pan, C. *Macromolecules*, **2003**, *36*, 5960.

77. (a) Kricheldorf, H. R.; Lee, S-R.; Schittenhelm, N. *Macromol. Chem. Phys*. **1998**, *199*, 273–282. (b) Kricheldorf, H. R.; Langanke, D.; Stricker, A.; Rader, H. J.

Macromol. Chem. Phys. **2002**, *203*, 405–412. (c) Ma, J. *Polym. Preprints (Am. Chem. Soc., Div. Polym. Chem.* **1993**, *34*, 626–627. (d) Hadjichristidis, N.; Iatrou, H. *Macromolecules* **2002**, *35*, 5426–5437. (e) Gan, Y.; Zoller, J.; Yin, R.; Hogen-Esch, T. E. *Makromol. Symp.* **1994**, *77*, 93–104. (f) Kricheldorf, H. R. *J. Polym. Sci. Part A: Polym. Chem*. **2004**, *42*, 4723–4742.

78. (a) Fustin, C. A.; Clarkson, G. J.; Leigh, D. A.; Van Hoof, F.; Jonas, A. M.; Bailly, C. *Macromolecules* **2004**, *37*, 7884–7892. (b) Gibson, H. W.; Nagvekar, D. S.; Yamaguchi, N.; Bhattacharjee, S.; Wang, H.; Vergne, M. J.; Hercules, D. M. *Macromolecules* **2004**, *37*, 7514–7529. (c) Watanabe, N.; Ikari, Y.; Kihara, N.; Takata, T. *Macromolecules* **2004**, *37*, 6663–6666.
79. (a) Gan, Y.; Dong, D.; Hogen-Esch, T. E. *Macromolecules* **2002**, *35*, 6799–6803. (b) Ohta, Y.; Kushida, Y.; Kawaguchi, D.; Matsushita, Y.; Takano, A. *Macromolecules* **2008**, *41*, 3957–3961.
80. Ishikawa, K.; Yamamoto, T.; Asakawa, M.; Tezuka, Y. *Macromolecules* **2010**, *43*, 168–176.
81. Cao, P.; Bunha, A.; Mangadlao, J.; Felipe, M. J.; Mongcopa, K.; Advincula, R. *Chem. Commun*. **2012**, *48*, 12094–12096.

Chapter 2: Synthesis of Polymer Catenanes *via* a Supramolecularly Templated ATRP Initiator

2.1. Introduction

Polymers with different types of topologies play an important role in tuning macromolecular properties.[1] Various polymers with special architectures, such as star, hyperbranched, dendronized, cylindrical, and macrocyclic, have been reported.[2-3] Although numerous examples of catenanes, rotaxanes, and trefoil knots with considerably low molecular weight have been reported in the literature,[4-7] obtaining such orderly entangled topology in the case of high molecular weight polymers as well as block copolymers remains challenging due to their synthetic obstacles. Nevertheless, the interest on entanglements is an integral part of modern polymer physics, notably in the fields of rheology,[8] adhesion,[9] crystallinity,[10] surface and interfaces,[11] block copolymers,[12] and viscoelasticity.[13] Many aspects of chemical topology from DNA to stereochemical reactions have been studied.[14] These topologies can be explained by the realm of orderly molecular entanglements of well-reported interlocked molecular and supramolecular architectures as demonstrated by Sauvage,[7] Stoddart,[4] Wasserman,[15] Busch,[16] and Walba.[17] A number of reports have demonstrated intricate sequences of steps (threading, cross-overs, ring closings, and other linkages) in order to form complicated orderly knot entanglements.[18]

The development of controlled radical polymerization methods, especially atom transfer radical polymerization (ATRP) and reversible addition fragmentation chain

transfer polymerization (RAFT), has opened the door to experimentally more lenient syntheses of well-defined telechelic linear precursors.[19] Since a catenane is an analogue of a cyclic ‘‘end-less’’ structure, there is a possibility of using existing methods of forming cyclic polymers, such as coupling reactions of telechelics in dilute solution to form polymer catenanes.[20-21] Herein, we report a synthetic strategy to obtain polymer catenanes by: (1) design and synthesis of supramolecularly templated ATRP initiators followed by polymerization, and (2) template-closure of the supramolecular polymer *via* an intra-molecular end-to-end cyclization step **(Scheme 2.1)**.

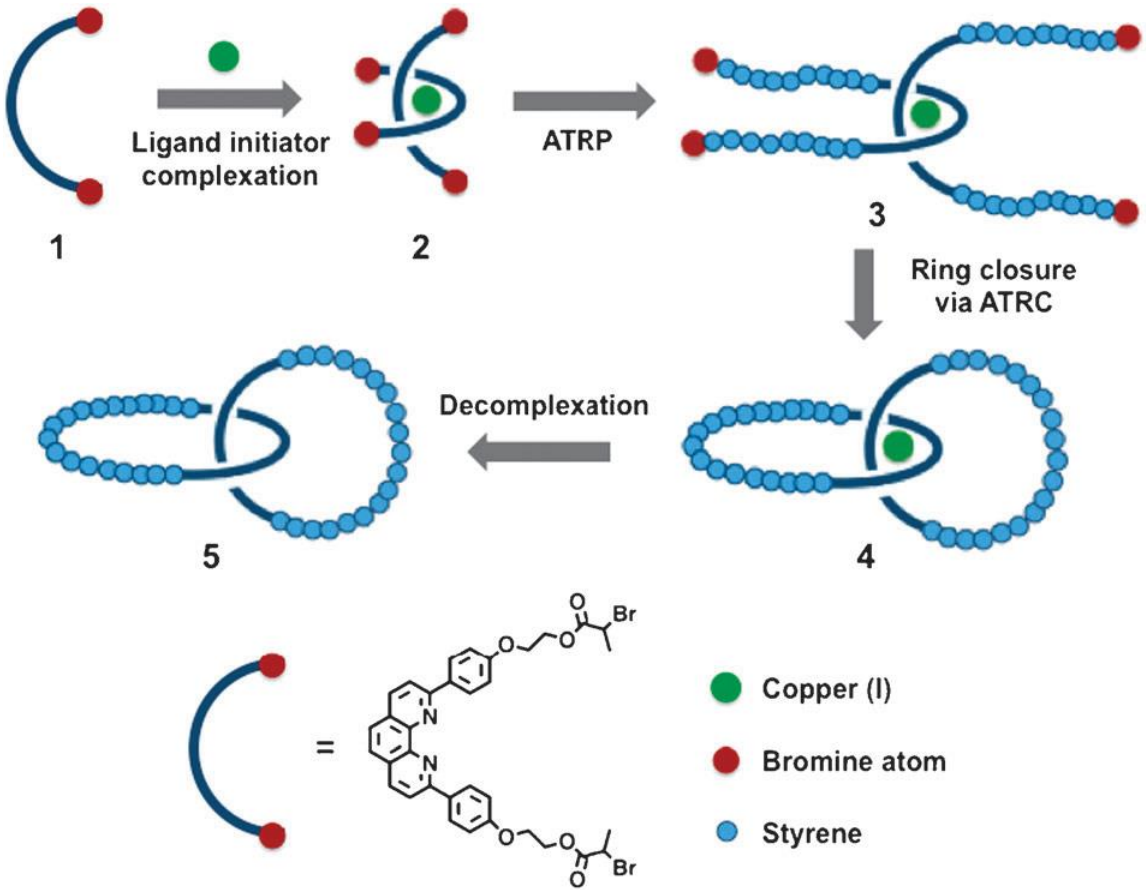

Scheme 2.1. Schematic route for the preparation of polymer catenanes from the supramolecularly templated ATRP initiator.

2.2. Results and Discussion

2.2.1. Design and synthesis of ATRP initiator Cu(I) complex

Synthesis of molecules with complex topologies such as catenanes, rotaxanes, and molecular knots requires the use of chemical templates. Various types of supramolecularly assembled templates have been reported based on metal-ion templates, hydrogen-bonded templates, and π-donor, π-acceptor templates.[5] A metal-ion template such as a phenanthroline Cu(I) complex as demonstrated by Sauvage and co- workers[4,22] could be the best choice for designing supramolecularly templated ATRP initiator because of the ease of end-group modifications in the 2,9-bis(p- hydroxyphenyl)- 1,10-phenanthroline ligand and the stability of the template under ATRP polymerization conditions.[22] The synthesis of the ATRP initiator (**1**) was reported in 68.8% yield using

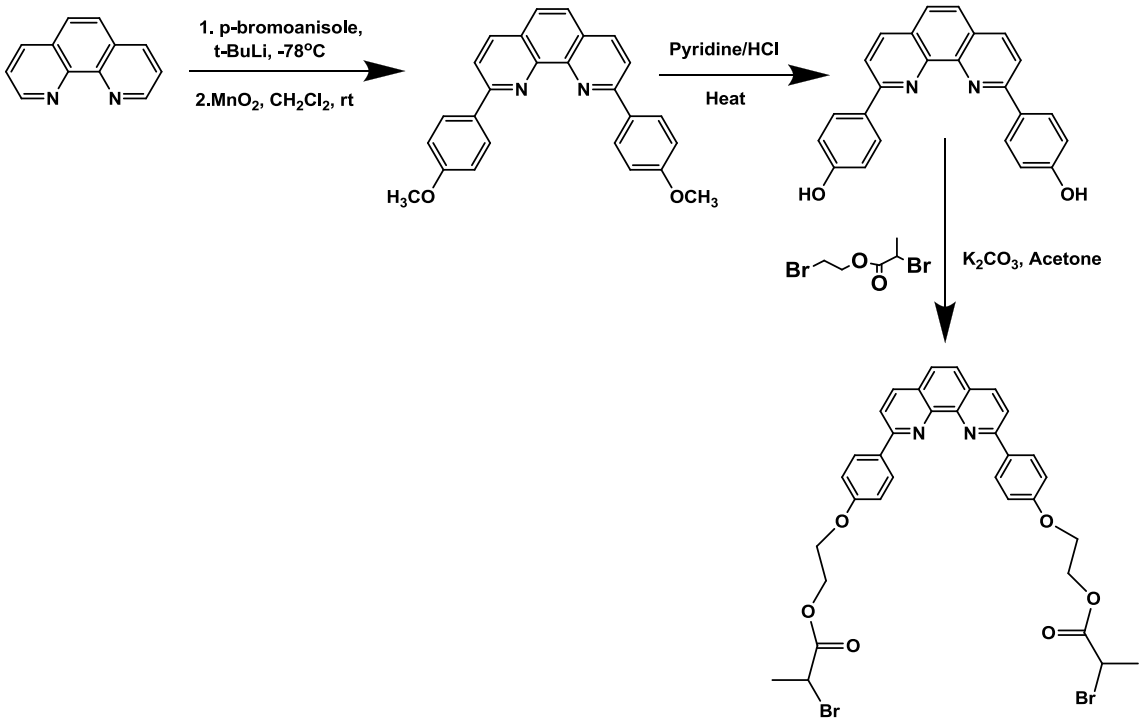

Scheme 2.2. Synthetic scheme for the ATRP initiator (**1**).

bromoethyl, 2-bromopropionic acid ester and the previously reported 2,9-bis(p-hydroxyphenyl)-1,10-phenanthroline ligand.

The supramolecular assembly of ATRP initiators (**1**) was formed by adding a degassed solution of $Cu(CH_3CN)_4PF_6$ in CH_2Cl_2 to the degassed solution of the ATRP initiator (2 eq.) in CH_2Cl_2. The resulting reddish solid product of the initiator complex was characterized by UV-Visible spectroscopy as shown in **Figure 2.1a**. The formation of the initiator complex (**2**) was confirmed by the presence of the intense ligand-centered

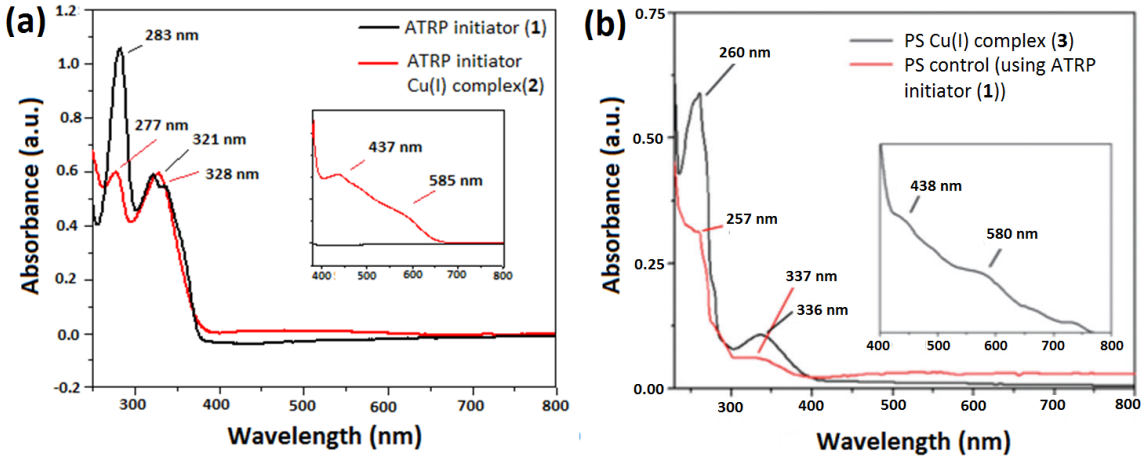

Figure 2.1. UV-Visible analysis of (a) ATRP initiator (**1**) and ATRP initiator Cu(I) complex (**2**) (inset: visible region of the ATRP initiator Cu(I) complex (**2**) spectrum), (b) PS Cu(I) complex (**3**) and PS control (inset: visible region of the PS complex (**3**) spectrum).

transitions at 277 nm and 328 nm and the weaker absorption peaks at the visible regions, 437 nm and 585 nm corresponding to metal-to-ligand (MLCT) and the ligand-to-metal (LMCT) charge-transfer transitions, respectively.[23]

2.2.2 Polymerization of styrene using ATRP initiator Cu(I) complex

Using the ATRP initiator Cu(I) complex (**2**), styrene was polymerized by the Cu(I)Br catalyst with the 1,1,4,7,10,10-hexamethyltriethylenetetraamine (HMTETA) ligand in anisole at 110 ^{o}C.

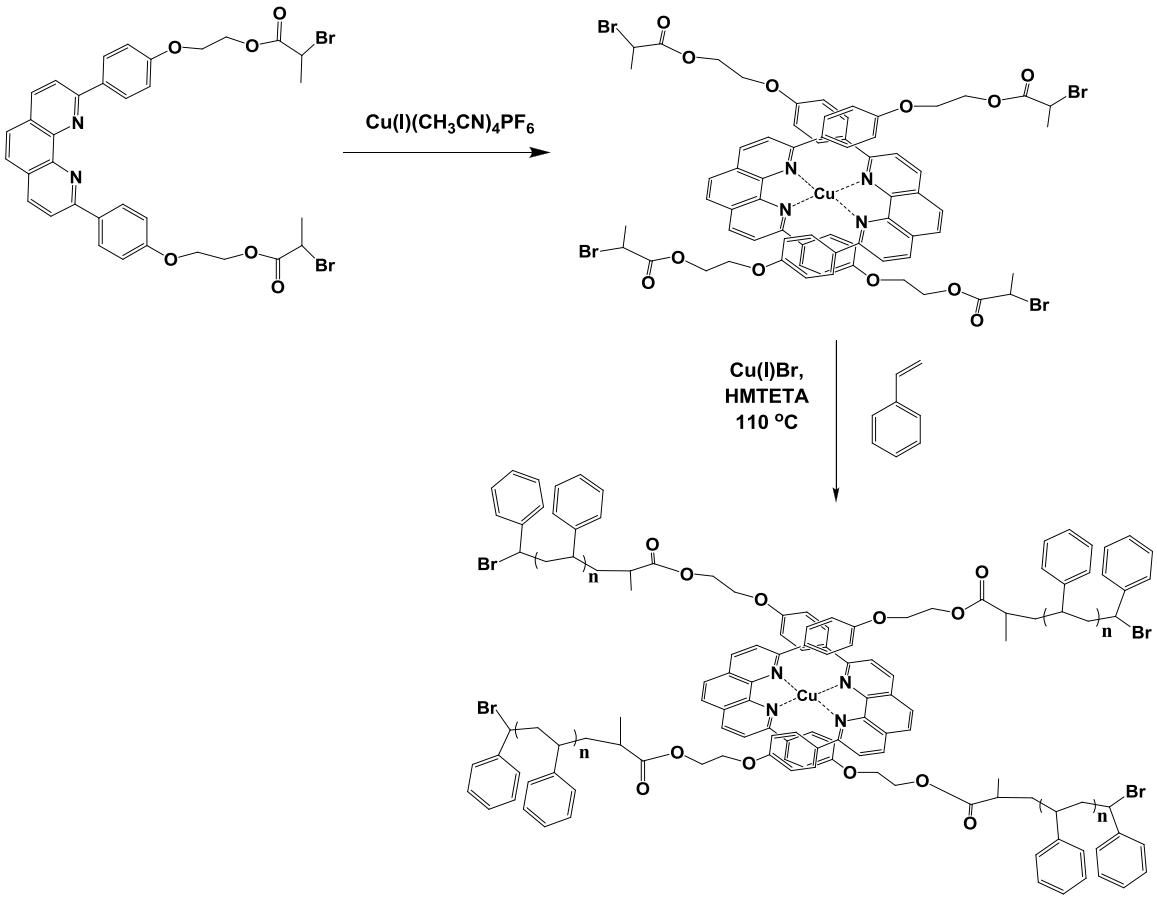

Scheme 2.3. Polymerization of styrene using ATRP initiator Cu(I) complex (**2**).

The resulting polystyrene (PS) Cu(I) complex (**3**) was purified by passing through a neutral alumina plug to remove the copper salts. The unreacted monomer and solvent were removed by precipitation of the polymer in cold methanol. The gel permeation chromatography (GPC) traces of the resulting PS Cu(I) complex (**3**) **(Figure 2.2)** show

narrow polydispersity with good control over molecular weight (M_n 6405 Da, M_w 7814 Da, PDI: 1.22). The integrity of the ligand Cu(I) complex within the backbone of the polymer was confirmed by the UV-Visible analysis as shown in **Figure 2.1b**, which still shows the ligand-centered bands (260 nm and 336 nm) and the MLCT and LMCT transition peaks (438 nm and 580 nm, respectively), consistent with the observed results of the ATRP initiator Cu(I) complex (**2**). The UV-Visible spectroscopy result was also supported by performing a control study of demetallation reaction of the PS Cu(I) complex (**3**) and characterization by GPC as discussed later in this chapter.

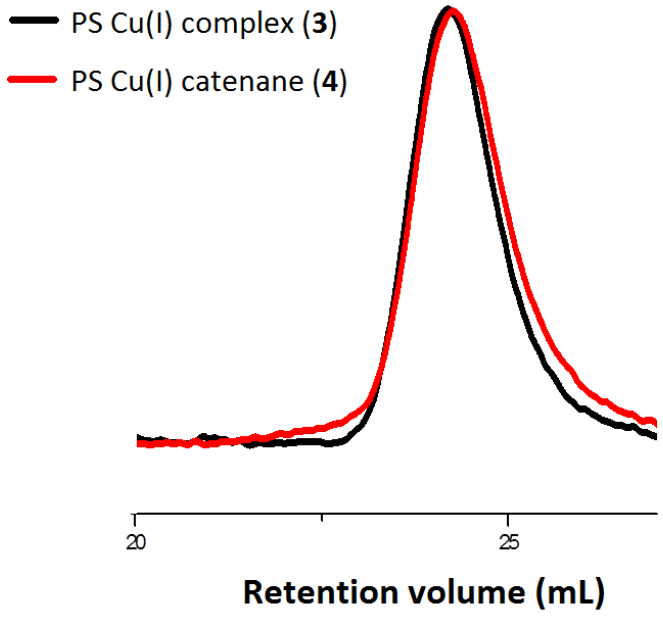

Figure 2.2. GPC traces of PS Cu(I) complex (**3**) and PS Cu(I) catenane (**4**).

2.2.3 Template-closing of PS Cu(I) complex *via* ATRC

Even though intra-molecular click chemistry[24] and ring-closing metathesis[25] have proven to be highly efficient in producing macrocycles, the synthetic modification of the

polymer chains prior to the cyclization reaction yields an additional step(s) to the overall synthetic route and could lead to multiple side products. We have utilized a simple method for the synthesis of the PS Cu(I) catenane (**4**) based on atom transfer radical coupling (ATRC) chemistry, which only involves one step towards tempate closure.[26]

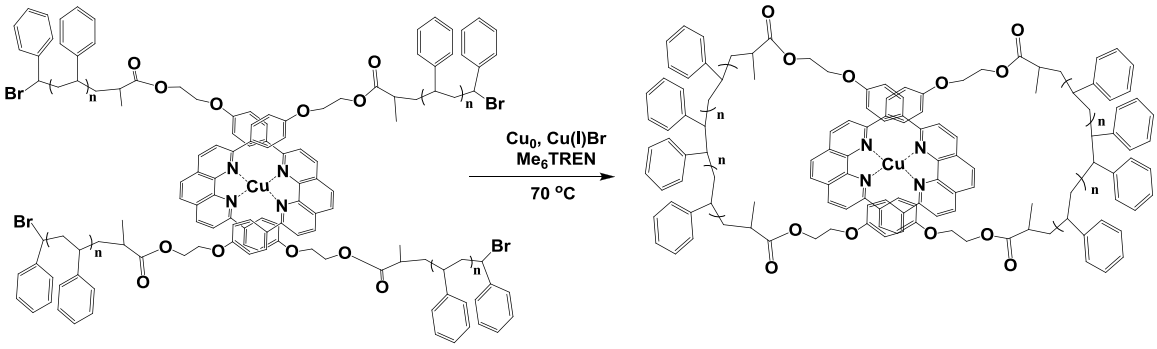

Scheme 2.4. Template-closing of PS Cu(I) complex (**3**) *via* ATRC.

The formation of the PS Cu(I) catenane (**4**) over step polymers can be favored by intra-molecular reaction of the PS Cu(I) complex (**3**) under pseudo-high dilution conditions. Thus, a THF solution of the PS Cu(I) complex (**3**) was added dropwise at a fairly low rate (0.75 mL/ h) into a refluxing THF solution of Cu(I)Br, Me_6TREN, and Cu(0). The GPC analysis of the closed PS Cu(I) catenane (**4**) (M_n 4188 Da, M_w 6533 Da) showed a very slight shift to a higher retention volume (R_v) (R_v = 24.27 mL) as compared to the open PS Cu(I) complex (**3**) (R_v=23.84 mL) **(Figure 2.2)**. This shift in the retention volume is due to the formation of the reduced hydrodynamic radius (R_h) of the PS Cu(I) catenane (**4**) (R_h = 4.6 nm) after the template-closure of the precursor PS Cu(I) complex (**3**) (R_h = 4.9 nm). As observed, the shift in R_v is not too evident as compared to other GPC traces reported in the literature that compares linear and cyclic polymer

counterparts. This observation could be explained by the fact that our open PS Cu(I) complex system (**3**) is not completely linear and is much closer to a semicyclic structure due to the geometric constraints coming from the complexed phenanthroline ligand in between the PS chains. The formation of a broader GPC peak for PS Cu(I) catenane (**4**) (PDI 1.56) as compared to PS Cu(I) complex (**3**) (PDI 1.22) signifies the presence of the mixture of PS Cu(I) catenane (**4**), unreacted PS complex (**3**) and the inter-molecular coupling product. Nonetheless, the observed ATRC products were predominantly PS Cu(I) catenane (**4**) as evidenced by a relatively high $<G_0>$ value (i.e. the ratio of the peak average molecular weight (M_p) of the coupled product relative to that of the acyclic precursor) of 0.79, which is comparable to other literature values of cyclic polymers produced by ATRC coupling[26] and anionic methods.[27]

2.2.4 Demetallation reaction of PS Cu(I) catenane

In order to obtain metal-free polymer catenanes, Cu(I) from the template was removed by stirring the PS Cu(I) catenane (**4**) with saturated solution of KCN in THF: methanol (3:1). The GPC traces of the demetallation step **(Figure 2.3)** of the PS

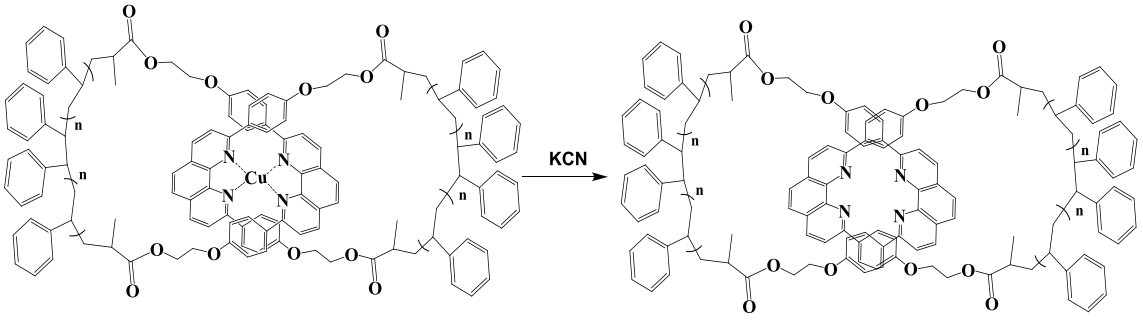

Scheme 2.5. Synthesis of PS catenane (**5**) *via* demetallation of PS Cu(I) catenane (**4**)

Cu(I) catenane (**4**) show that the molecular weight of the PS catenanes (**5**) (M_n 7374 Da, M_w 7922 Da) barely changed even after removing the copper, indicating an interlocked structure of cyclic polymers. The peak broadening of the GPC trace of the PS Cu(I) catenane (**4**) due to the unreacted acyclic precursor was also supported by the GPC analysis of the demetallation step. The appearance of the broad shoulder at a higher

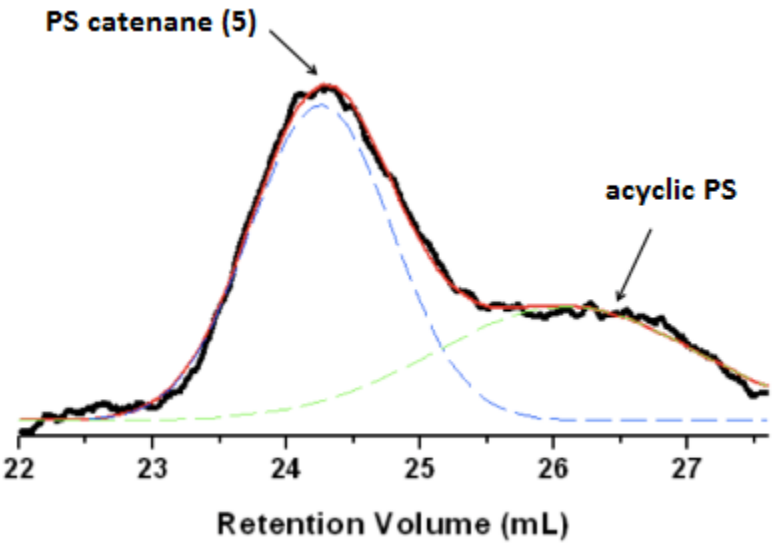

Figure 2.3. The GPC traces of the PS catenanes (**5**) after demetallation.

retention volume (M_n 2769 Da, M_w 2982 Da) denotes the formation of decomplexed acyclic PS with approximately half the molecular weight of the PS Cu(I) complex (**3**). On the basis of the relative area under curve of the GPC traces of the PS catenanes (**5**), the amount of polymer catenanes (**5**) formed in the reaction was estimated to be 60% of the product mixture.

To investigate the stability of supramolecular template during polymerization and to test the efficiency of metal removal, demetallation of the PS Cu(I) complex (**3**) (M_n

4,341 Da, PDI 1.25) was performed and analyzed by GPC as shown in **Figure 2.4**. The demetallation of PS Cu(I) complex (**3**) was performed using the same procedure as followed for PS Cu(I) catenanes (**4**). The GPC traces show the appearance of peak at a higher retention volume with M_n 2,738 Da, which is approximately half of the molecular weight of the PS Cu(I) complex (**3**). This result clearly indicates that the template is very stable under ATRP that the template is very stable under ATRP conditions and that the resulting polymers have a polymer-metal complex architecture.

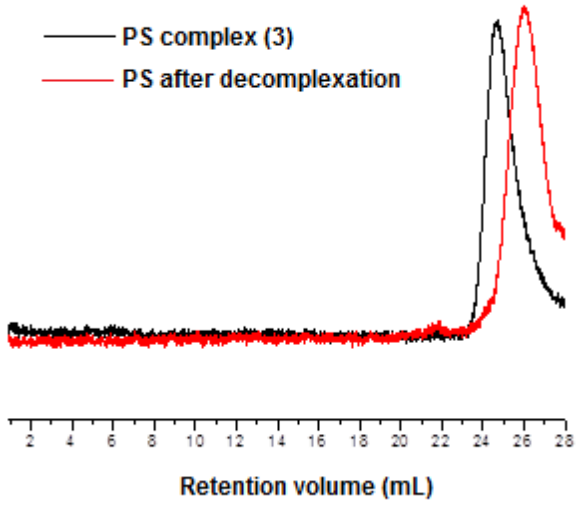

Figure 2.4 The GPC traces of the demetallation study of PS complex.

2.2.5. AFM imaging of PS catenanes

To give a visual representation of the PS catenanes (**5**), AFM imaging was also performed. The samples of PS catenanes (**5**) for AFM analysis were prepared by spin-coating a very dilute solution of the polymer in dry THF onto freshly cleaved mica. As shown in **Figure 2.5**, interlocked cyclic structures of polymers were statistically

observed, exhibiting different orientations on the surface. Line profile analysis of the structure revealed the presence of the cavities inside the catenanes where the overlapping region (middle of the catenanes) is double the height of the individual ring of a catenane.

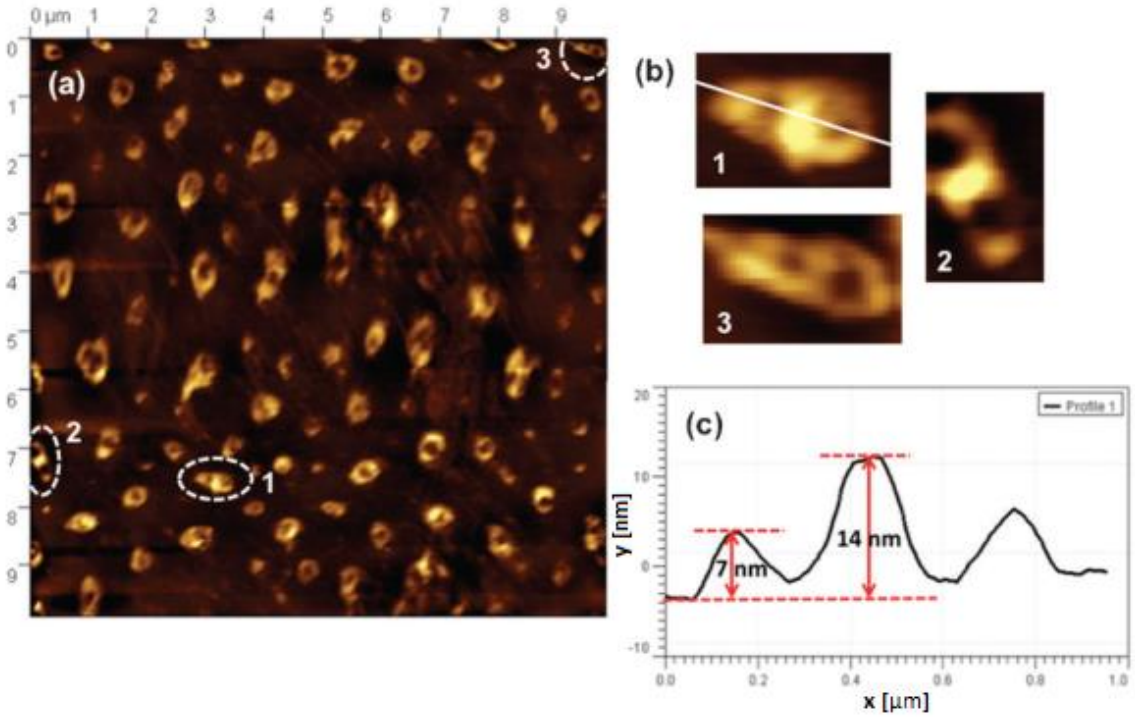

Figure 2.5. (a) AFM image of the PS catenanes (**5**) on a 9 x 9 mm scale on mica, (b) magnified images of the representative PS catenanes from (a), and (c) line profile of one of the PS catenanes from (b).

Statistically, other structures could represent partial open arms or inter-molecular coupling of the four-armed type PS complex (**3**), or simply different conformations of catenanes.

2.3. Conclusions

A new, simple, and versatile method for the synthesis of polymer catenanes with complex and higher order of cyclic topology was demonstrated. The supramolecularly assembled ATRP initiator Cu(I) complex was able to polymerize styrene with a good control over molecular weight. The intra-molecular template-closing of the PS Cu(I) complex *via* ATRC was proven to be an effective method to obtain polymer catenanes based on the UV-Visible spectroscopy, AFM imaging and GPC results. The presented method is promising in extending the synthesis to higher order knotted polymeric structures like trefoil knots through designed templates. This would open doors for the investigation of important physicomechanical properties and possible applications of these knotted structures. Moreover, it is also possible to extend this towards other ring-expansion living polymerization methods as well as block copolymer topologies.

2.4. Experimental Section

2.4.1. Materials

All chemicals were purchased from Aldrich Chemical Company and were used directly without further purification unless otherwise indicated. All solvents were aspirated with nitrogen gas before use.

2.4.2. Instrumentation

^{1}H NMR spectra were recorded on a JEOL ECS 500 spectrometer (500MHz). GPC was carried out on a Viscotek 270 instrument with a triple detector array (RALS, IV, RI, or UV) equipped with 2 GMHHR-M and 1 GMHHR-L mixed bed ViscoGel columns (eluent: THF; flow rate: 1 mL min-1). All atomic force microscopy (AFM) images were recorded in air under ambient conditions on PicoScan 2500 (Agilent Technologies formerly Molecular Imaging, Corp.) equipped with an 8 × 8 μm scanner. Intermittent contact mode was used for all imaging. The AFM tip used was a silicon-nitride AFM probe from Ted Pella Inc. UV-Visible measurements were taken on an Agilent technologies 8453 spectrometer.

2.4.3. Synthesis of 2,9-di(p-anisyl)-1,10-phenanthroline

para-bromoanisole 4.23 mL (34 mmol) was dissolved in 100 mL degassed ether. After cooling the solution to -30 ^{o}C, tert-BuLi 50 mL (1.7 mol/L, 85 mmol) was added by cannula. After stirring this mixture for 1.5 h, it was transferred to the solution of pre-dried 1, 10-phenanthroline (1.76 g, 9.78 mmol) in 20 mL degassed toluene. The reaction mixture then stirred under nitrogen for 40 h. After hydrolysis with water at 0 ^{o}C, the bright yellow toluene layer was decanted and the aqueous layer was extracted three times with dichloromethane. The combined organic layer was rearomatized by the addition of MnO_2 (35 g), with efficient stirring. The yellow color partially disappeared. After MnO_2 was filtered and the solvent removed, the crude product was recrystallized from toluene. Final purification was achieved by silica column chromatography using dichloromethane/methanol (100:1) as eluent to yield 1.6 g (3.9 mmol, 40%) of an

amorphous white solid. ^{1}H NMR ($CDCl_3$): 8.42 (m, 4H, H_o), 8.30 (d, 2H, $H_{4,7}$), 8.11 (d, 2H, $H_{3,8}$),7.78 (s, 2H, $H_{5,6}$), 7.14 (m, 4H, H_m), 3.92 (s, 6H, -OCH_3).

2.4.4. Synthesis of 2,9-di(p-phenol)-1,l0-phenanthroline

Technical grade pyridine (16 mL) was placed in a 100 mL three-necked round-bottomed flask fitted with a thermometer and a magnetic stirrer. With rapid stirring concentrated hydrochloric acid (17.6 mL) was added. The flask was equipped for distillation, and water was distilled from the mixture until its internal temperature rose to 210 ^{o}C. After cooling to 140 ^{o}C, **1** (6.27 g, 16 mmol) was added as a solid and the reaction flask was fitted with a reflux condenser connected to a source of argon. The yellow mixture was stirred and refluxed for three hours (190-220 ^{o}C). The hot reaction mixture was then diluted with 10 mL warm water and slowly poured into 60 mL hot water. The resulting bright yellow suspension was refrigerated overnight. After cooling, the precipitated solid was filtered by suction, and washed with cold water. Crude acidic diphenol was suspended (it dissolves partially) in an ethanol-water mixture (250/8.5 mL) and neutralized with a dilute NaOH solution. After this pH-meter monitored neutralization (end-point: pH = 7.321), the solution was diluted with hot water (300 mL). Neutral diphenol precipitated as beige solid during cooling down. Filtered by suction, the solid was air dried to yield 5.85 g of an ochre solid. Upon further drying (high vacuum in presence of P_2O_5) the latter turned bright red (5.31 g, 92% yield) and could be utilized without further purification. ^{1}H-NMR (d-DMSO): 10.14 (s, 2H, -OH), 8.56 (d, 4H, H_o), 8.55 (d, 2H, $H_{4,7}$), 8.37 (d, 2H, $H_{3,8}$), 7.98 (s, 2H, $H_{5,6}$), 7.14 (d, 4H, H_m).

2.4.5. Synthesis of bromoethyl, 2-bromo priopionic acid ester

In a round bottom flask, 2-bromo propionic acid (1.22 g, 4 mmol), 2-bromoethanol (0.5 g, 4 mmol) and DMAP (146.4 mg, 0.6 mmol) in dry CH_2Cl_2 was mixed together and DCC (2.3 g, 4.4 mmol) was added slowly to reaction mixture. The solution was stirred overnight under argon atmosphere. After that solution was filtered to remove DCU solid and evaporation of solvent yields colorless liquid. The product was further purified by column chromatography using dichloromethane as an eluent to yield colorless liquid (1.5 g, 79% yield). ^{1}H NMR ($CDCl_3$): 4.41 (t, 2H, -CH_2-O(CO)), 4.39 (q, 1H, -CH(Me)Br), 3.49 (t, 2H, -CH_2Br), 1.77 (d, 3H, -CH_3).

2.4.6 Synthesis of ATRP initiator

In a round bottom flask, 2, 9-di(p-phenol)-1, l0-phenanthroline (0.364 g, 1 mmol), bromoethyl, 2-bromo priopionic acid ester (0.138 g, 2 mmol), anhydrous K_2CO_3 (0.264 g, 10 mmol), and 18-crown-6 (74 mg, 0.1 mmol) were mixed together in acetone and stirred overnight at room temperature under argon atmosphere. The solvent was evaporated under vacuum and the residue was extracted by CH_2Cl_2. The organic layer was washed twice with 1M HCl and one time with water. The organic layer was then dried by anhydrous sodium sulfate and the solvent was evaporated to yield a crude product, which was further purified by recrystalization using toluene as solvent to yield a yellow solid (0.5 g, 69% yield)**.** ^{1}H NMR ($CDCl_3$): 8.41 (m, 4H, H_o), 8.25 (d, 2H, $H_{4,\ 7}$), 8.08 (d, 2H, $H_{3,\ 8}$), 7.74 (s, 2H, $H_{5,\ 6}$), 7.10 (m, 4H, H_m), 4.95 (q, 2H, -CH(Me)Br), 4.51 (t, 4H, -CH_2-O(CO)), 3.52 (t, 4H, -PhOCH_2), 1.71 (d, 6H, -CH_3). Anal. calc. for $C_{36}H_{30}N_2O_6Br_2$: C, 56.53; H, 4.19; N, 3.88; Br, 22.12 Found : C, 56.47; H, 4.43; N, 4.04; Br, 20.84.

2.4.7 Synthesis of PS Cu(I) complex

The general polymerization procedure is as follows: styrene (430 mg, 4.1 mmol), HMTETA (12.7 mg, 0.0278 mmol), initiator **1** (10 mg, 0.0138 mmol), $Cu(CH_3CN)_4PF_6$ (3.1 mg, 0.0278 mmol), and Cu(I)Br (3.97 mg, 0.0278mmol) were mixed in 5 mL anisole. After the mixture was degassed by three freeze-evacuate-thaw cycles, the tube was sealed under vacuum and then subjected to polymerization in oil bath at 110 ^oC under nitrogen atmosphere for 5 h. The reaction was terminated by exposing to atmosphere oxygen and the copper residue was removed by passing through neutral alumina. After concentrating the polymer solution, the PS Cu(I) complex (**3**) was precipitated from cold methanol and was characterized by GPC and UV-Visible spectroscopy.

2.4.8. Synthesis of PS Cu(I) catenane

A 500 mL Schlenk flask containing a 100 mL THF solution of Cu(I)Br (574 mg, 4.0 mmol, 40 mM), and nanosized copper (254 mg, 4.0 mmol, 40 mM) was sealed with a rubber septum, evacuated with 4 freeze-pump-thaw cycles, backfilled with N_2, and sealed from the Schlenk line. The flask was then placed in an oil bath and was stirred at 75 ^oC. After allowing the metal solution to reach the temperature of the bath, Me_6TREN (1.07 mL, 4.0 mmol, 40 mM) was introduced *via* a nitrogen flushed syringe. A syringe pump held a 50 mL syringe containing an 18 mL THF solution of PS Cu(I) complex (**3**) (M_n 6,405 Da, 5.5 mg; 1.383 μmol; 76.3 μM solution), which had separately been subjected to three freeze-pump-thaw cycles and backfilled with N_2. The solution of PS Cu(I) complex (**3**) was slowly dripped through a needle piercing the rubber septum into the stirring THF

solution of the metal ligand, over approximately 24 h (approximate rate = 0.75 mL/h, 2 μmol/h). After the contents of the syringe had been added to the reaction mixture, the reaction mixture was stirred for an additional 1 h. The resulting PS Cu(I) catenane (**4**) was passed through an alumina column and precipitated into cold methanol prior to characterization by GPC and AFM analysis.

2.4.9. Synthesis of PS catenanes

KCN (0.1 g. 1.53 mmol) dissolved in water (10 mL) were added to PS Cu(I) catenane (**4**) (3.5 mg, 0.88 μmol) in 40 mL mixture of THF: methanol (3:1) and stirred for 24 h at room temperature. After stirring THF was evaporated to under vacuum and resulting precipitates of polymers were isolated by centrifugation. After purifying by re-dissolving in THF and precipitating out from methanol, the resulting PS catenanes (**5**) was characterized by GPC.

2.5. References

1. (a) Nasongkla, N.; Chen, B.; Macaraeg, N.; Fox, M. E.; Frechet, J. M. J.; Szoka, F. C. J. *J. Am. Chem. Soc.* **2009**, *131*, 3842–3843. (b) Eugene, D. M.; Grayson, S. M. *Macromolecules* **2008**, *41*, 5082–5084. (c) Guan, Z. J. *J. Polym. Sci., Part A: Polym. Chem.* **2003**, *41*, 3680–3692. (d) Guan, Z. *Chem.–Eur. J.* **2002**, *8*, 3086–3092. (e) Harth, E. M.; Hecht, S.; Helms, B.; Maelmstrom, E. E.; Frechet, J. M. J.; Hawker, C. J. *J. Am. Chem. Soc.* **2002**, *124*, 3926–3938. (f) Edgecombe, B. D.; Stein, J. A.; Frechet, J. M. J.; Xu, Z.; Kramer, E. J. *Macromolecules* **1998**, *31*, 1292–1304. (g)

Rose, J. B. in *High Performance Polymers: Their Origin and Development*, R. B. Seymour and G. S. Kirshenbaum, Elsevier, New York, 1986, p. 187.

2. For reviews, see: (a) Matyjaszewski, K.; Xia, J. *Chem. Rev*. **2001**, *101*, 2921–2990. (b) Kamigaito, M.; Ando, T.; Sawamoto, M. *Chem. Rev*. **2001**, *101*, 3689–3746. (c) Schluter, A. D.; Rabe, J. P. *Angew. Chem., Int. Ed*. **2000**, *39*, 864–883.

3. (a) Tezuka, Y.; Fujiyama, K. *J. Am. Chem. Soc*. **2008**, *128*, 6266–6270. (b) Jeong, W.; Hedrick, J. L.; Waymouth, R. M. *J. Am. Chem. Soc*. **2007**, *129*, 8414–8415. (c) Culkin, D. A.; Jeong, W.; Csihony, S.; Gomez, E. D.; Balsara, N. P.; Hedrick, J. L.; Waymouth, R. M. *Angew. Chem., Int. Ed*. **2007**, *46*, 2627–2630. (d) Pyun, J.; Kowalewski, T. Matyjaszewski, K. *Macromol. Rapid Commun*. **2003**, *24*, 1043–1059. (e) Bosman, A. W.; Vestberg, R.; Heumann, A.; Frechet, J. M. J.; Hawker, C. J.; *J. Am. Chem. Soc*. **2003**, *125*, 715–728. (f) Shu, L.; Schluter, A. D.; Ecker, C.; Severin, N.; Rabe, J. P. *Angew. Chem., Int. Ed*. **2001**, *40*, 4666–4669.

4. Amabilino, D. B.; Stoddart, J. F. *Chem. Rev*. **1995**, *95*, 2725–2828.

5. Sauvage, J. P. *Acc. Chem. Res*. **1990**, *23*, 319–327.

6. Vogtle, F.; Dunwald, F.; Schmidt, T. *Acc. Chem. Res*. **1996**, *29*, 451–460.

7. Dietrich-Bucheker, C. O.; Sauvage, J. -P. *Chem. Rev*. **1987**, *87*, 795–810.

8. (a) Graessley, W. W.; *Adv. Polym. Sci*. **1974**, *16*, 1–3. (b) Graessley, W. W. *Adv. Polym. Sci*. **1982**, *47*, 68.

9. Wu, S. *Polymer Interface and adhesion*, Marcel Dekker, New York, 1982.

10. (a) Plummer, C. J. G.; Mauroux-Cudre, N.; Kaush, H. H. *Polym. Eng. Sci*. **1994**, *34*, 318. (b) Ottani , S.; Porter, R. S. *Macromol. Rapid Commun*. **1995**, *16*, 813.

11. Brown, H. R.; Russell, T. R. *Macromolecules*, **1996**, *29*, 798.

12. Zhang, Y.; Wiesner, U. *J. Chem. Phys*. **1995**, *103*, 4784.

13. Grassley, W. W. *Viscoelasticity and Flow in Polymer Melts and Concentrated Solutions*, Physical Properties of Polymers, Symposium Series no 84, American Chemical Society, Washington DC, 1984, pp. 97–153.

14. Schill, G. *Catenanes, Rotaxanes and Knots*, Academic Press, 1971.

15. Wasserman, E. *J. Am. Chem. Soc*. **1960**, *82*, 4433.

16. Busch, D. H.; Stephenson, N. A.; *Chem. Rev*. **1990**, *100*, 119–154.

17. Walba, D. M. *Tetrahedron* **1985**, *41*, 3161.

18. Sauvage, J. -P. *Chem.–Eur. J*. **2005**, *11*, 4374–4386.

19. Sarbu, T.; Lin, K. Y.; Spanswick, J.; Gil, R. R.; Siegwart, D. J.; Matyjaszewski, K. *Macromolecules*, **2004**, *37*, 9694–9700.

20. Rique-Lurbet, L.; Schappacher, M.; Deffieux, A.; *Macromolecules* **1994**, 27, 6318.

21. Kricheldorf, H. R.; Bohme, S.; Schwarz, G.; Kruger, R. P.; Schulz, G. *Macromolecules* **2001**, *34*, 8886.

22. Smith, A. P.; Fraser, C. L. *Macromolecules* **2002**, *35*, 594–596.

23. Yang, P.; Yang, X.; Wu, B. *Eur. J. Inorg. Chem*. **2009**, 2951–2958.

24. Laurent, B. A.; Grayson, S. M. *J. Am. Chem. Soc*. **2006**, *128*, 4238–4239.

25. Adachi, K.; Honda, S.; Hayashi, S.; Tezuka, Y. *Macromolecules* **2008**, *41*, 7898–7903.

26. Voter, A. F.; Tillman, E. S. *Macromolecules*, **2010**, *43*, 10304–10310.

27. Alberty, K. A.; Hogen-Esch, T. E. Carlotti, S. *Macromol. Chem. Phys*. **2005**, *206*, 1035–1042.

Chapter 3: Synthesis of Block Copolymer Catenanes *via* Supramolecularly Templated ATRP Initiator Approach

3.1. Introduction

The synthesis of topologically interesting molecules such as catenanes, rotaxanes, and trefoil knots has attracted considerable attention in recent years.[1] The synthesis and study of such compounds show interesting relationship about molecular architecture and intra-molecular interactions, which occasionally lead to new materials with unusual properties.[2] The synthesis of low-molecular-weight (M_w < 2000 Da) catenanes has been studied intensively over the past few years. However, demonstrating this type of orderly entangled topology in large molecules such as polymers is still a challenge due to synthetic obstacles. The topologically self-constrained structures of catenated polymers are of high interest for the study of chain entanglement phenomenon in polymer physics.[3] Several strategies have been reported to demonstrate successful formation of polymer catenanes such as: (a) statistical threading, in which one of the macrocycles is used in large concentrations and threading of the linear precursor is predominantly entropy driven,[4-5] and (b) template-directed threading, which involves an enthalpic driving force such as transition metal coordination,[6] hydrogen bonding,[7] etc.

Block copolymers with incompatible components can form nanophase-separated structures in concentrated solutions or in bulk due to the direct constraint of covalent bonds.[8] Catenated block copolymers should show unique phase separation behavior compared with its cyclic or linear analogue due to lack of chemical or physical bond between two interlocked polymer rings.[5] Several attempts have been made to synthesize

catenated block copolymers. Hogen-Esch and co-workers have reported the synthesis of a catenated polystyrene–*b*–poly(2-vinylpyridine) copolymer using statistical threading approach.[4] Similarly Takano and co-workers[5] have demonstrated the synthesis of catenated polystyrene–*b*–polyisoprene copolymers with comparatively high molecular weight and studied their phase separation behavior. However, these methods require several steps for purification and give comparatively low yield. Recently, we have reported the synthesis of catenated polystyrene *via* supramolecularly templated atom transfer radical polymerization (ATRP) initiator.[6] In addition; it was of our interest to demonstrate the feasibility of this approach to make various types of block copolymer catenanes. Herein, we demonstrate the concept with synthesis of polystyrene–*b*–polymethylmethacrylate (PS–b–PMMA) catenanes **(Scheme 3.1)**.

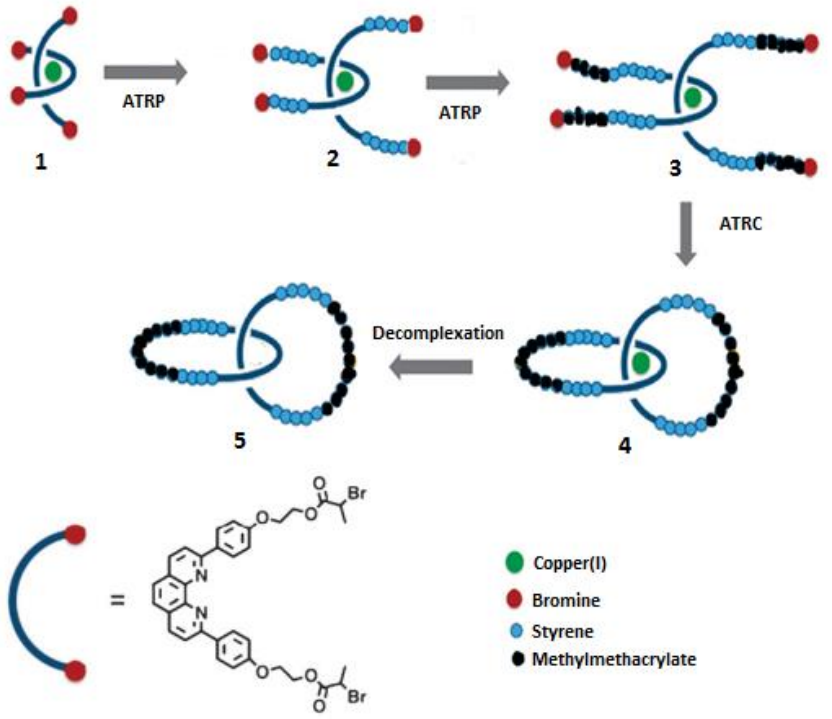

Scheme 3.1. Schematic route for the preparation of block copolymer catenanes from the supramolecularly templated ATRP initiator.

3.2. Results and Discussion

3.2.1. Polymerization of styrene using ATRP initiator Cu(I) complex

Using the previously reported ATRP initiator Cu(I) complex (**1**),[6] styrene was polymerized in the presence of Cu(I)Br/hexamethyltriethylenetetraamine (HMTETA) as catalyst, in anisole at 110 °C for 5h. The GPC traces of the resulting PS Cu(I) complex (**2**) **(Figure 3.1a)** shows narrow polydispersity with good control over molecular weight (M_n 2781 Da, PDI 1.16). ^{1}H NMR of PS complex **(Figure 3.2a)** showed the signals attributed to aromatic protons of styrene at 7.2–6.8 ppm and methylene and methine

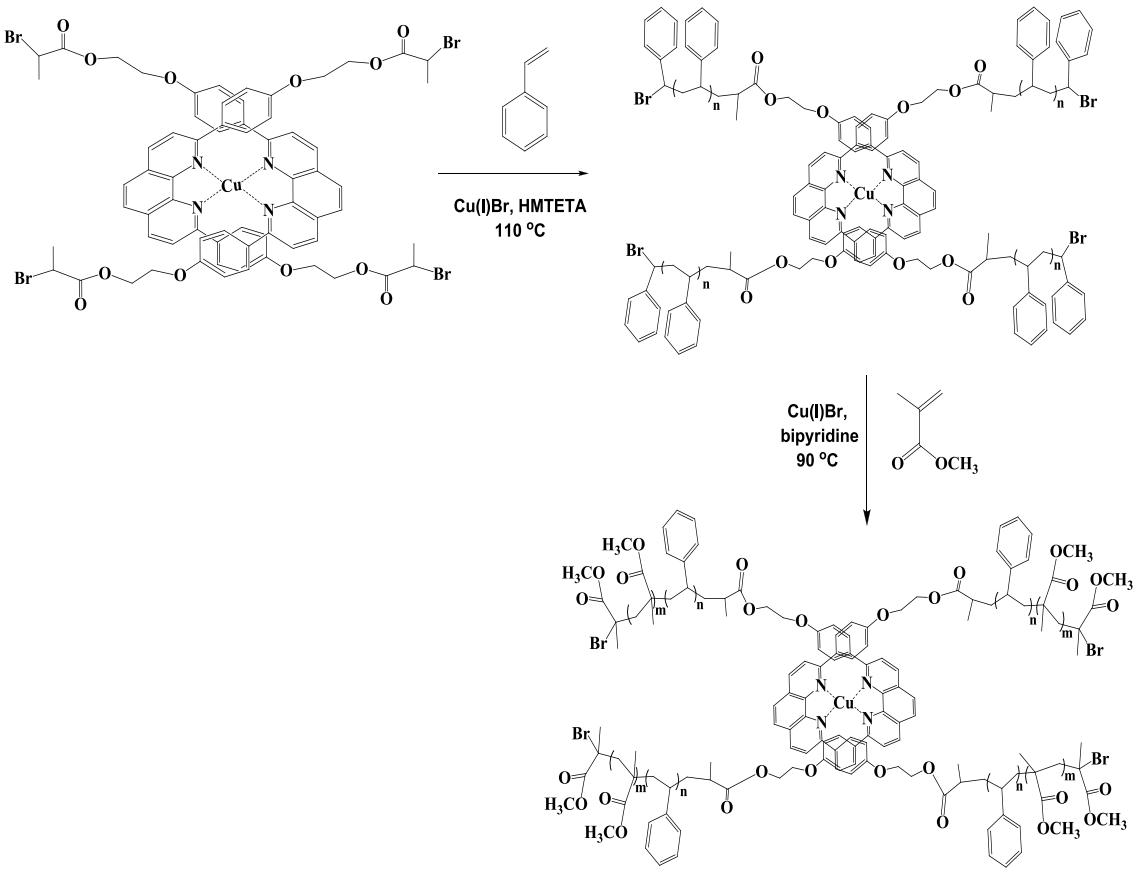

Scheme 3.2. Synthesis of PS-b-PMMA Cu(I) complex (**3**) using PS Cu(I) complex (**2**) macroinitiator.

protons in the main chain at 2.2–1.7 and 1.7–1.2 ppm, respectively. The integrity of the ligand copper (I) complex within the backbone of the polymer was confirmed by UV–Visible spectral analysis in our previous work, which showed the ligand centered bands (260 and 336 nm) and the MLCT and LMCT transition peaks (438 and 580 nm, respectively).[6]

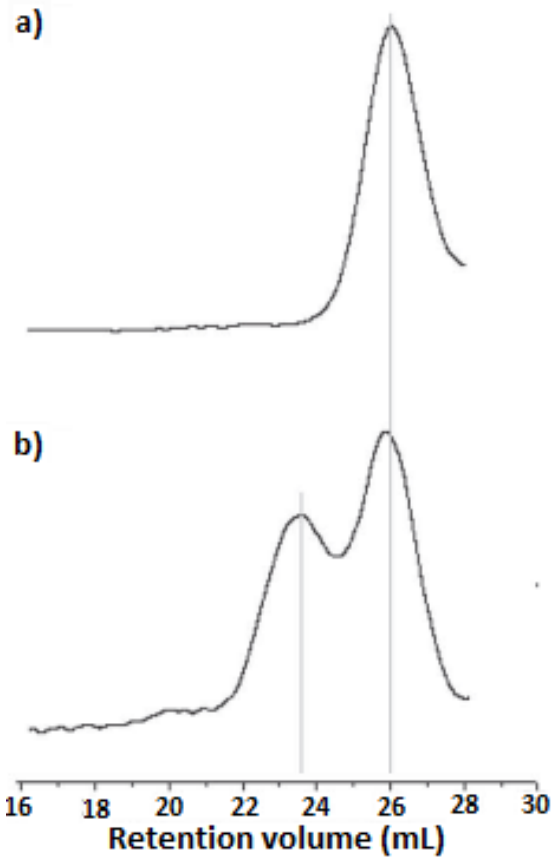

Figure 3.1. a) GPC traces of (a) PS Cu(I) complex (**2**), b) PS-b-PMMA Cu(I) complex (**3**).

3.2.2. Chain extension of PS Cu(I) complex *via* ATRP of methyl methacrylate

ATRP of methyl methacrylate (MMA) was carried out using the PS Cu(I) complex (**2**) as a macroinitiator and bipyridine/Cu(I)Br as catalyst to produce a PS-b-PMMA Cu(I) complex (**3**). GPC traces **(Figure 3.2b)** of block copolymers (**3**) show an increase of M_n 4694 Da, PDI 1.7 resulting from chain extension by MMA polymerization. ^{1}H NMR spectrum of the resulting block copolymer (**3**) in $CDCl_3$ **(Figure 3.2b)** shows peaks from the pendant methyl protons at 3.6 ppm, methylene and methyl protons in the main chain at 1.8–1.7 and 0.9–0.8 ppm, respectively, and benzene ring protons of a PS block at 7.2–6.8 ppm confirming the formation of a PS-b-PMMA Cu(I) complex (**3**).

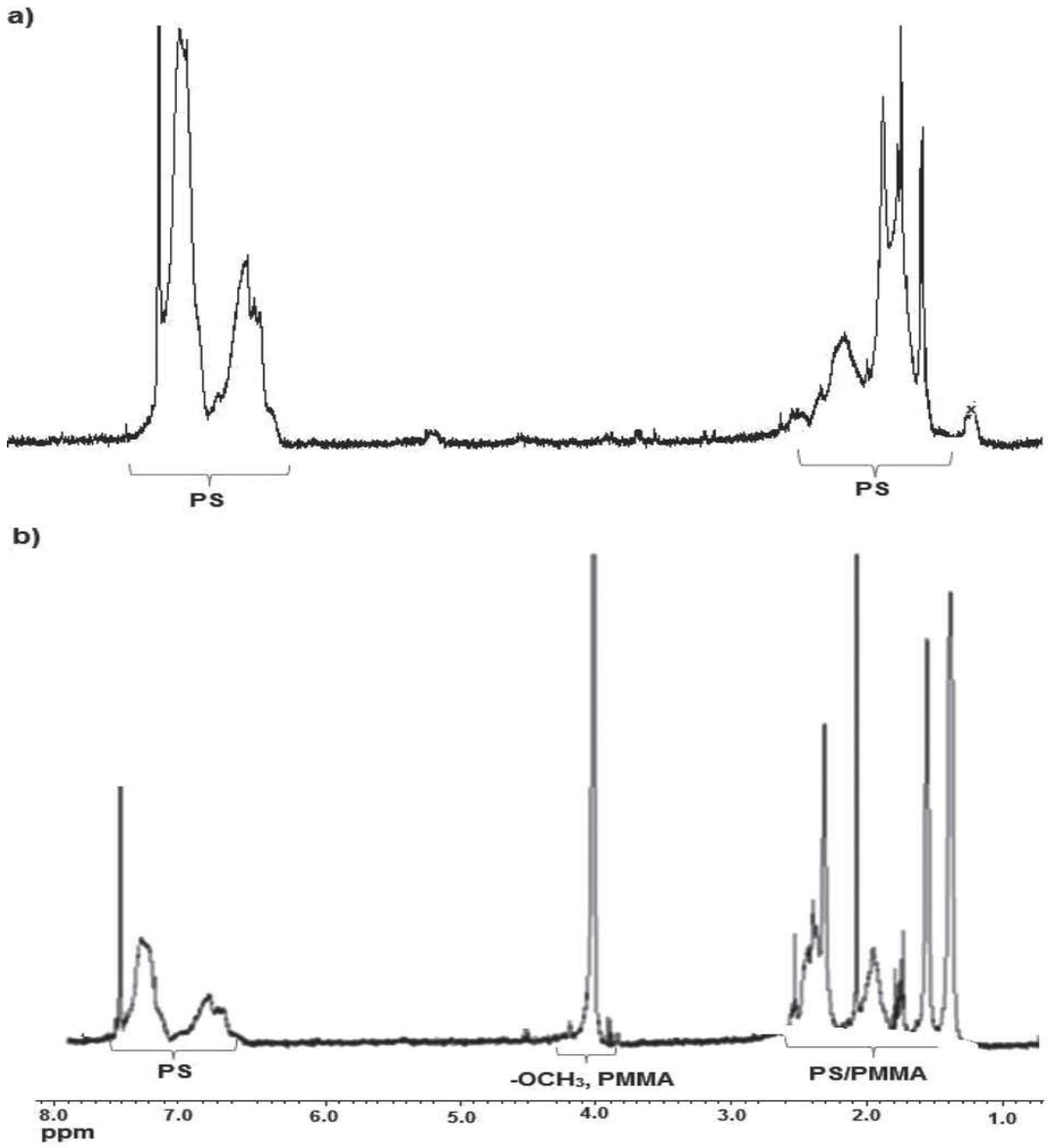

Figure 3.2 ^{1}H NMR of a) PS Cu(I) complex (**2**), b) PS-b-PMMA Cu (I) complex (**3**) in $CDCl_3$.

In the bimodal curve of the GPC, the position of the higher elution time peak is at the same position as the peak of the homopolymer starting material. This suggests the presence of unreacted PS homopolymer with the PS- b-PMMA copolymer, causing an increase in the polydispersity. Similar difficulties were reported by the Matyjaszewski and co-workers attempting to synthesize block copolymers of PMMA from a chloride

end-capped polyacrylate macroinitiator *via* ATRP techniques.[10] They found that the higher propagation rate of MMA and the ineffectiveness of secondary halides of polyacrylate to initiate methyl methacrylate result in slow or incomplete initiation of the PMMA. In the PS Cu(I) complex (**2**) macroinitiator, the bromide-capped styrene used to prepare the PS-b-PMMA Cu(I) complex (**3**) is a secondary halide, and therefore initiation of MMA may be slow compared with propagation, resulting in residual unreacted homopolymer (**2**). Matyjaszewski has utilized a halide exchange system to overcome this obstacle, where Cu(I)Cl was used as the catalyst to improve the initiation efficiency of secondry Br-terminated macroinitiator.[11] The use of a halide exchange system in the preparation of block copolymer catenanes with improved polydispersity is underway.

3.2.3. Template-closing of PS-b-PMMA Cu(I) complex *via* styrene assisted ATRC

High yield macrocyclic PS has been reported *via* intramolecular ATRC of dibrominated PS (Br-PS-Br) at high temperature.[12] On the other hand, ATRC of the PMMA precursor could be performed at low temperature due to the lower activation energy. Nevertheless, disproportionation reaction of PMMA radical rather than coupling limits the use of this strategy.[13] Yokozawa and co-workers have demonstrated the use of styrene during ATRC of PMMA precursors giving better coupling efficiency.[9] Their result shows that the generated PMMA radicals can rapidly cross-propagate to styrene and the resulting styryl radicals undergo coupling of the polymer chain at low temperature, rather than chain extension. Following this, we have performed intra-molecular ATRC of PS-b-PMMA Cu(I) complex (**3**) by dropwise addition of a toluene solution of copolymer (**3**) precursor/styrene at a very slow rate (0.75 mL h^{-1}) into a

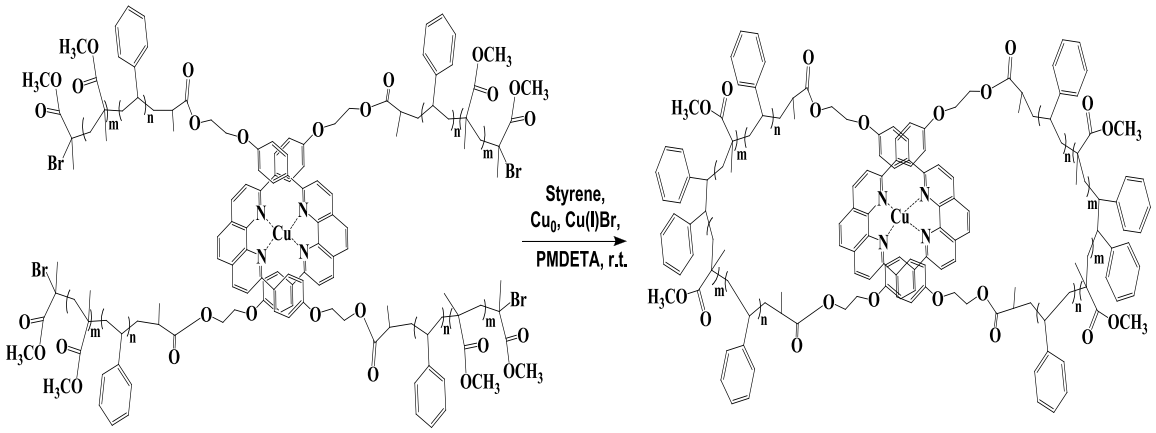

Scheme 3.3. Styrene assisted low temperature ATRC of PS-b-PMMA Cu(I) complex (**3**).

toluene solution of Cu(I)Br, PMDETA, and Cu(0) heated to 25 °C. GPC analysis of the resulting PS-b-PMMA Cu(I) catenane (**3**) **(Figure 3.3a)** showed a slight increase in M_n 4861 Da, PDI 1.8 because of the styrene insertion and no significant shift to higher molecular weight was observed, which suggest that intra-molecular coupling was favorable than inter-molecular coupling. As observed, the shift in the hydrodynamic radius (R_v) of resulting Cu(I) catenane (**4**) is not significant as compared with GPC traces of its linear counterparts (**3**)**,** which could be explained by the fact that the open PS-b-PMMA Cu (I)complex (**3**) is not completely linear and is much closer to a semicyclic structure due to the geometric constraints coming from the complexed phenanthroline ligand in between.

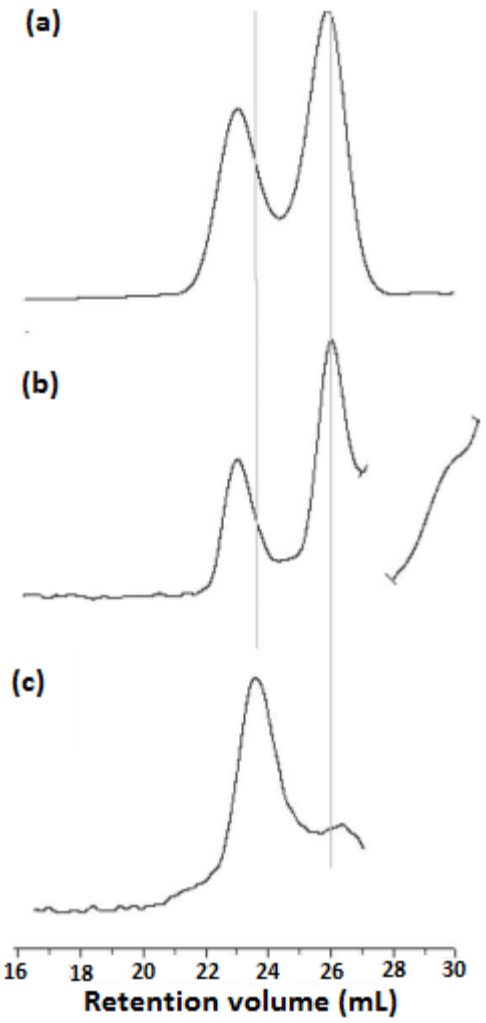

Figure 3.3. GPC traces of a) PS-b-PMMA Cu(I) catenane (**4**), b) PS-b-PMMA catenanes (**5**), and c) Purified PS-b-PMMA catenanes (**5**).

3.2.4. Demetallation reaction of PS-b-PMMA Cu(I) catenane

In order to obtain metal-free block copolymers catenanes, Cu(I) from the template was removed by stirring the PS-b-PMMA Cu(I) catenane (**4**) with saturated solution of KCN in THF:methanol (3:1). The GPC traces of the demetallation step product **(Figure 3.3b)** show that the molecular weight of the resulting PS-b-PMMA catenanes (**5**) (M_n 5876 Da) barely changed even after removing the copper, indicating an interlocked

structure of block copolymers catenanes (**5**). It is also worth to note that the right choice of using a phenanthroline Cu(I) complex as a template over other types of metal templates[14,15] and the control of the polymer arm length of the precursor (**3**) favor the formation of the catenated structure over the topologically trivial figure-of-eight isomer. Moreover, the isomeric structures of catenanes and figure-of-eight[14] can be distinguished by monitoring the change in hydrodynamic volume after demetallation reaction. As per our knowledge, the figure-of-eight isomer would generate a large single ring upon demetallation and so its resulting hydrodyamic volume would be larger than the interlocked cyclic structure of catenanes. However, the GPC traces of block copolymer catenanes (**5**) **(Figure 3.3b)** show a similar hydrodynamic volume compared with the PS-b-PMMA Cu(I) catenane (**4**), which further confirms the formation of a catenated structure rather than a figure-of-eight isomer by ATRC. In addition to this, the GPC traces of the PS-b-PMMA catenane (**5**) also show the low molecular peaks at a retention volume of 28.9 and 29.5 mL, which can be attributed to the acyclic and/or cyclic block copolymers and homopolymer generated upon demetallation of uncyclized or partially cyclized polymer complex (**3**) by ATRC. The large difference in molecular weight of the block copolymer catenanes and homopolymer catenanes enabled us to isolate the block copolymer (**5**) by dialysis in THF. The GPC traces of purified block copolymer catenanes **(Figure 3.3c)** show an almost complete removal of the homopolymer imputiry from the mixture.

3.2.5. AFM imaging of PS-b-PMMA catenanes

We have also tried to visualize the PS-b-PMMA catenanes (**5**) directly by AFM. A very dilute solution of the polymer (10^{-8} M) in chloroform was spin casted onto freshly cleaved mica. The topography image by AFM **(Figure 3.4)** clearly shows interlocked cyclic structures of block copolymers catenanes. The different in shape of copolymer catenanes compare to homopolymer catenanes could be result of exhibiting different orientations, degree of overlap, or phase incompatibility on the surface. Line profile analysis of the structure revealed the profile thickness, which confirms the presence of the cavities inside the catenated structures. Further studies on the phase separation and thermal properties are underway.

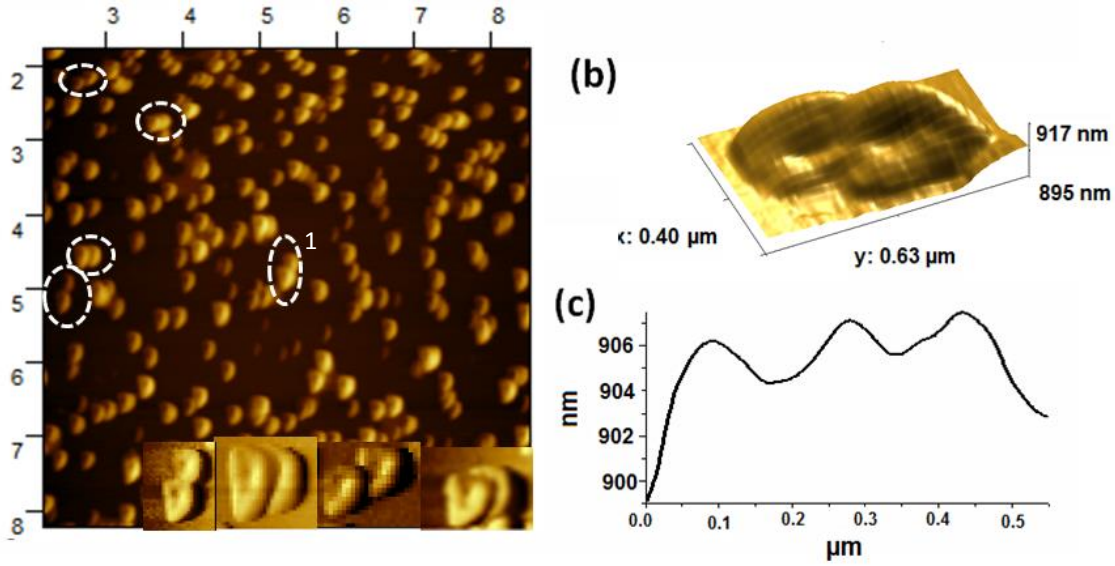

Figure 3.5. a) AFM image PS-b-PMMA catenanes (**5**) on mica (inset: magnified image of highlighted structures), (b) 3-D image of catenane 1, and (c) line profile of catenane 1.

3.3. Conclusions

A novel route to prepare block copolymer catenanes demonstrated *via* a supramolecularly templated ATRP initiator approach. The styrene assisted low temperature ATRC was able to couple the halide terminated PMMA block. Formation of the interlocked block copolymer catenanes was confirmed by GPC, ^{1}H NMR spectroscopy, and AFM analysis. Since ATRP is applicable for the production of various types of block copolymers, this method can be applied for the preparation of other complex block copolymers with the combination of not only different block segments but also higher ordered interlocked cyclic topologies. These activities are currently in progress in our laboratory.

3.4. Experimental Section

3.4.1. Materials

All chemicals were purchased from Aldrich Chemical Company and were used directly without further purification unless otherwise indicated. All solvents were aspirated with nitrogen gas before use.

3.4.2. Instrumentation

^{1}H NMR spectra were recorded on a JEOL ECS 500 spectrometer (500 MHz). Gel permeation chromatography (GPC) was carried out on a Viscotek 270 instrument with a triple detector array (RALS, IV, RI, or UV) equipped with 2 GMHHR-M and 1

GMHHR-L mixed bed ViscoGel columns (eluent: THF; flow rate: 1 mL min^{-1}). All atomic force microscopy (AFM) images were recorded in air under ambient conditions on PicoScan 2500 (Agilent Technologies formerly Molecular Imaging, Corp.) equipped with an 8 × 8 μ m scanner. Intermittent contact mode was used for all imaging. The AFM tip used was a silicon nitride AFM probe from Ted Pella Inc.

3.4.3. Synthesis of ATRP initiator Cu(I) complex

Using the double-ended needle transfer technique, 3 mg (8.06 μmol) of $Cu(CH_3CN)_4PF_6$ in 3 mL degassed acetonitrile was transferred under nitrogen at room temperature to a stirred degassed solution of ATRP initiators coupled to phenanthroline ligand[6] (10 mg, 7.14 μ mol) in 3 mL DCM. The mixture turned dark red instantaneously, indicating the formation of ATRP initiator Cu(I) complex (**1**). After stirring the solution for 1 h under nitrogen at room temperature, the solvents were evaporated to dryness to obtain dark red solids of **1** in quantitative yield (12 mg). Complex (**1**) was used without further purification.

3.4.4. Synthesis of PS Cu(I) complex

Styrene (318 mg, 3.05 mmol), HMTETA (7 mg, 0.003 mmol), initiator (**1**) (12 mg, 750 μmol)**,** and Cu(I)Br (4.4 mg, 0.003 mmol) were mixed in 5 mL anisole. After the mixture was degassed by three freeze-evacuate-thaw cycles, the tube was sealed under vacuum and then subjected to polymerization at 110 °C under nitrogen atmosphere for 5 h. The reaction was terminated by exposing to atmosphere and the copper residue was

removed by passing through neutral alumina. After concentrating the polymer solution, it was precipitated from cold methanol and characterized by GPC and ^{1}H NMR.

3.4.5 Synthesis of PS-b-PMMA Cu(I) complex

Methylmethacrylate (MMA) (66.6 mg, 0.66 mmol), bipyridine (1 mg, 6.41 μmol), PS Cu(I) complex macroinitiator (5 mg, 1.79 μ mol)**,** and Cu(I)Br (0.5 mg, 0.0012 mmol) were mixed in 2 mL DMF. After the mixture was degassed by three freeze-evacuate-thaw cycles, the tube was sealed under vacuum and then subjected to polymerization at 90 °C under nitrogen atmosphere for 5 h. The reaction was terminated by exposing to atmosphere and the copper residue was removed by passing through neutral alumina. After concentrating the copolymer solution, it was precipitated from cold methanol and was characterized by GPC and ^{1}H NMR.

3.4.6. Synthesis of PS-b-PMMA Cu(I) catenane

ATRC was performed as per literature procedure:[9] The reagents were used in following ratio, Styrene/PS-b-PMMA Cu(I) complex (**3**)/Cu(I)Br/Cu(0) /PMDETA = 40/1/1/4/2.5. A 50 mL Schlenk flask containing a 10 mL toluene solution of Cu(I)Br (0.22 mg, 1.53 μmol) and copper (0.4 mg, 6.15 μmol) was sealed with a rubber septum, evacuated with four freeze-pump-thaw cycles, backfilled with N_2 , and sealed from the Schlenk line. The flask was then placed in an oil bath and stirred at 25 °C. After allowing the metal solution to reach the temperature of the bath, PMDETA (0.55 mg, 3.82 μmol) was introduced *via* a nitrogen flushed syringe. A syringe pump held a 10 mL syringe containing mixture of copolymer **3** (8 mg, M_n 4694 Da) and styrene (0.16 mg, 0.061

mmol) in 8 mL toluene, which had separately been subjected to three freeze-pump-thaw cycles and backfilled with N_2 . A solution mixture of copolymer **3** and styrene was slowly dripped through a needle piercing the rubber septum into the stirring toluene solution of the metal ligand, over approximately 10 h (approximate rate 0.75 mL h^{-1}). After the contents of the syringe had been added to the reaction mixture, the reaction mixture was stirred for an additional 1 h. The resulting polymer was passed through an alumina column and precipitated into cold methanol prior to characterization by GPC and ^{1}H NMR.

3.4.7. Synthesis of PS-b-PMMA catenanes

Demetallation of PS-b-PMMA Cu(I) catenane (**4**) was performed as per the following procedure: KCN (100 mg, 1.53 mmol) dissolved in water (2 mL) was added to copolymer (**4**) (3.5 mg, 0.72 μ mol) in 6 mL mixture of THF: methanol (3:1) and stirred for 24 h at room temperature. After stirring, solvent was evaporated to under vacuum and resulting polymers were extracted by DCM: water mixture twice. The DCM layer was collected, dried over sodium sulfate, and evaporated under vacuum yields PS-b-PMMA catenane (**5**) and characterized by GPC.

3.5. References

1. (a) Dietrich-Buchecker, C. O.; Sauvage, J.-P. *Angew. Chem., Int. Ed.Engl.* **1989**, *28*, 189. (b) Harrison, J. T.; Harrison, S. *J. Am. Chem. Soc.* **1967**, *89*, 5723. (c) Schill, G. *Catenanes, Rotaxanes and Knots,* Academic Press , New York **1971**.

2. (a) Li, Q. Y.; Vogel, E.; Parham, A. H.; Nieger, M.; Bolte, M.; Frohlich, R.; Saarenketo, P.; Rissanen, K.; Vogtle, F. *Eur. J. Org. Chem.* **2001**, *21*, 4041. (b) Reuter, C.; Schmieder, R.; Vogtle, F. *Pure Appl. Chem.* **2000**, *72*, 2233. (c) Takata, K. T. J. *Synth.Org. Chem. Jpn.* **2001**, *59*, 206. (d) Zhao, X.; Jiang, X. K.; Shi, M.; Yu, Y. H.; Xia, W.; Li, Z. T. *J. Org. Chem.* **2001**, *66*, 7035.

3. (a) Graessley, W. W. *Adv. Polym. Sci.,* **1974**, *16*, 1. (b) W. W. Graessley, *Adv. Polym. Sci.*, **1982**, *47*, 68.

4. Gan, Y.; Dong, D.; Hogen-Esch, T. E. *Macromolecules* **2002**, *35*, 6799.

5. Ohta, Y.; Kushida, Y.; Kawaguchi, D.; Matsushita, Y.; Takano, A. *Macromolecules* **2008**, *41*, 3957.

6. Bunha, A.; Tria, C.; Advincula, R. *Chem. Commun.* **2011**, *47*, 9173.

7. Ishikawa, K.; Yamamoto, T.; Asakawa, M.; Tezuka, Y. *Macromolecules* **2010**, *43*, 168.

8. (a) Hashimoto, T.; Shibayama, M.; Kawai, H. *Macromolecules* **1980**, *13*, 1237. (b) Matsushita, Y. J. *J. Polym. Sci., Part B: Polym. Phys.* **2000**, *38*, 1645.

9. Huang, C.; Ohta, Y.; Yokoyama, A.; Yokozawa, T. *Macromolecules* **2011**, *44*, 4140.

10. Shipp, D. A.; Wang, J.; Matyjaszewski, K. *Macromolecules* **1998**, *31*, 8005.

11. Matyjaszewski, K.; Wang, J.-L.; Grimaud, T.; Shipp, D. A. *Macromolecules* **1998**, *31*, 1527.

12. Voter, A.; Tillman, E. *Macromolecules* **2010**, *43*, 10304.

13. Jiang, Z.; Vamvakaki, M.; Narain, R. *Macromolecules* **2010**, *43*, 3228.

14. Belfrekh, N.; Dietrich-Buchecker, C.O.; Sauvage, J.-P. *Inorg. Chem.* **2000**, *39*, 5169.

15. Beves, J. E.; Blight, B. A.; Campbell, C. J.; Leigh, D. A.; McBurney, R. T. *Angew. Chem. Int. Ed.* **2011**, *50*, 9260.

Chapter 4: Synthesis of Polymer Catenanes *via* Combination of "Grafting to" Approach by Click Method and Atom Transfer Radical Coupling

4.1. Introduction

Over the past few decades, synthesis of novel polymer structures has become an interesting topic of research due to their potential in providing a wider range of properties. The chemical composition of the polymer chains as well as the architectural aspects, such as chain conformations and chain interactions plays an important role on the fundamental properties of polymers.[1] One of the interesting architectural features which can be introduced to a polymer is by mechanically interlocking the cyclic polymer chains, known as polymer catenanes.[2] Despite the broad exploration of the synthesis of small molecule catenanes over the past decades, polymer catenanes with relatively high molecular weight are still the most challenging targets in synthetic polymer chemistry.

The commonly used synthetic method for polymer catenanes include threading and a subsequent cyclization step; where a linear polymer threads into a cyclic polymer ring which after cyclization of the resulting pseudorotaxane, gives polymer catenanes.[3] However, the thermodynamically unfavorable statistical threading and difficulties associated with purification results in very poor yield of polymer catenanes. Recently, our group has demonstrated the synthesis of homopolymer and blockcopolymer catenanes *via* controlled radical polymerization from supramolecularly templated ATRP initiators followed by template-closing *via* Atom Transfer Radical Coupling (ATRC).[4] This approach not only allows one to improve the yield of polymer catenanes, but also opens

the door for synthesis of a wide variety of structurally different homopolymer and blockcopolymer catenanes.

In our effort to demonstrate other possible efficient method for synthesis of polymer catenanes, we have considered the use of the copper(I)-catalyzed alkyne-azide cycloaddition (CuAAC) reaction also known as "click" reaction. The click chemistry has been broadly taken up by synthetic chemists and has found extensive use in the design and synthesis of new polymeric materials.[5] In particular, the CuAAC click reaction has been proven as a promising tool for the synthesis of mechanically interlocked molecules because it can be performed at room temperature in a variety of solvents, allowing the optimization of noncovalent bonding interactions in the precursors.[6] In this work, we have demonstrated another versatile approach for the synthesis of polymer catenanes by; 1) grafting alkyne-functionalized linear polymer to azide-functionalized supramolecularly template *via* CuAAC click method, and 2) template-closing of a four-armed type polymer *via* intra-molecular coupling ATRC as shown in **Scheme 4.1**.

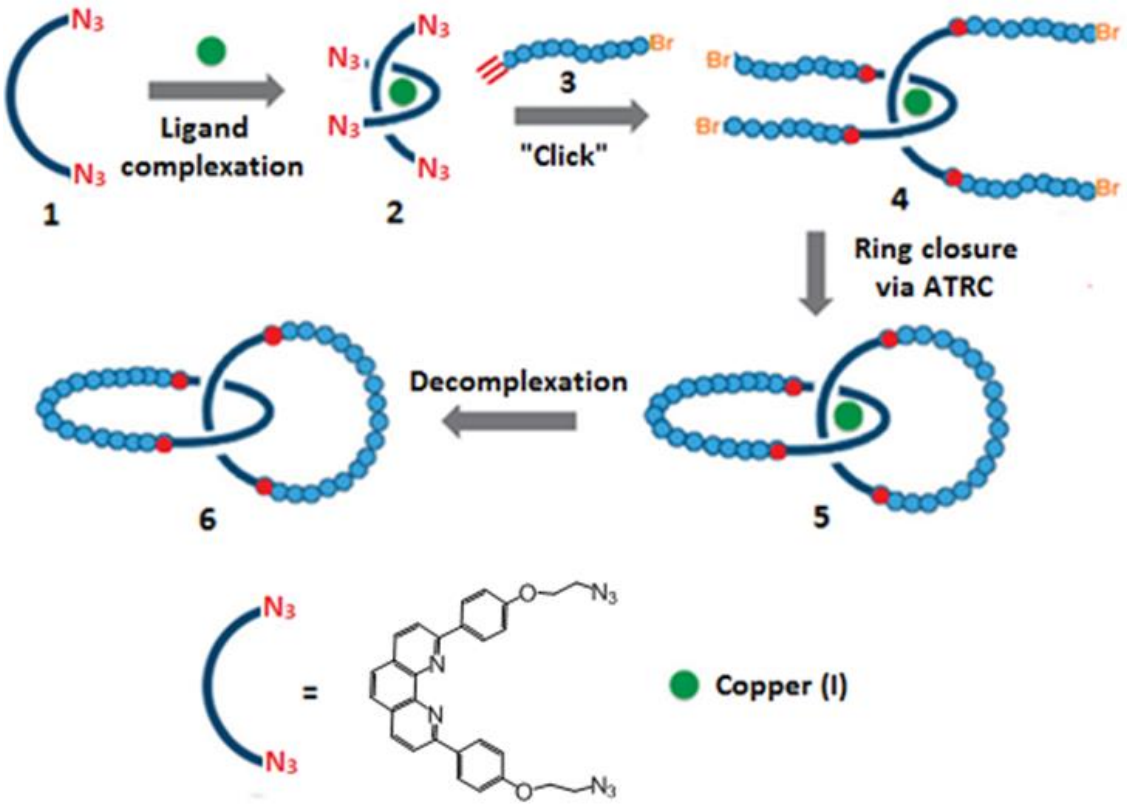

Scheme 4.1. Schematic route for the preparation of polymer catenanes *via* "grafting to" approach.

4.2. Results and Discussion

4.2.1. Design and synthesis of azide-functionalized ligand Cu(I) complex

The classic Sauvage group strategy of forming tetrahedral complex using two phenanthroline ligands and Cu(I) metal ion has been utilized in the synthesis of many types of mechanically interlocked molecules. In addition, the CuAAC click reaction has been proven to be a very effective method for constructing various catenanes in good yield using a Cu(I)-phenanthroline complex core.[11] Considering this, the azide functionalized phenanthroline ligand (ligand-N_3 (**1**)) was afforded in good yield by reaction of 2,9-bis(4-(hydroxy)phenyl))-1,10-phenanthroline with 2-azidoethyl 4-

methylbenzenesulfonate in basic condition. The supramolecular assembly of ligand-N_3 (**1**) in the presence of $Cu(I)(CH_3CN)_4PF_6$ yields a dark red solid of ligand-N_3 Cu(I) complex (**2**).

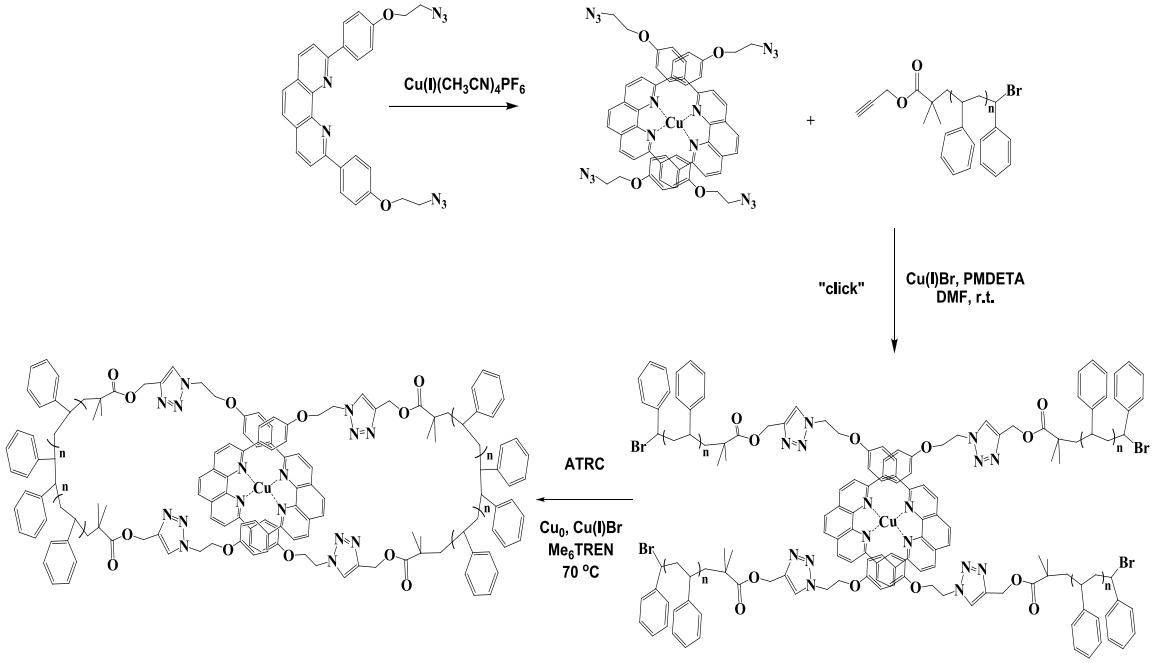

Scheme 4.2. Synthesis route for PS catenane *via* "grafting to" click reaction and ATRC.

The UV-Visible analysis of ligand-N_3 Cu(I)complex (**2**) **(Figure 4.1)** shows intense ligand-centered transition at 283 nm and 321 nm and weaker absorption peak at 437 nm corresponding to metal-to-ligand charge transfer (MLCT), which was found to be consistent with reported literature value.[12]

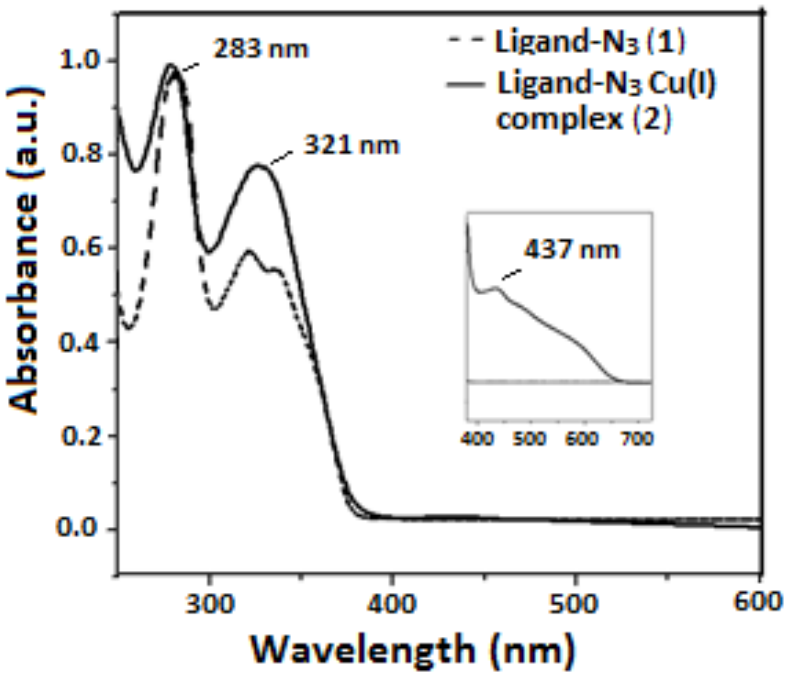

Figure 4.1. UV-Visible spectra of Ligand-N_3 (**1**) and Ligand-N_3 Cu(I) complex (**2**) (inset: visible region of the Ligand-N_3 Cu(I) complex (**2**) spectrum).

4.2.2. Synthesis of alkyne-functionalized PS *via* ATRP

The alkyne functionalized linear polystyrene (alkyne-PS (**3**)) was prepared as a precursor for "grafting to" CuAAC click reaction with ligand-N_3 Cu(I)complex (**2**). The bulk polymerization of styrene using propargyl 2-bromoisobutyrate as initiator and Cu(I)Br/PMDETA as catalyst yield alkyne-functionalized PS (**3**). Further confirmation of end-group functionality in polymer was accomplished by ^{1}H NMR spectroscopy **(Figure 4.2)**. GPC data shows **(Figure 4.3a)** good control over molecular weight with low polydispersity (M_n 3,373 Da, PDI: 1.05).

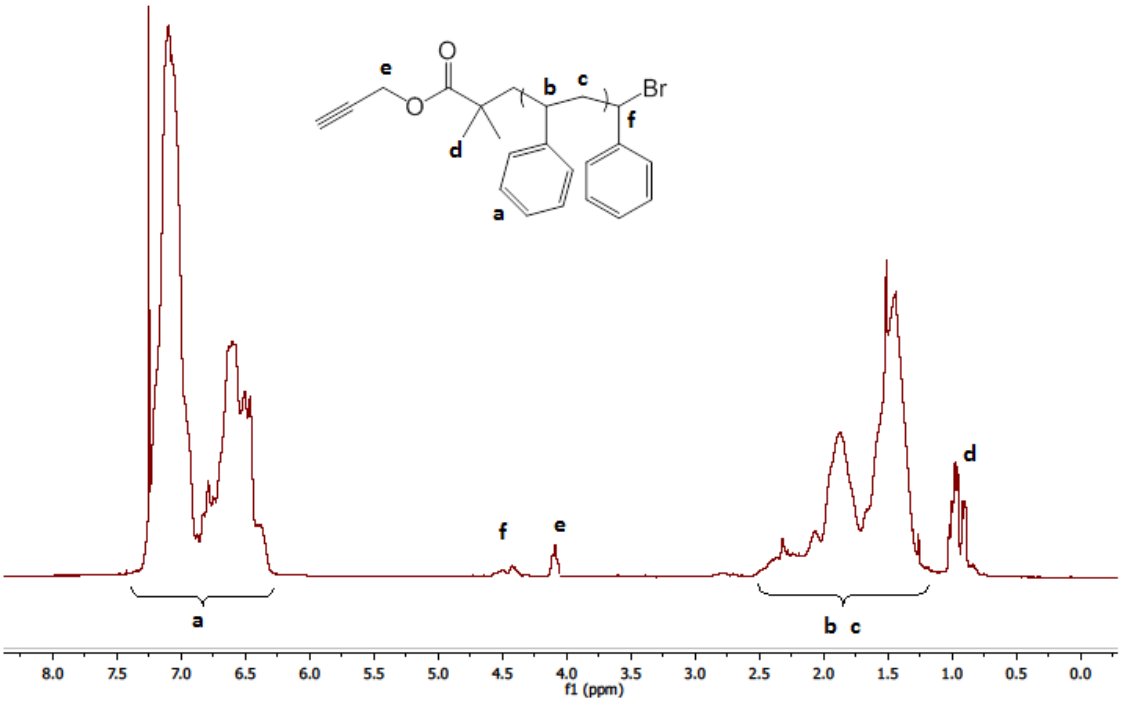

Figure 4.2. ^{1}H NMR of alkyne-functionalized PS (**3**).

4.2.3. Synthesis of PS Cu(I) complex *via* "grafting to" click reaction

The CuAAC click reaction between alkyne-PS (**3**) and the ligand-N_3 Cu(I) complex (**2**) in DMF using CuBr/PMDETA as catalyst produced PS Cu(I) complex (**4**). The alkyne-PS (**3**) was used in excess to ensure complete conversion of the ligand-N_3 complex (**2**) to PS Cu(I) complex (**4**)**.** An efficient click reaction was evidenced by GPC analysis **(Figure 4.3b)** which shows a clear shifting of peak corresponding to PS Cu(I) complex (**4**) toward high molecular weight compared to linear precursor PS-alkyne (**3**). On the basis of the calibration curve with linear PS as standard, the apparent molecular weight of PS Cu(I) complex (**4**) was 4,878 Da, which was found to be smaller than the theoretical value. This deviation was due to the compact structure of PS Cu(I) complex

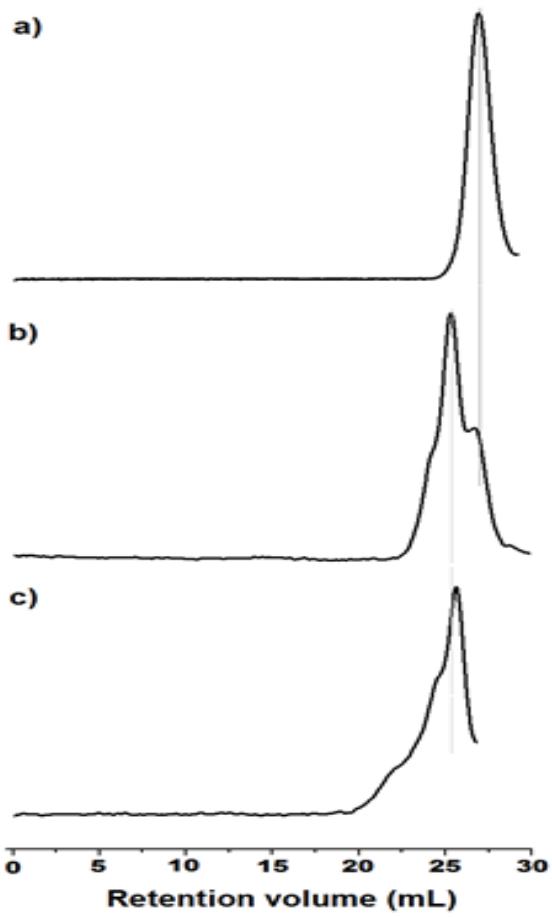

Figure 4.3. GPC traces of a) alkyne-PS (**3**), b) PS Cu(I) complex (**4**), and c) PS Cu(I) catenane (**5**)**.**

(**4**) (four- armed type polymers), which have a smaller hydrodynamic radius compared to its linear analogue. Further evidence of efficient click reaction was obtained from FT-IR analysis **(Figure 4.4)** of PS Cu(I) complex (**4**), which shows absence of the azide peak at 2090 cm^{-1}.

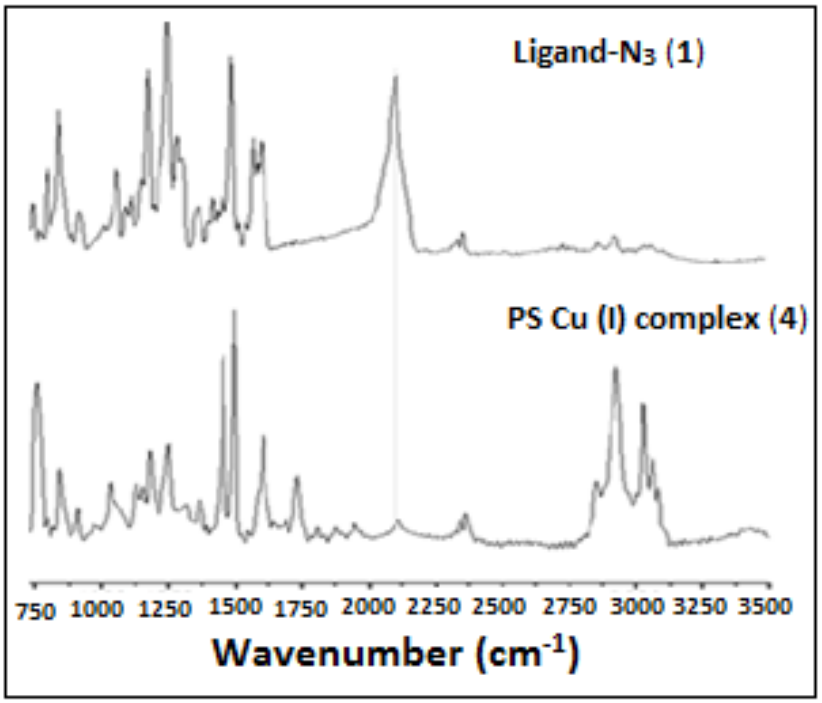

Figure 4.4. FT-IR spectram of a) Ligand-N_3 (**1**), b) PS-Cu(I) complex (**4**).

4.2.4. Template-closing of PS Cu(I) complex *via* ATRC

The intra-molecular ATRC of dibrominated PS (Br-PS-Br) at high temperature have been reported for the synthesis of macrocyclic polystyrene.[10] Similarly, the formation of the PS Cu(I) catenane (**5**) can be achieved by intra-molecular ATRC of dibrominated PS arms of Cu(I) complex (**4**) under pseudo-high dilution conditions. Thus, a THF solution of the PS Cu(I) complex (**4**) was added dropwise at a fairly low rate (0.75 mL h^{-1}) into a refluxing THF solution of catalyst CuBr/Me_6TREN and Cu(0). The GPC trace of resulting PS Cu(I) catenane (**5**) **(Figure 4.3c)** show slight shifting toward higher retention volume as a result of reduced hydrodynamic radius upon template-closing by ATRC. However, the coexistence of the inter-molecular coupling product was evidenced by a small shoulder at smaller retention volume.

4.2.5. Demetallation reaction of PS Cu(I) catenane

A metal-free PS catenane (**6**) was obtained by reacting PS Cu(I) catenane (**5**) with a saturated solution of KCN in THF: methanol (3:1). The GPC traces of the resulting PS catenane (**6**) **(Figure 4.5a)** show that the retention volume peak has not shifted to low molecular

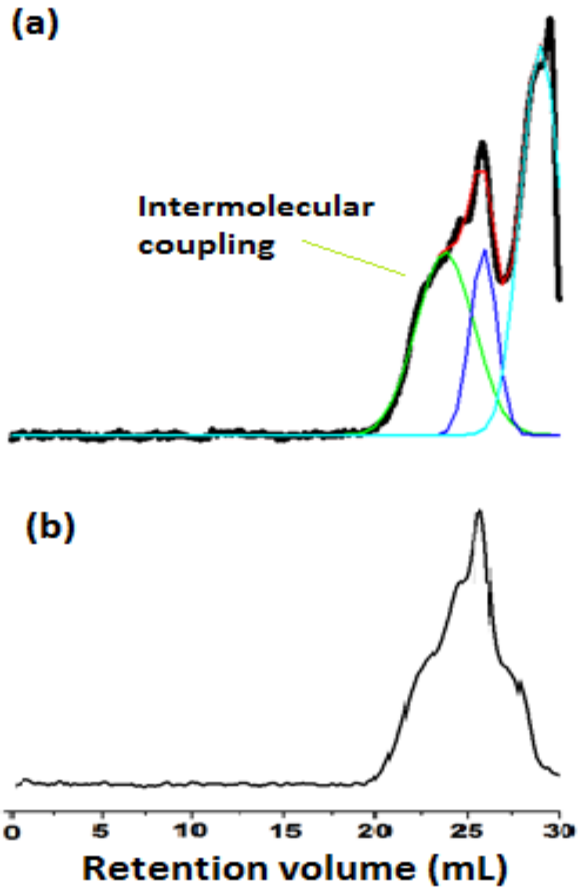

Figure 4.5. GPC traces of (a) crude PS catenane (**6**), (b) purified PS catenane **(6)**.

weight region after removing the copper, indicating an interlocked structure of PS catenane (**6**). The possible side reaction of ATRC where the polymer chains couples

laterally instead of "beyond" the metal center, which results to the formation of a "figure--of-eight" shaped PS polymers was also evident from GPC analysis.[13] After the demetallation step, "figure-of-eight" shaped PS generated cyclic PS with higher hydrodynamic volume compared to its catenated form. GPC traces also show the low molecular weight peak at a retention volume of 28.9 mL which can be attributed to side product of demrtallation reaction and the acyclic and/or cyclic polymers generated upon demetallation of uncyclized or partially cyclized polymer complex (**4**) during ATRC. The low molecular weight side products of demetallation step togather with unreacted alkyne-PS (**3**) as impurities in final polymer catenane (**6**) was removed by dialysis in THF. The GPC traces of purified PS catenane (**6**) **(Figure 4.5b)** show an almost complete removal of the low molecular weight fraction.

To test the integrity of Cu(I) complex during click reaction and efficiency of metal removal from template, a control experiment was performed by demetallation of PS Cu(I) complex (**4**) using same reaction conditions. GPC traces **(Figure 4.6)** of resulting polymer clearly suggest that the peak of of PS Cu(I) complex (**4**) shifted toward higher retention volume as polymer chains decoupled from Cu(I) metal center, resulting to an overall decrease in the molecular weight of polymers.

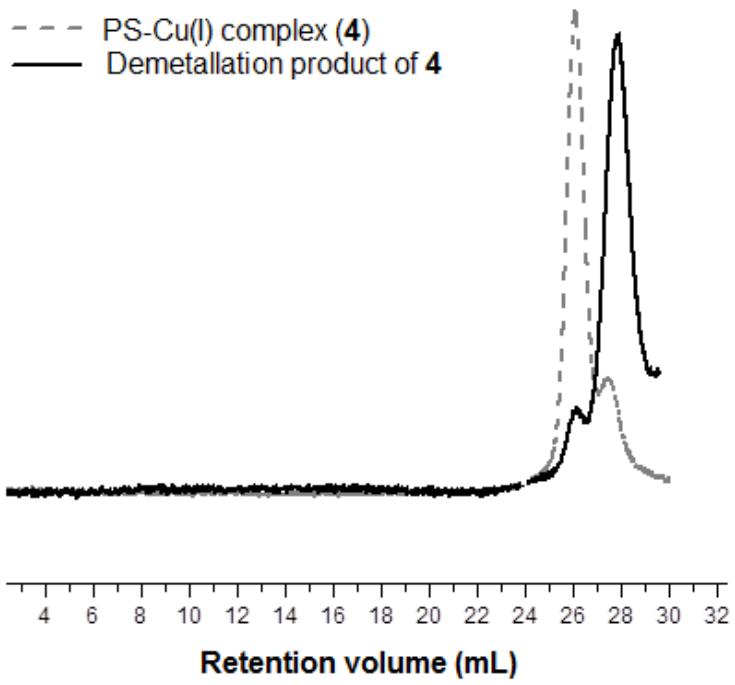

Figure 4.6. GPC traces of demetallation study of PS-Cu(I) complex (**4**).

4.2.6. AFM imaging of PS catenanes

To provide direct proof of formation of polymer catenanes, AFM imaging was also performed. The samples of PS catenanes (**6**) for AFM analysis were prepared by spin-coating a very dilute solution of the polymer in $CHCl_3$ onto freshly cleaved mica. As shown in **Figure 7**, interlocked cyclic structures of PS catenanes (**6**) were statistically observed, exhibiting different orientations on the surface. In addition, the line profile analysis of individual structure revealed the presence of the cavities inside the catenanes and the height doubled at overlapping point of polymer chain.

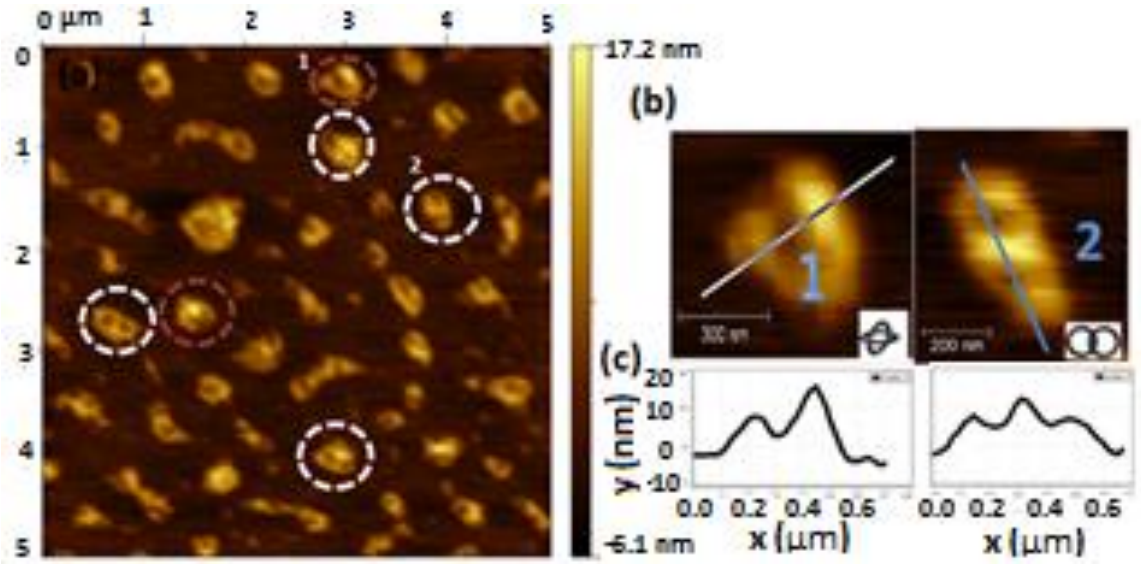

Figure 4.7. (a) AFM image of the PS catenanes (**6**) on a 8 x 8 µm scale on mica, (b) magnified images of the representative PS catenanes from (a), and (c) line profile of the PS catenanes

The presence of inter-molecular coupling product as observed in GPC trace was also supported by AFM image, where it shows interlocked multicyclic polymer rings in the form of polycatenanes. Similarly, a large single cyclic polymer as a topological isomer of catenanes was also observed with the presence of a single cavity measured by line profile analysis **(Figure 4.8)**.

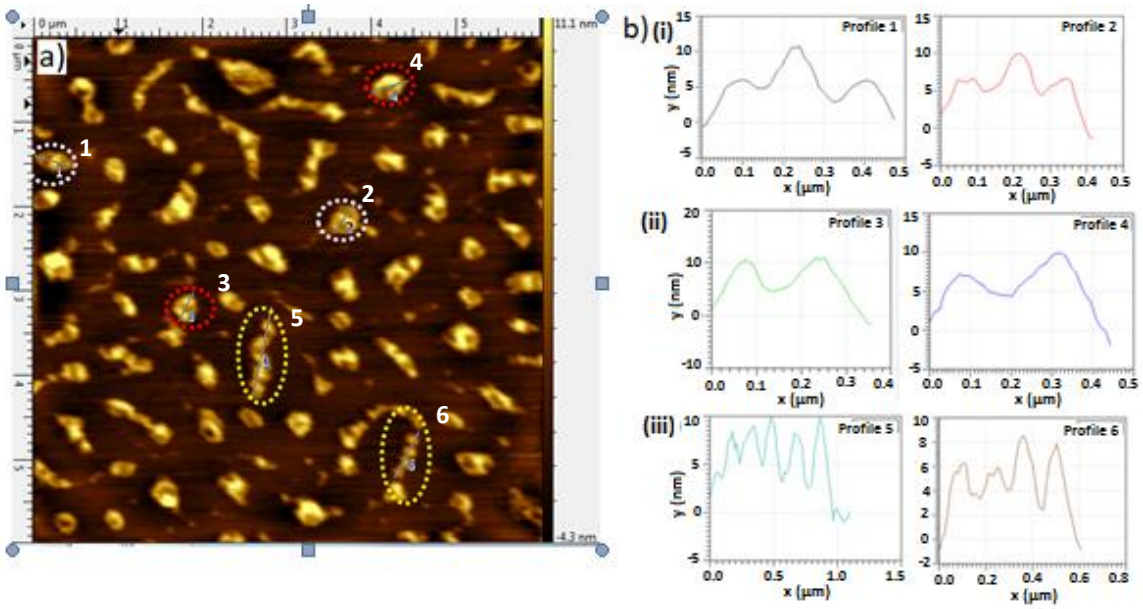

Figure 4.8. (a) AFM image of the PS catenanes (**6**) on a 6 x 6 µm scale on mica, (b) line profile of the representative samples of (i) PS catenanes, (ii) cyclic isomer of PS catenanes, and (iii) inter-molecular coupling product of ATRC from image (a).

4.3. Conclusions

The 'grafting to' approach as a novel route to synthesize polymer catenanes was demonstrated. The CuAAC click reaction has been proven to be an efficient way to couple alkyne-functionalized polymers to azide-functionalized ligand Cu(I) complex. The template-closing *via* intra-molecular ATRC enabled the formation of polymer catenanes which was further characterized by GPC and AFM to confirm its interlocked structure. Due to the presence of 4 reactive groups, intermolecular coupling products can also be observed. As the alkyne functionality can be easily introduce in variety of polymers, this approach can further explore to obtain structurally different homopolymer and blockcopolymer catenanes.

4.4. Experimental Section

4.4.1. Materials

All chemicals were purchased from Aldrich Chemical Company and were used directly without further purification unless otherwise indicated. All solvents were degassed with nitrogen gas before use.

4.4.2. Instrumentation

^{1}H NMR spectra were recorded on a JEOL ECS 500 spectrometer (500MHz). GPC was carried out on a Viscotek 270 instrument with a triple detector array (RALS, IV, RI) equipped with 2 GMHHR-M and 1 GMHHR-L mixed bed ViscoGel columns (eluent: THF; flow rate: 1 mL min^{-1}). UV-Visible measurements were taken on an Agilent technologies 8453 spectrometer. The FTIR spectra were obtained on a Digilab FTS 7000 equipped with a HgCdTe detector from 4000 to 600 (cm^{-1}) wavenumbers. All atomic force microscopy (AFM) images were recorded in air under ambient conditions on PicoScan 2500 (Agilent Technologies formerly Molecular Imaging, Corp.) equipped with an 10 × 10 μm scanner. The AFM tip used was a silicon-nitride AFM probe from Ted Pella Inc.

4.4.3. Synthesis of 2,9-bis(4-(2-azidoethoxy)phenyl))-1,10-phenanthroline

The solution of 2,9-bis(4-(hydroxy)phenyl))-1,10-phenanthroline[7] (0.21 g, 0.50 mmol) and 2-azidoethyl 4-methylbenzenesulfonate[8] (0.22 g, 0.75 mmol) in DMF (15 mL) was added to K_2CO_3 (0.21 g, 1.5 mmol) and the suspension was heated to 80 °C for 18 h. After cooling to room temperature, the reaction mixture was poured into mixture of ethyl acetate: water (50 mL). The aqueous layer was extracted with ethyl acetate (3 × 50 mL), and the combined organic fractions were washed with brine (50 mL), dried over $MgSO_4$, filtered and concentrated under reduced pressure. The resulting crude oil was then purified by precipitating from hexane to yield ligand-N_3 **(1**) as a pale yellow solid (0.2 g, yield 74%). ^{1}H NMR ($CDCl_3$): 8.43 (m, 4H, H_o), 8.25 (d, 2H, $H_{4,\ 7}$), 8.08 (d, 2H, $H_{3,\ 8}$), 7.74 (s, 2H, $H_{5,\ 6}$), 7.14 (m, 4H, H_m), 4.26 (t, 4H, -CH_2-N_3), 3.66 (t, 4H, -PhOCH_2).

4.4.4. Synthesis of Ligand-N_3 Cu(I) complex

By the double-ended needle transfer technique, 3 mg (0.60 mmol) of $Cu(CH_3CN)_4PF_6$ in 3 mL degassed CH_3CN was transferred under nitrogen at room temperature to a stirred degassed solution of **1** (10 mg, 3.0 mmol) in 3 mL DCM. The mixture turned dark red instantaneously, indicating the formation of Ligand-N_3 Cu(I) complex (**2**). After the solution was stirred for 1 h under nitrogen at room temperature, the solvents were evaporated to dryness to obtain dark red solid of crude **2** in quantitative yield (12 mg, 1.5 mmol). Complex **2** was used without further purification.

4.4.5. Synthesis of alkyne-PS

A mixture of styrene (16.0 mL, 139.2 mmol), anisole (1.60 mL) and PMDETA (600 µL, 2.89 mmol) was deoxygenated in a dry Schlenk flask by performing four freeze–pump–thaw cycles. The contents were frozen again and Cu(I)Br (207.5 mg, 1.44 mmol) was added. The freeze–pump–thaw cycle was repeated two more times, after which the mixture was allowed to melt. The Schlenk flask was immersed in an oil bath at a preset temperature of 90 ^{o}C. Propargyl 2-bromoisobutyrate [9] (800 mg, 2.89 mmol) initiator was added using a N_2 purged syringe. The polymerization was stopped after 2 h. The mixture was then diluted with THF and passed through a neutral alumina column to remove the catalyst. The polymer was precipitated in methanol.

4.4.6. Synthesis of PS Cu(I) complex

Ligand-N_3 Cu(I) complex (**2**) (10 mg, 0.12 mmol), alkyne-PS (**3**) (75.0 mg, 0.9 mmol), PMDETA (3.24 mg, 0.9 mmol) and 3 mL DMF were added to a Schlenk flask. The solution was purged with nitrogen and degassed by performing four freeze–pump–thaw cycles and then Cu(I)Br (1.49 mg, 0.9 mmol) was added. The resulting homogeneous reddish brown solution was stirred at room temperature for 24 h. After passing the solution through alumina, the PS Cu(I) complex (**4**) was precipitated from methanol.

4.4.7. Synthesis of PS Cu(I) catenane

ATRC was performed as per literature procedure[10]: A 500 mL Schlenk flask containing a 100 mL THF solution of Cu(I)Br (574 mg, 4.0 mmol) and nanosized copper (254 mg, 4.0 mmol) was sealed with a rubber septum, evacuated with four freeze-pump-thaw cycles, backfilled with N_2, and sealed from the Schlenk line. The flask was then placed in an oil bath and stirred at 75 ^oC. After allowing the metal solution to reach the temperature of the bath, Me_6TREN (1.07 mL, 4.0 mmol) was introduced via a nitrogen flushed syringe. A syringe pump held a 50 mL syringe containing an 18 mL THF solution of PS Cu(I) complex (**4**) (10 mg), which had separately been subjected to three freeze-pump-thaw cycles and backfilled with N_2. The solution of PS Cu(I) complex (**4**) was slowly dripped through a needle piercing the rubber septum into the stirring THF solution of the metal ligand, over approximately 24 h (approximate rate = 0.75 mL/h). After the contents of the syringe had been added to the reaction mixture, the reaction mixture was stirred for an additional 1 h. The resulting polymer Cu(I) catenane (**5**) was passed through an alumina column and precipitated into cold methanol.

4.4.8. Synthesis of PS catenanes

Demetallation of PS CuI) catenane (**5**) was performed as per following procedure. KCN (100 mg, 1.53 mmol) dissolved in water (2 mL) was added to PS CuI) catenane (**5**) (3.5 mg, 0.88 μmol) in 6 mL mixture of THF: methanol (3:1) and stirred for 24 h at room temperature. After stirring, the solvent was evaporated under vacuum, and the resulting polymer was extracted twice by DCM: water mixture. The DCM layer containing the

polymers were mixed together and dried over anhydrous Na_2SO_4 which upon evaporation under vacuum, yields PS catenane (**6**).

4.5. References

1. (a) Nasongkla, N.; Chen, B.; Macaraeg, N.; Fox, M. E.; Frechet, J. M. J.; Szoka, F. C. J. *J. Am. Chem. Soc.* **2009**, *131*, 3842–3843. (b) Eugene, D. M.; Grayson, S. M. *Macromolecules* **2008**, *41*, 5082–5084. (c) Guan, Z. J. *J. Polym. Sci., Part A: Polym. Chem.* **2003**, *41*, 3680–3692. (c) Guan, Z. *Chem.–Eur. J.* **2002**, *8*, 3086–3092. (d) Harth, E. M.; Hecht, S.; Helms, B.; Maelmstrom, E. E.; Frechet, J. M. J.; Hawker, C. J. *J. Am. Chem. Soc.* **2002**, *124*, 3926–3938.

2. (a) Dietrich-Buchecker, C. O.; Sauvage, J.-P. *Angew. Chem., Int. Ed. Engl*. **1989**, *28*, 189. (b) Harrison, J. T.; Harrison, S. *J. Am. Chem. Soc.* **1967**, *89*, 5723. (c) Schill, G. *Catenanes, Rotaxanes and Knots;* Academic Press: New York, 1971.

3. (a) Gan, Y.; Dong, D.; Hogen-Esch, T. E. *Macromolecules* **2002**, *35*, 6799–6803. (b) Ohta, Y.; Kushida, Y.; Kawaguchi, D.; Matsushita, Y.; Takano, A. *Macromolecules*, ***2008***, *41*, 3957–3961.

4. (a) Bunha, A.; Tria, C.; Advincula, R. *Chem. Commun.* **2011**, *47*, 9173–9175. (b) Bunha, A.; Mangadlao, J.; Felipe, M.; Pangilinan, K.; Advincula, R. *Macromol. Rapid Commun*. **2012**, *33*, 1214–1219.

5. (a) Tsarevsky, N. V.; Bernaerts, K. V.; Dufour, B.; Du Prez, F. E.; Matyjaszewski, K. *Macromolecules* **2004**, ***37***, 9308–9313. (b) Steffensen, M. B.; Simanek, E. E. *Angew. Chem., Int. Ed.* **2004**, *43*, 5178–5180. (c) Ergin, M.; Kiskan, B.; Gacal, B.; Yagci, Y. *Macromolecules* **2007**, *40*, 4724–4727. (d) Q. Liu, P. Zhao, Y. Chen, *J. Polym. Sci. Polym. Chem.*, 2007, **45**, 3330–3341.

6. (a) Dichtel, W. R.; Miljanic, O.S.; Spruell, Heath, J. R.; Stoddart, J. F. *J. Am. Chem. Soc.* 2006, **128**, 10388–10390. (b) Loethen, S.; Ooya, T.; Choi, H.-S.; Yui, N.; Thompson, D. H. *Biomacromolecules* **2006**, *7*, 2501–2506. (c) Mobian, P.; Collin, J.-P; Sauvage, J.-P. *Tetrahedron Lett.* **2006**, *47*, 4907–4909.

7. Dietrich-Bucheker, C. O.; Sauvage, J.-P. *Tetrahedron* **1990,** *46*, 502.

8. Zhan, J.; Zhu, X.; Fang, F.; Miao, F.; Tian, D.; Li, H. *Tetrahedron* **2012**, *68*, 5579–5582.

9. Shi, G.; Tang, X.; Pan, C. *J. Polym. Sci. Polym. Chem.* **2008**, *46*, 2390.

10. Voter, A. F.; Tillman, E. S. *Macromolecules* **2010**, *43*, 10304–10310.

11. Megiatto, J. D.; Schuster, D. I. *J. Am. Chem. Soc.* **2008**, *130*, 12872–12873.

12. Yang, P.; Yang, X.; Wu, B. *Eur. J. Inorg. Chem.* **2009**, 2951–2958.

13. Belfrekh, N.; Dietrich-Buckecker, C. O.; Sauvage, J.-P. *Inorg. Chem.* **2000**, *39*, 5169–5172.

Chapter 5: Synthesis of Cyclic Polymer *via* Ring-Expansion Polymerization from Cyclic RAFT initiator

5.1. Introduction

Over the last decade, much attention was given towards the design and synthesis of cyclic polymers because of its distinct properties compared to their linear counterparts, such as glass transition temperature, order-disorder transition, hydrodynamic volume, intrinsic viscosity, and fluorescene enhancement.[1-3] In addition, a cyclic polymer is also a topologically interesting material due to the stringent restrictions on the backbone conformation and the absence of chain ends.[4] The discovery of natural DNA rings, where the two strands of the double helix form a high order link has further stimulated the importance of synthesis and study of well-defined macrocycles.[5]

The usual route for the synthesis of cyclic polymers indeed relies on the end-to-end coupling of linear precursors. The advances in controlled living radical polymerization made possible the formation of well-defined linear precursors with functional end-groups suitable for the cyclization reactions.[6-7] However, the synthesis *via* this approach requires very dilute solution conditions to favor cyclization over inter-molecular coupling. Moreover, incomplete cyclization can lead to linear polymers as contaminants and further purification steps are required to remove undesirable impurities. On the other end, ring-expansion polymerization is an emerging route for the synthesis of cyclic polymer which does not require high dilute solution conditions. This technique, when optimized, should be amenable to larger scale synthesis. Typically, a cyclic catalyst or initiator has been used to yield a growing cyclic polymer chain held together by a

relatively labile bond (e.g. organometallic or electrostatic). Propagation occurs by insertion of new monomer into this weak bond, and in some cases also thermodynamically driven due to ring strain in the monomer. The cyclic structure is maintained throughout propagation which allows preparation of high molecular weight polymers without the entropic penalty associated with the ‘‘ring-closure’’ approach. Several research groups have explored the potential of a ring-expansion strategy. For example, Kricheldorf and Lee have pioneered the work on ring-expansion polymerization using lactide monomers and cyclic tin oxide catalyst.[8] Bielawski *et al*. demonstrated an elegant application of ring opening metathesis catalysts to enable cyclic ring-expansion by use of a cyclic Ru catalyst.[9] In later process, the cyclic Ru catalyst inserts itself into the cyclooctene monomer to initiate the ring-expansion polymerization.

However, only few reports have appeared on the synthesis of cyclic polymer *via* combination of ring-expansion strategy and controlled radical polymerization (CRP) method. This approach is particularly attractive because of the variety of monomers that can be polymerized by CRP and the preparation of functionalized cyclic polymers is achievable. Pan and co-worker have reported ^{60}Co γ-ray-induced low temperature polymerization of methylacrylate (MA) in the presence of cyclic Reversible Addition Fragmentation Chain Transfer (RAFT) initiator.[10] As shown in **Scheme 5.1**, initiation results in homolytic cleavage of the weak C-S bond in cyclic initiator and forms active radical and a stable sulfur radical. The former radical initiates the polymerization of monomer, forming a propagating radical. The temperature of polymerization was kept at -30 ^{o}C to maintain slow propogation and lower diffusion rate in order to generate

monodispersed cyclic polymer. In addition, for the process to be successful, the reversible termination must be fast enough for competing effectively deleterious irreversible termination. In this work, the termination rate constant (k_t = 0.95x10^7 for MA) was much higher than the propagation rate constant (k_p= 2.09x10^3). Therefore, only few monomers were added before reversible termination occurs. Cyclic poly(methyl acrylate) with a predetermined molecular weight was obtained in considerably good yield (77%) without high dilution reaction conditions. However, the low temperature polymerization condition requirement of this method limits the use of commonly used thermal initiation method, since the ^{60}Co γ-ray source is commonly not available.

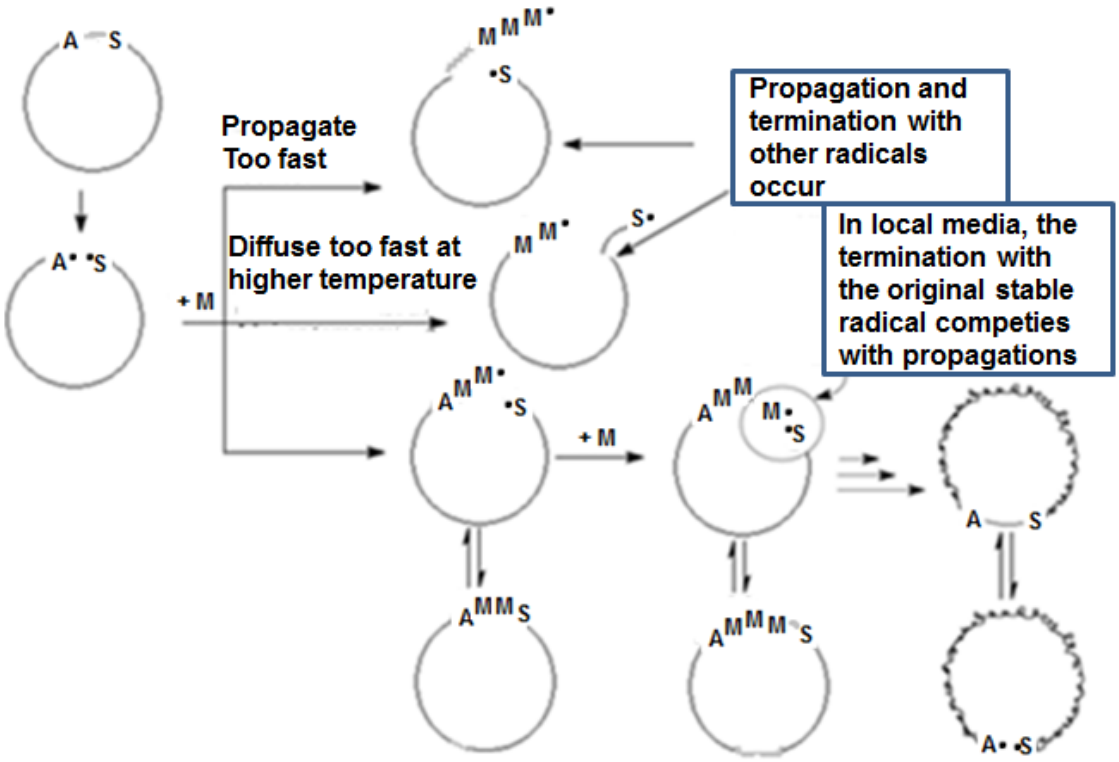

Scheme 5.1. Kinetics of ring-expansion RAFT polymerization.

In another development, Narumi et al. have prepared a novel cyclic NMP initiator *via* an intra-molecular azide/alkyne-‘‘click’’-reaction and tested it for the polymerization of styrene at 130 ^{o}C **(Scheme 5.2)**.[11] As expected, the results showed the formation of a mixture of products, containing different ring size polymers with an average of three to four alkoxyamine functionalities per chain. These observations were explained by the occurrence of radical crossover reaction due to high temperature polymerization condition, which further confirmed the challenges associated with ring-expansion by controlled radical polymerization technique.

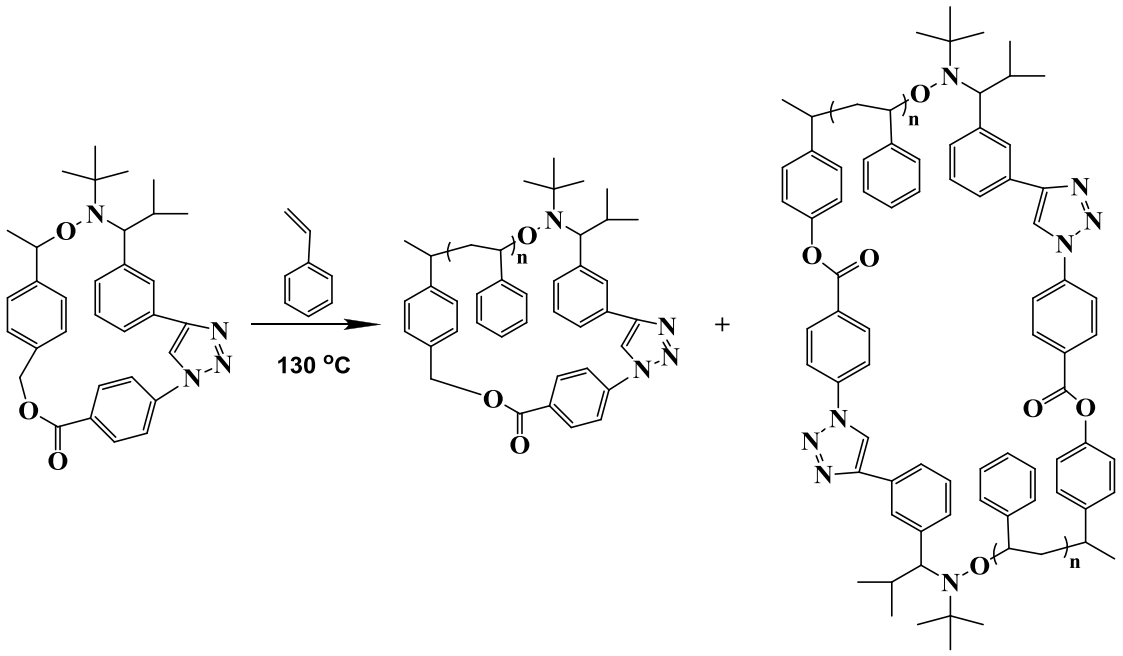

Scheme 5.2. Ring-expansion polymerization initiated by a cyclic alkoxyamine derivative producing macrocyclic polystyrene.

The detailed insights of complex macromolecular architectures are sometimes too difficult to obtain by standard polymer analysis techniques. Classical methods such as Gel permeation chromatography, NMR spectroscopy or scattering techniques measure

average information and therefore give only a general description of polymer properties. Recent advances in single-molecule spectroscopy and imaging open additional opportunities for characterizations and analysis of complex synthetic macromolecules. For example, single-molecule fluorescence spectroscopy, single-molecule force measurements, and scanning tunneling microscopy (STM) not only allow the visualization of discrete macromolecules but also give insight into the physics of single polymer chains, such as measurements of chain conformation, dynamics and micromechanics.[12] So far, these analytical methods have been used mainly to study proteins and nucleic acids. However, they have significant potential for the characterization of synthetic polymers. The first convincing examples of visualization of single polymer chains have been obtained by Atomic Force Microscopy (AFM).[13] Interestingly, direct correlation made possible between polymer synthesis and observation *via* single-chain visualization. For instance, polydispersity, structural defects and side reactions have been directly evaluated from AFM images.[14-15] Recently, AFM imaging have been explored as important tool for direct evidence of the formation of cyclic and complex topological polymers.[16]

Herein, we demonstrate ring-expansion polymerization by RAFT for future polymer catenane synthesis projects. A cyclic dixanthate initiator with phenanthroline moiety was prepared and evaluated for its efficiency to control thermally initiated free radical polymerization of N-vinylcarbazole (NVK). Characterization of the macromolecules in solution, XPS, and AFM imaging confirmed the viability of this approach.

5.2. Results and Discussion

5.2.1. Design and synthesis of cyclic dixanthate RAFT initiator

Xanthates have been studied as chain transfer agents in the controlled/living free-radical polymerizations of vinyl monomers under thermal initiation, and the polymerizations have good living characteristics in the presence of S-benzyl O-ethyl dithiocarbonate.[17] In this study, we designed and synthesized a novel cyclic dixanthate initiator (**1**) (**Scheme 5.3**), which similarly includes two molecules of S-benzyl O-ethyl dithiocarbonate.

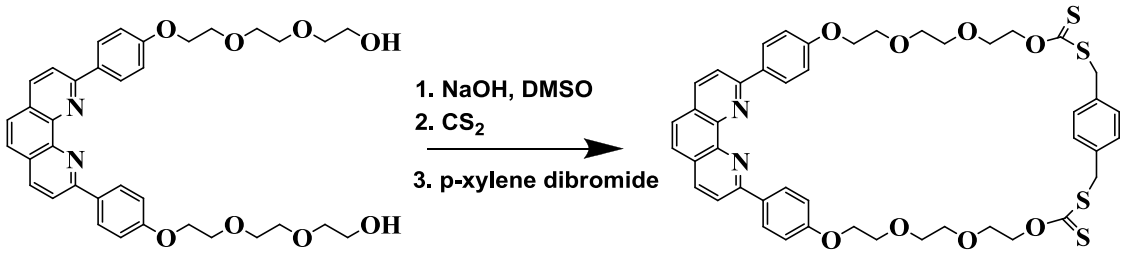

1

Scheme 5.3. Synthetic pathway for the formation of cyclic dixanthate initiator (**1**).

The cyclic initiator (**1**) was obtained in 30% yield *via* one pot reaction of phenanthroline diol with carbon disulfide and p-xylene dibromide. The structure and purity of the initiator was confirmed by ^{1}H NMR. The molecular ion peak obtained by the MALDI-TOF is 883.9, which further confirms the cyclic structure of (**1**).

5.2.2. Ring-expansion polymerization of NVK using cyclic dixantate initiator

RAFT polymerization of NVK has been reported to be well controlled with xanthates as the chain transfer agents.[18] To investigate polymerization behavior in the presence of **1,** we carried out free radical polymerization of NVK *via* thermal initiation **(scheme 5.4)**.

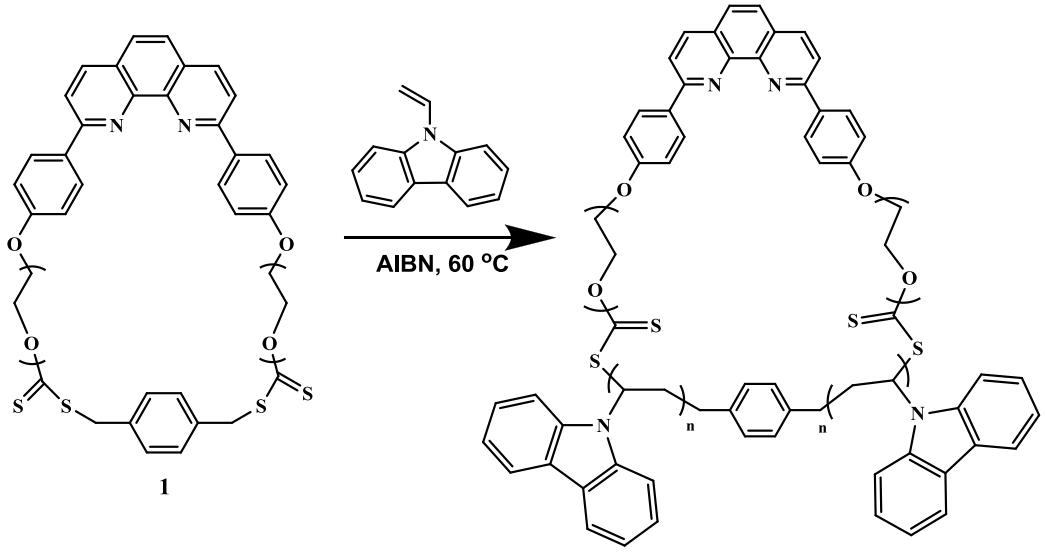

Scheme 5.4. RAFT polymerization of N-vinylcarbazole using cyclic initiator (**1**).

The solution polymerization was conducted in dioxane at 60 ^{o}C, using a 200:5:2.5 molar ratio of NVK to **1** to AIBN. During the polymerization process, the reaction solution remained transparent with a slight increase in the viscosity with time. In order to determine the living nature of polymerization, the samples were withdrawn at specific time intervals. The polymers were recovered by precipitation, and dried under vacuum before characterization. The GPC curves of the cyclic polyvinylcarbazole (Cyclic PVK) obtained from different polymerization times are shown in **Figure 5.1a**.

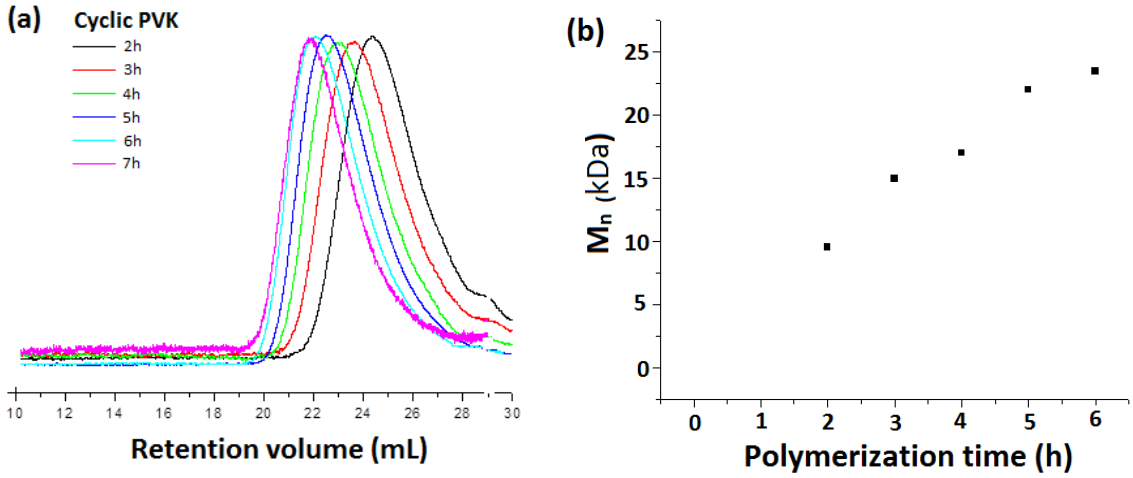

Figure 5.1. (a) GPC traces of cyclic PVK samples obtained at different time interval of RAFT polymerization, (b) Kinetic plot of M_n vs polymerization time.

All the curves are unimodal and symmetrical, and are continuously shifted to less elution time with increase of polymerization time, indicating molecular weight increase of the resulting polymers with time of polymerization. The kinetic results for the polymerization of N-vinylcarbazole are shown in **Figure 5.1b**. A linear relationship between M_n and polymerization time was observed and indicates the living nature of the RAFT polymerization. The molecular weight data and polydispersity index information obtained from GPC are shown in Table 5.1.

Table 5.1. GPC results of thermally initiated RAFT polymerization of NVK using cyclic dixanthate initiator (**1**).

Sample	Polymerization Time (h)	M_n (Da)	M_w (Da)	PDI
1	2	9,536	15,568	1.63
2	3	14,950	24,982	1.67
3	4	17,015	31,825	1.87
4	5	21,997	36,393	1.65
5	6	23,465	41,215	1.75
6	7	33,333	77,151	2.3

The structural composition of cyclic PVK was confirmed from ^{1}H NMR spectra as shown in **Figure 5.2**. It can be seen that the typical signals of PVK are quite diffusive due to the restricted rotation of the bulky carbazole groups combined with ring current effects of neighboring rings.[19-20] Most of the signals from initiator part are overlapped with those of the main chain and the pendant carbazole groups, except the methylene protons of triethylene glycol at δ 4.24 ppm. This suggests that cyclic initiator has successfully incorporated in polymer chain during the polymerization in order to control the molecular weight and polydispersity.

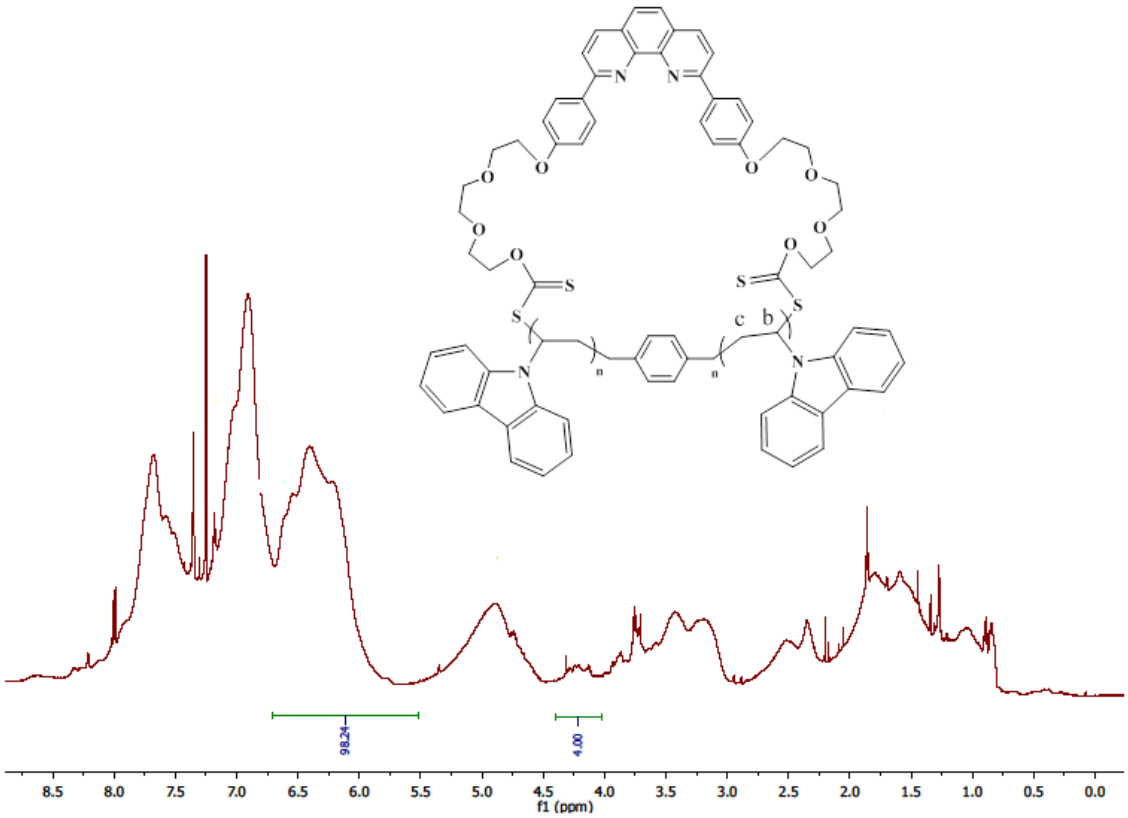

Figure 5.2. ^{1}H NMR spectra of cyclic PVK (sample 5).

Assuming that each cyclic polymer contains one cyclic initiator unit, the number-average molecular M_n,NMR, can be calculated according to eq. 1

$$M_{n,\,NMR} = (I_{6.15}/3) \times 193 + 883 \qquad (1)$$

where $I_{6.15}$ is the integral values of three carbazole proton at δ 6.15 relative to the integral value of four methylene proton from initiator at δ 4.24; 193 and 883 are the molecular weights of monomer N-vinylcarbazole and cyclic initiator **1**, respectively. The M_n,NMRs of the polymers obtained during different polymerization time were calculated and plotted versus the polymerization time. The kinetic plot shown in **Figure 5.3**

indicates a linear increase in M_n with polymerization time, which is also in a good agreement with M_n obtained from GPC.

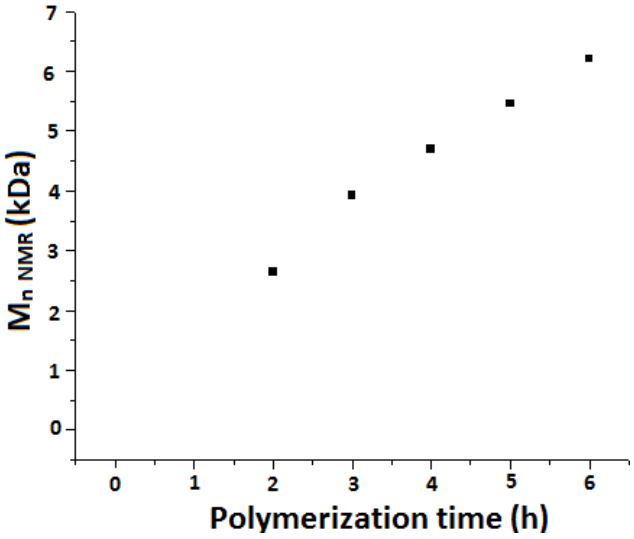

Figure 5.3 Relationship $M_{n,NMR}$ vs polymerization time for polymerization of NVK in the presence of cyclic initiator **1**.

In addition, it also indicates increase in intensity of polymer protons (δ 6.15) with respect to initiator proton (δ 4.24) and confirms the chain growth from single cyclic initiator. It is reasonable that M_n NMR is different from M_n GPC because the GPC instrument is calibrated with linear polystyrene standards and has the hydrodynamic volume factor.

To further confirm the elemental composition of the synthesized cyclic polymers, X-ray photoelectron spectroscopy (XPS) was performed. The sample for XPS measurement was dropcasted on a 1x1 cm O_2 plasma-cleaned silicon wafer. A total of 200 mL of 2mg/mL sample in THF was dropcast per substrate. The samples were then dried overnight in vacuum at room temperature. Survey scans of two different molecular weight polymer samples in **Figures 5.4** reveal the presence of carbon (C1s), nitrogen (N1s) and a weak signal for sulfur (S2p). High resolution scans (inset) for 25 cycles were

performed in order to amplify the S2p signal. The well-defined S2p band further confirms the preservation of the xanthate moiety which is essential not only to maintain the

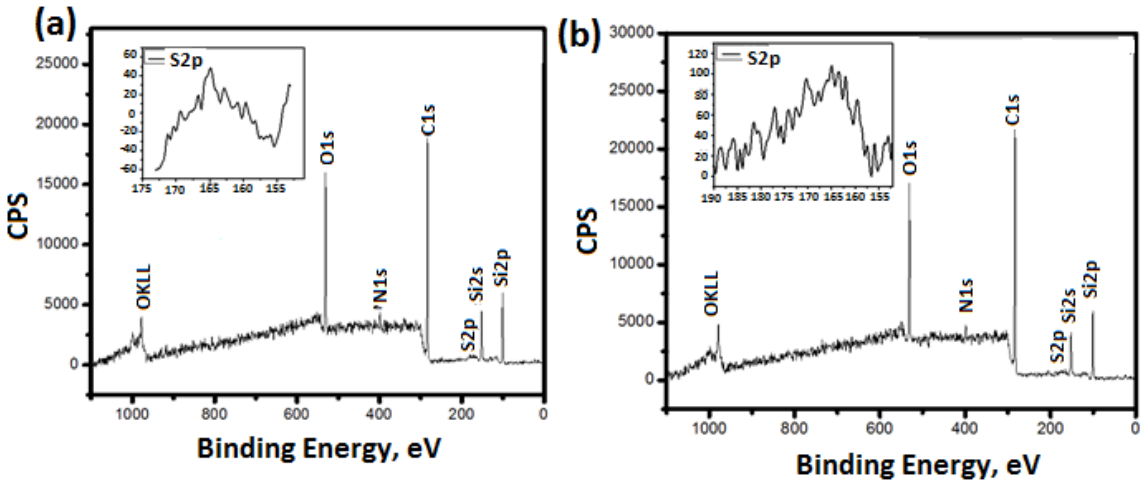

Figure 5.4. XPS survey spectrum of cyclic PVK (a) sample 4, (b) sample 5 from Table 5.1 (Inset: High-resolution XPS spectrum of the S2p region).

living nature of the polymer but also its cyclic structure. Due to the high population of carbon and other major species in the sample, atomic percentage of sulfur could not be accurately measured as it falls below the detection limit of the instrument (<.1%). However, it is worth noting that the atomic percentages of N1s and C1s, excluding other elements present, are 7.6 and 92.4%, respectively. This is in close agreement to elemental composition of the monomer N-vinyl carbazole which constitutes 7.25% of nitrogen. Meanwhile, the O1s, Si2s and Si2p signals are from the silicon wafer substrate.

5.2.3 AFM and DLS analysis of cyclic PVK

For a better understanding of the topological aspect of the polymer, we turned our attention toward visualization of the polymers v*ia* AFM. Samples of cyclic PVK (Sample 4, Table 5.1) were prepared by spin-coating a 9 ng/mL solution of the polymer in $CHCl_3$ onto freshly cleaved mica. Multiple rings were observed **(Figure 5.5a)** without any detectable linear polymers, and analysis of the line scans of the toroids revealed highly uniform line profile features indicating presence of cavity.

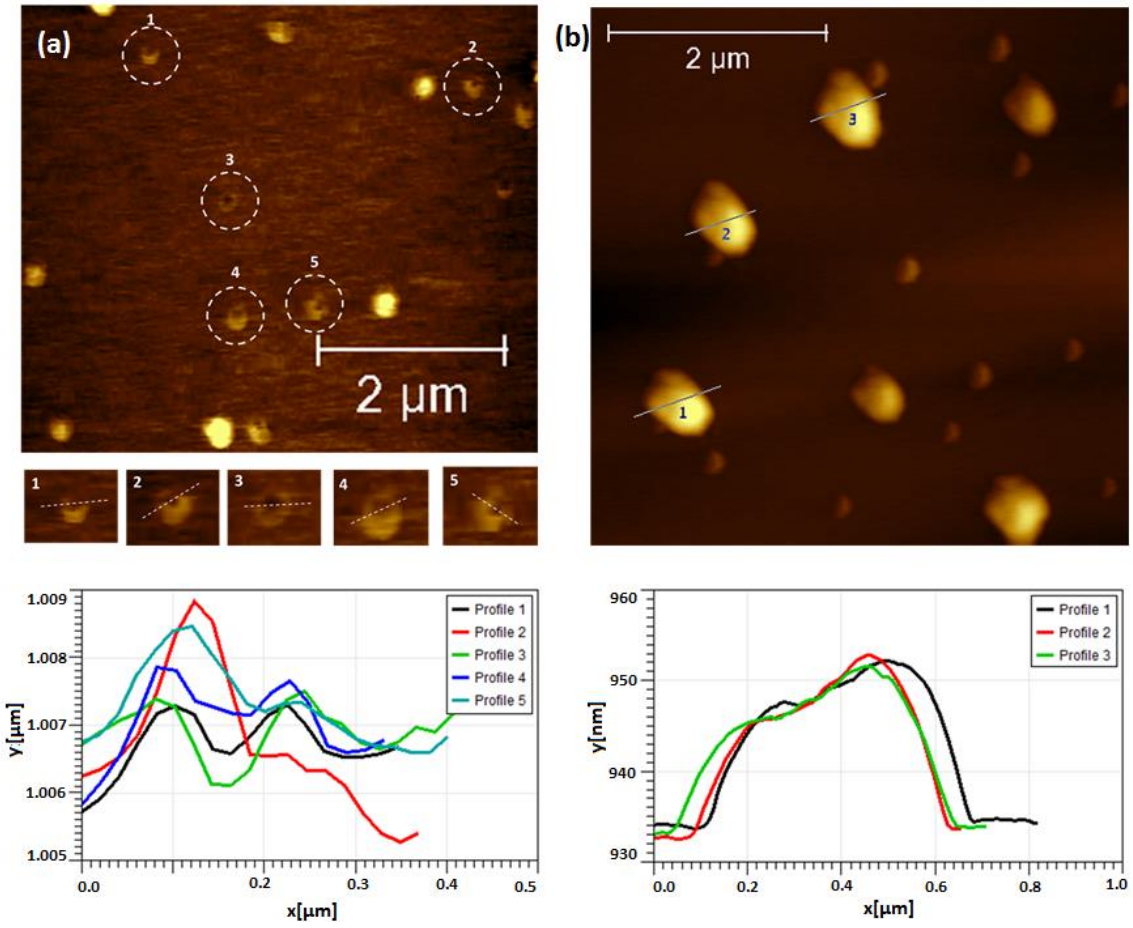

Figure 5.5. AFM image of cyclic PVK on mica (a) sample 4, and (b) sample 6 from Table 5.1.

To compare the relative size of cyclic PVK with different molecular weight samples, another AFM sample was prepared by using high molecular weight cyclic PVK (Sample 6, Table 5.1). As expected, the overall diameter of the torroids is relatively larger in size compared to the low molecular weight sample (**Figure 5.5b)**. The line profile shows slight decrease in thickness over the middle of the structure indicating presence of the cavity but not as significant as compared to sample 4. This could be the result of contracted conformation of the high molecular weight polymer as the chain flexibility increases with molecular weight on a non-wetting selective surface.

To examine the size distribution of cyclic PVK in THF solution, dynamic light scattering (DLS) was used to measure hydrodynamic radius (R_h) of the polymers. DLS analysis was conducted with 0.015 wt% of cyclic polymer in THF at 25 ^{o}C. The DLS data for low and high molecular weight cyclic PVK (M_n 21,997 Da and M_n 33,333 Da, respectively) are plotted in **Figure 5.6**.

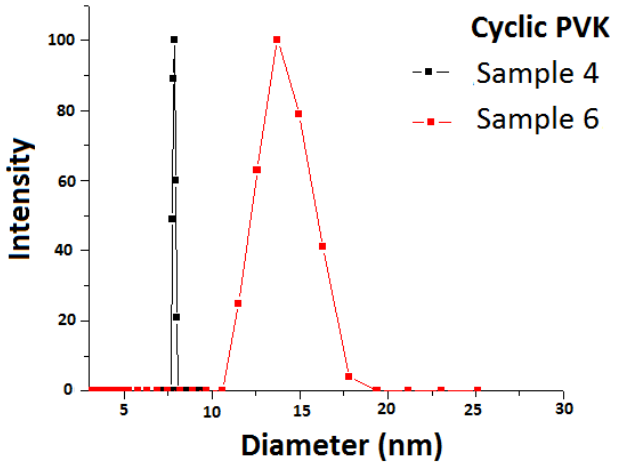

Figure 5.6. DLS analysis of cyclic PVK in THF.

As expected from the living nature of RAFT polymerization by cyclic initiator **1**, the sizes of the cyclic PVK increase with the increased molecular weight. The relatively narrow size distribution of sample 4 (7.8 nm) compared to sample 6 (14.3 nm) also shows good agreements with polydispersity data and toroid sizes from GPC and AFM respectively.

5.2.4. Ring-opening study of cyclic PVK

The broad size distribution of polymer could be a result of inter-molecular chain transfer reaction due to high temperature polymerization condition. As demonstrated by Pan *et al*. and other group, increasing the temperature will increase the diffusion rate of the radicals and may favor the propogation and termination with other radicals in local media. Therefore as shown in **Scheme 5.5**, chain transfer reaction would result to larger macrocyles with more than one cyclic dixanthate moiety in single polymer chain.

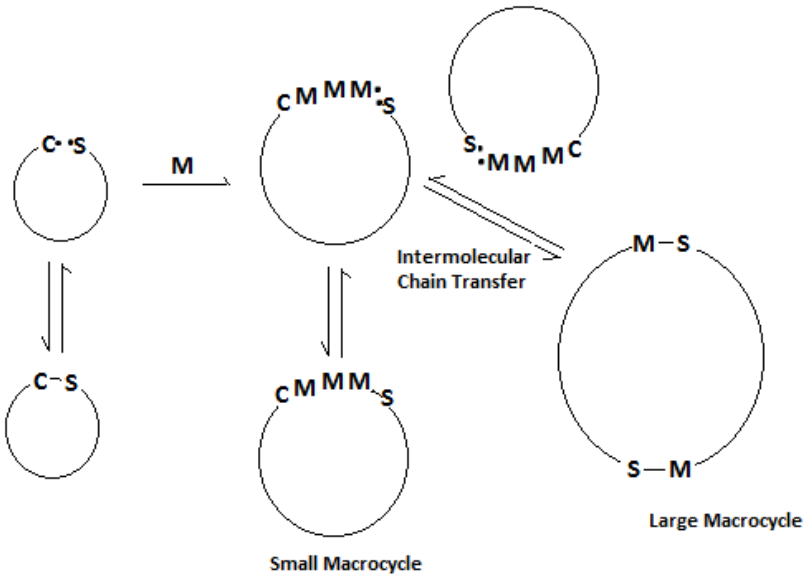

Scheme 5.5. Mechanism of formation of large macrocycle during RAFT polymerization.

The further insight of polymerization mechanism can be obtained by ring opening reaction of cyclic PVK to its linear analogue **(Scheme 5.6)**. Polymer chain can be easily broken down at the location of xanthate group. There are three general methods for xanthate group removal/transformation: aminolysis, thermal elimination, and radical-induced reduction.[21-23] We have used radical-induced reactions with tributylstannane as the most effective H atom donor to remove the xanthate groups. The tributylstannane was

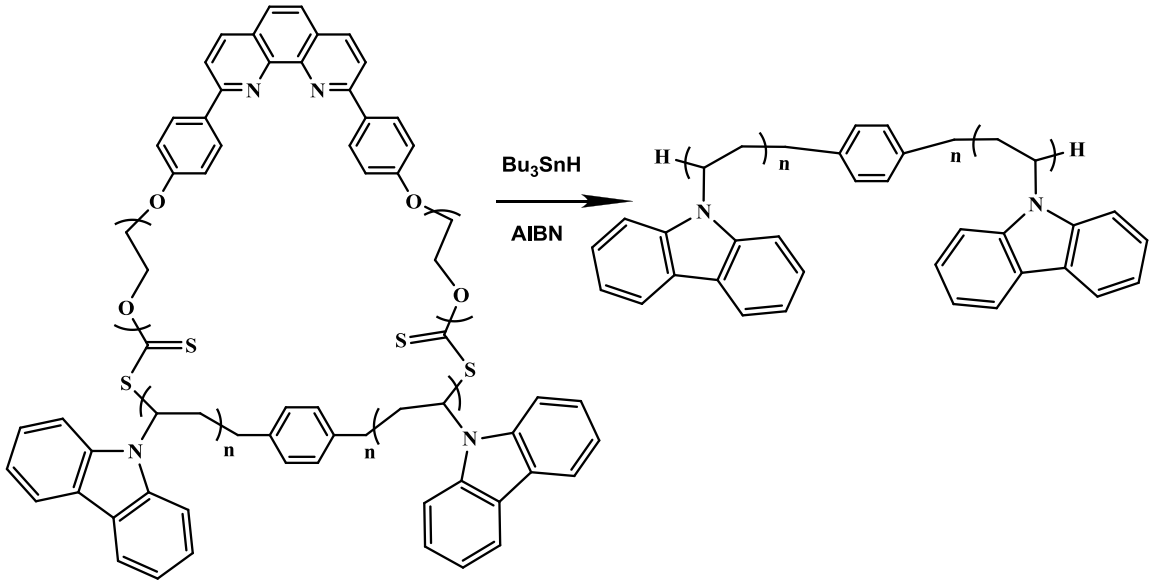

Scheme 5.6. Ring-opening reaction of cyclic PVK by radical induced reduction of xanthate group.

used in excess with respect to polymer in order to guarantee a quantitative removal. The yellow color of polymer solution disappeared after reduction indicates successful removal of xanthate group. The GPC results of the treated polymer shows substantially decreased molecular weight **(Figure 5.7)**, which indicates presence of more than two xanthate group per chain before cleavage. Approximately 65% of the polymer chain contains more than two xanthate groups as calculated from the ratio of M_n of treated polymer vs.

untreated cyclic polymer. This size distribution also shows an agreement with size distribution in AFM result.

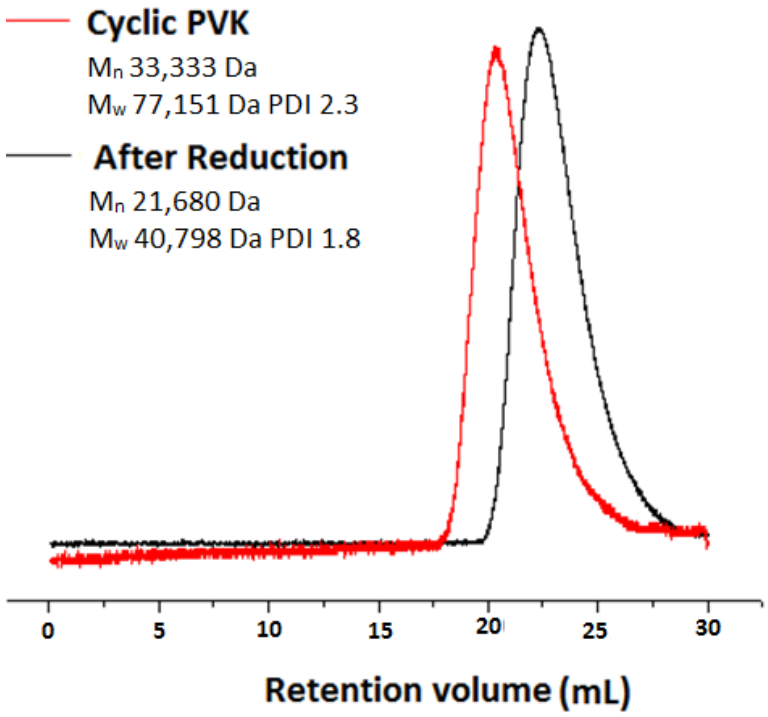

Figure 5.7. GPC traces of cyclic PVK before and after radical induced reduction of xanthate group.

For comparison, we also performed AFM study of linear analogues resulting from radical reduction of cyclic PVK. The image of sample did not show any ring structures and only shows some aggregated structures, which is more commonly observed in AFM imaging of the linear polymers.

5.3. Conclusions

Thermally initiated ring-expansion RAFT polymerization of N-vinylcarbazole was demonstrated using novel cyclic dixanthate RAFT initiator. The controlled molecular weights versus polymerization time indicate that the polymerization is a controlled free-radical process and progressed through cyclic initiator. The structural composition of cyclic PVK was characterized well by NMR and XPS analysis. GPC results show relatively broad distribution of polymer, which can be attributed as results of chain transfer due to relatively high temperature polymerization condition. The direct visualization of polymers by AFM reveals interesting information about topology, where most of the polymer chains are cyclic in structure. The mixture of small and larger macrocycle in AFM image and broad size distribution of polymer sample 6 in DLS further confirms chain transfer reaction during polymerization. The experimental results suggest low temperature polymerization condition is necessary to prevent chain transfer and to obtain monodispersed macrocycles. Thus, ongoing research is directed to perform low temperature polymerization by other initiation methods. Other possible extension of this work is in progress in our lab, where catenane type RAFT initiator can be synthesized by using cyclic dixanthate initiator as a precursor and well defined polymer catenane can be obtained by ring-expansion strategy.

5.4. Experimental Section

5.4.1. Materials

All chemicals were purchased from Aldrich Chemical Company and were used directly without further purification unless otherwise indicated. All solvents were degassed with nitrogen gas before use.

5.4.2. Instrumentation

^{1}H NMR spectra were recorded on a VARIAN 600 spectrometer (600MHz). GPC was carried out on a Viscotek 270 instrument with a triple detector array (RALS, IV, RI) equipped with 2 GMHHR-M and 1 GMHHR-L mixed bed ViscoGel columns (eluent: THF; flow rate: 1 mL min^{-1}). All atomic force microscopy (AFM) images were recorded in air under ambient conditions on PicoScan 2500 (Agilent Technologies formerly Molecular Imaging, Corp.) equipped with a 10 × 10 μm scanner. The AFM tip used was a silicon-nitride AFM probe from Ted Pella Inc. MALDI-TOF mass spectra were recorded in a Bruker OmniFLEX MALDI-TOF MS Spectrometer. This instrument was operated at an accelerating potential of 20kV in linear mode. The mass spectra represent an average over 250 consecutive laser shots. The mass scale was calibrated using the matrix peaks and the calibration software available from Bruker OmniFLEX. Mentioned *m/z* values correspond to monoisotopic masses. XPS analysis was conducted on a PHI 5000 Versa Probe^{TM} x-ray photoelectron spectrometer equipped with monochromatic Al Ka x-ray source (hn = 1486.6 eV) incident at 90° relative to the axis of a hemispherical energy analyzer. Low and high resolution spectra were collected with pass energies of 23.5 and

187.85 eV, respectively, a photoelectron take off angle of 45° from the surface, and an analyzer spot of 1400 micron x 1500 micron size. DLS data was obtained from Brookhaven 90Plus using ZetaPALS particle sizing software

5.4.3. Synthesis of dixanthate cyclic initiator

A mixture of 2,9-bis(*p*-{2-[2'-hydroxyethoxy(ethoxy(ethoxy))]}phenyl)-1,10-phenanthroline (220 mg, 0.35 mmol) and NaOH (27.9 mg, 0.70 mmol) in DMSO:H_20 (100 mL) was added to a 250 mL flask at room temperature. After stirring for 4 h, carbon disulfide (79.6 mg, 75 mmol) was added dropwise. The reaction mixture was stirred overnight at room temperature. P-xylene dibromide (92.1 mg, 0.70 mmol) in DMSO (18 mL) was introduced slowly (1.5 mL/h) at room temperature. After the addition was completed, the reaction mixture was stirred for another 5 h. The reaction mixture was poured into ice water (300 mL) and extracted with DCM (3 x 200 mL). The combined organic extracts were washed with water (2 x 150 mL), dried over anhydrous Na_2SO_4 and evaporated to afford a crude product, which was purified by silica gel column chromatography (DCM: methanol (96:4) as an eluent) to give a yellow solid (30 % yield). ^{1}H NMR($CDCl_3$): δ ppm: 8.45 (d, 2H), 8.37 (d, 4H), 8.20 (d, 2H), 7.84 (s, 2H), 7.30 (s, 4H), 7.12 (d, 4H), 4.73 (t, 4H), 4.30 (t, 4H), 4.23 (t, 4H), 3.93 (t, 4H), 3.85 (t, 4H), 3.78 (t, 4H), 3.72 (t, 4H). m/z (+FAB) found 883.98 $[M+H]^+$, calculated: 883.13 for $C_{46}H_{46}N_2O_8S_4$.

5.4.4. Synthesis of cyclic PVK *via* RAFT polymerization

A mixture of cyclic dixanthate initiator (**1)** as the chain transfer agent (50 mg, 5.6 x 10^{-5} mol), AIBN (4.64 mg, 2.8 x 10^{-5} mol), NVK (1.6 g, 0.011 mol), and dioxane (8 mL) was degassed by three freeze-pump-thaw cycles, sealed under vacuum, and heated at 60 ^{o}C. The different molecular weight cyclic polymers were obtained by withdrawing sample at specific time interval, precipitating the reaction mixture in a large excess of methanol. Polymer samples were recovered by centrifugation and dried under vacuum before characterizations.

5.4.5. Typical procedure for xanthate group removal with tributylstannane

A mixture of cyclic PVK (28 mg, Mn 33,333, PDI 2.3), tributylstannane (2.5 mg, 9.6 x 10^{-5} mol), AIBN (0.5 mg, 4.38 x 10^{-6} mol), and chlorobenzene (0.5 mL) was degassed by three freeze-pump-thaw cycles, sealed under vacuum and heated at 80 ^{o}C for 3 h. Then the reaction mixture was precipitated in a large excess of hexane, and the polymer was isolated by filtration. This step was repeated three more times to remove all the residual tin-products.

5.5. References

1. Roovers, J. in *Cyclic Polymers*, 2nd ed. (Ed.: Semlyen J. A.), Kluwer, Dordrecht, 2000, 347.

2. Gan, Y.; Dong, D.; Carlotti, S.; Hogen-Esch, T. E. *J. Am. Chem. Soc.* **2000**, *122*, 2130–2131.

3. Hadjichristidis, N.; Iatrou, H.; Pitsikalis, M.; Mays, J. *Prog. Polym. Sci*. **2006**, *31*, 1068–1132.

4. Hogen-Esch, T. E. *J. Polym. Sci. Part A: Polym. Chem*. **2006**, *44*, 2139–2155.

5. Fiers, W.; Sinsheimer, R. L. *J. Mol. Biol*. **1962**, *5*, 424.

6. Geiser, D.; Hocker, H. *Polym. Bull*. **1980**, *2*, 591–597.

7. Hild, G.; Kohler, A.; Rempp, P. *Eur. Polym. J.* **1980**, *16*, 525–527.

8. Kricheldorf, H. R. *J. Polym. Sci. Part A: Polym. Chem*. **2004**, *42*, 4723–4742.

9. Bielawski, C. W.; Benitez, D.; Grubbs, R. H. *Science*, **2002**, *297*, 2041.

10. He, T.; Zheng, G.; Pan, C. *Macromolecules* **2003**, *36*, 5960.

11. Narumi, A.; Zeidler, S.; Barqawi, H.; Enders, C.; Binder, W. H. *J. Polym. Sci. Part A: Polym. Chem.* **2010**, *48*, 3402–3416.

12. Granick, S. *J. Polym. Sci.Part B: Polym. Phys.* **2010**, *48***,** 2542–2543.

13. Kumaki, J.; Nishikawa, Y.; Hashimoto, T. *J. Am. Chem. Soc.* **1996**, *118***,** 3321–3322.

14. Sheiko, S. S.; Sumerlin, B. S.; Matyjaszewski, K. *Prog. Polym. Sci.* **2008**, *33***,** 759–785.

15. Schappacher, M.; Deffieux, A. *Science* **2008**, *319*, 1512–1515.

16. (a) Boydston, A. J.; Holcombe, T. W.; Unruh, D. A.; Frechet, J. M. J.; Grubbs, R. H. *J. Am. Chem. Soc.* **2009**, *131*, 5388–5389. (b) Bunha, A.; Tria, C.; Advincula, R. *Chem. Commun.* **2011**, *47*, 9173–9175.

17. Chen, F.; Cheng, Z.; Zhu, J.; Zhang, W.; Zhu, X. *European Polymer Journal* **2008**, *44*, 1789–1795.

18. Hu, N.; JI, W.; Tong, Z.; Li, Z.; Chen, E. *J. Polym. Sci. Part A: Polym. Chem.* **2010**. *48*, 4621–4626.

19. Natansohn, A. *J. Polym Sci Part A: Polym Chem* **1989**, *27*, 4257–4265.

20. Karali, A.; Froudakis, G. E.; Dais, P.; Heatley, F. *Macromolecules* **2000**, *33*, 3180–3183.

21. Chong, Y. K.; Moad, G.; Rizzardo, E.; Thang, S. H. *Macromolecules* **2007**, *40*, 4446–4455.

22. Moad, G.; Chong, Y. K.; Postma, A.; Rizzardo, E.; Thang, S. H. *Polymer* **2005**, *46*, 8458–8468.

23. Chen, M.; Moad, G.; Rizzardo, E. *J. Polym Sci Part A: Polym Chem* **2009**, *47*, 6704–6714.

Chapter 6: Knotty Polymer *via* "Grafting to" Click Reaction and Atom Transfer Radical Coupling

6.1. Introduction

The mathematical study of knots and links began in the 19th century with the efforts of Kelvin and Tait.[1] Soon after which, much progress has been made toward understanding knots in a topological framework, which reveals deep connections between knot topological invariants and statistical mechanics.[2] The scientific study of knots in polymers has also been a long standing interest in polymer physics to solve complex problems in the field of entanglements, rheology, etc. Some basic theoretical questions about polymeric knots have been answered with the help of powerful numerical techniques such as discovering the probability that a polymer is knotted[3] and the distribution of random knots[4]. However, the topological effects of knotted polymers on its static and dynamic properties are less understood.[5] Interest in this topic is further motivated by the possible industrial applications of knotted polymers such as the influence of topology on viscoelastic properties[6], and their relevance in biology and biochemistry[7].

The first experimental study on chemical knots was demonstrated well by Wang[8], Wasserman and Cozzarelli[9], and others in their work of elucidating the role of topology in the life processes of DNA. Various types of DNA nanoarchitectures have been exploited extensively by Seeman *via* programmed assembly of single stranded DNA.[10] The reliability of the Watson–Crick hydrogen-bonded pairs within DNA strands allows the easy formation of mechanically interlocked molecular entities. The nucleic acid

double-helical half twist is a perfect molecular tool to introduce the topological crossover point, node, or unit tangle in the construction of knots and links.[11] The right-handed B-DNA helps to generate negative (−) nodes, while the left-handed Z-DNA allows access to positive (+) nodes. Although the B-DNA conformation is the more common, naturally occurring motif, it is also capable of conversion to Z-DNA in solutions of high ionic strength or cationic effectors such as $[Co(NH_3)_6]^{3+}$. Seeman and co-workers have demonstrated an excellent example of the versatility and adaptability of DNA in the preparation of topologically interesting molecules **(Figure 6.1)**.[12]

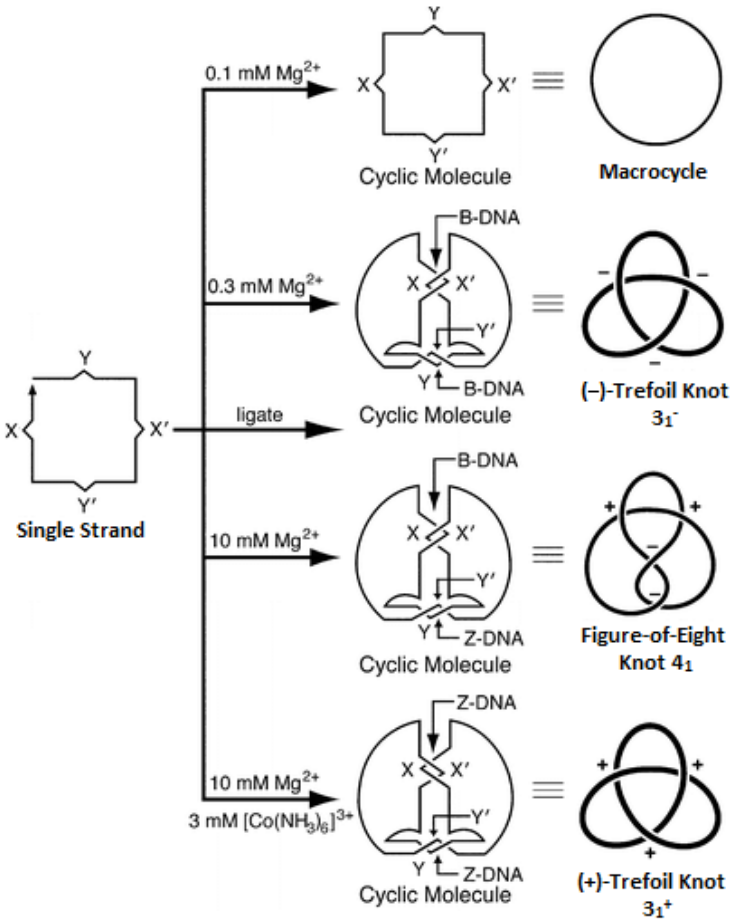

Figure 6.1. A schematic diagram illustrating the synthesis of four topologically distinct entities from one single strand of DNA.[12]

The concept utilizes an aforementioned strategy of using a single strand of DNA containing two complementary pairing regions, but, in this case, both were capable of undergoing transformation from B-DNA to Z-DNA in different ionic strength conditions. The careful control of ligation conditions results in the formation of four separate products: (i) the trivial unknot, or macrocycle, (ii) a trefoil knot with all negative nodes, containing all B-DNA, ligated at low ionic strength, (iii) a figure-of-eight knot with two positive and two negative nodes, containing a mixture of B-DNA and Z-DNA, ligated at high ionic strength, and (iv) a trefoil knot with all positive nodes, comprising only Z-DNA, ligated at high ionic strength and in the presence of $[Co(NH_3)_6]^{3+}$. This strategy allows precise control over molecular architecture compared to the earlier methods of DNA knot preparation using DNA topoisomerases, which generates various knotted species with no regulation of the outcomes of the process.

Despite the advances in the synthesis of DNA knots, the experimental studies of knots and links in a polymer continue to face setbacks due to their synthetic challenges. However, theoretical calculations suggest that linear knots are statistically probable in long polymer strands, and commonly generates in the crystallization of polymers from the melt.[13] Recently, Deffieux has reported a direct proof of existing of catenanes and trefoil knots in their study of long chain cyclized triblock copolymers *via* AFM imaging **(Figure 6.2)**.[14]

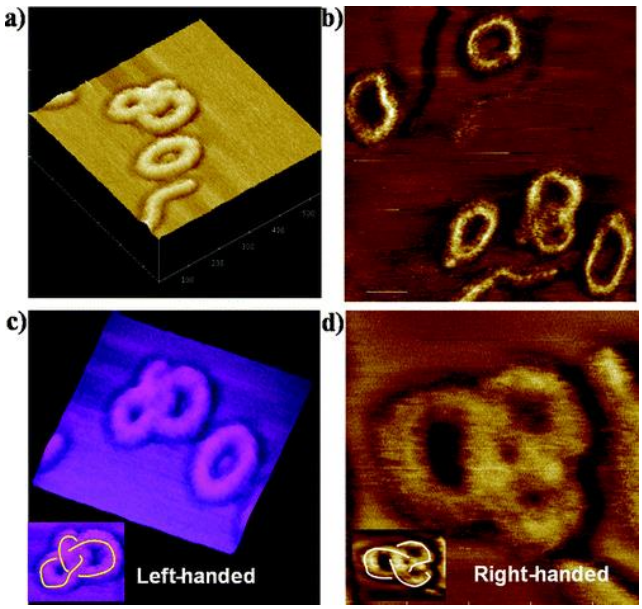

Figure 6.2. Topographic (a,c) and phase (b,d) AFM images of polymeric trefoil knots prepared by the cyclization of triblock copolymers.[14]

The key challenge in the formation of well-defined knotted polymer architectures is the controlled threading of polymer chains to generate crossing points and links. The answer to this problem lies possibly in the success of a metal template-directed synthesis of small molecular weight catenanes and trefoil knot.[15] Various other types of template and self-assembly methods including the use of π-π interactions,[16] hydrogen bonding,[17] hydrophobic interactions,[18] and anions[19] have also been proven to be powerful tools in the synthesis of higher order links and knots.

In addition, the recent advances in controlled radical polymerization method and usefulness of the azide/alkyne click reaction has enabled the synthesis of complex polymeric architectures such as star-polymers,[20] rod-coil-block copolymers,[21] dendrimers,[22] etc. Moreover, the end-to-end linking of linear analoues to generate

macrocycles has also been well demonstrated in literature, which further solves the key issue of fixing the interlocked structure of polymeric catenanes and knots.[23] The aforementioned developments in chemical synthesis suggest that nearly every polymeric architecture is now achievable by proper design and planning.

In this work, we have demonstrated for the first time, a template directed synthesis of a knotty (trefoil knot) polymer in two major steps: 1) grafting of alkyne-functionalized linear polymer to the azide-functionalized double helical metal template *via* click method, and 2) template-closing of four-armed type polymer *via* intra-molecular atom transfer radical coupling (ATRC) as shown in **Scheme 6.1**.

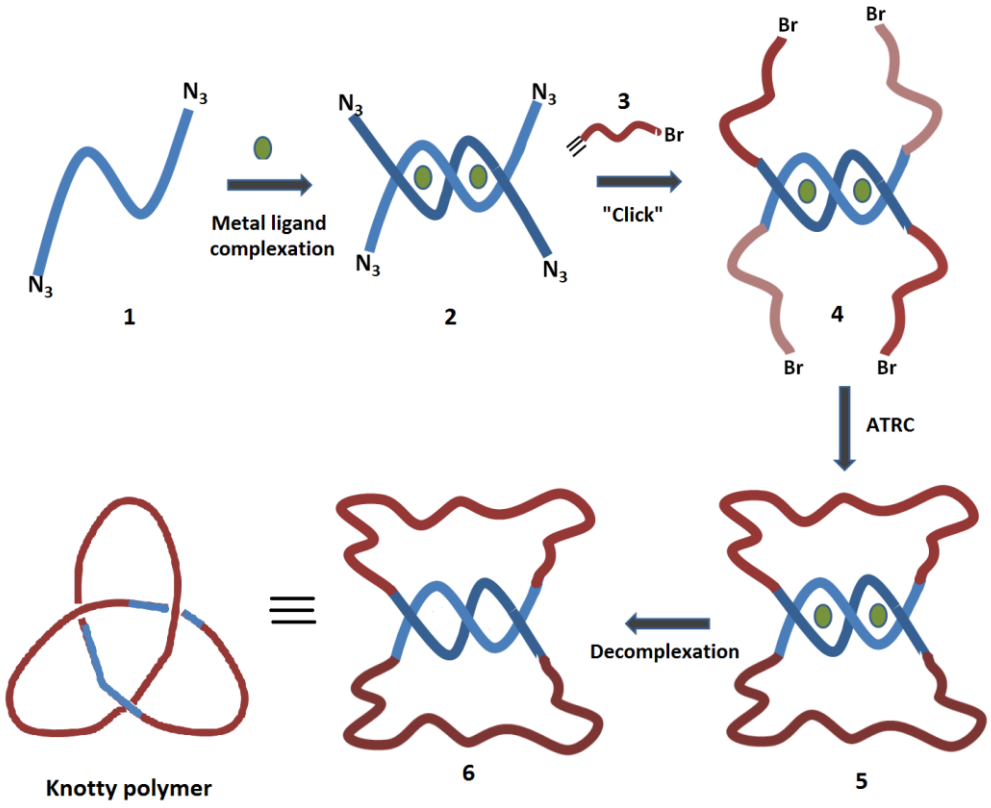

Scheme 6.1. Schematic route for the preparation of knotty polymers.

6.2. Results and Discussion

6.2.1. Design and synthesis of azide-functionalized double helix metal complex

Among the various phenanthroline ligands developed by the Sauvage group as a precursor for trefoil knot synthesis, we have used the most efficient one which contains two 1,10-phenanthroline units connected by a 1,3 phenylene group as shown in **Scheme 6.2**.[24] The azide group functionality in the ligand (helix precursor-N_3 (**1**)) was introduced quantitatively by reacting a hydroxyl ligand with 2-(2-(2-azidoethoxy)ethoxy)ethyl 4-methylbenzenesulfonate[25] in the presence of K_2CO_3. The double helix-N_3 diCu(I) complex **(2)** was formed quantitatively by the addition of $Cu(I)(MeCN)_4PF_6$ dissolved in ACN onto a DCM solution of **1** under argon.

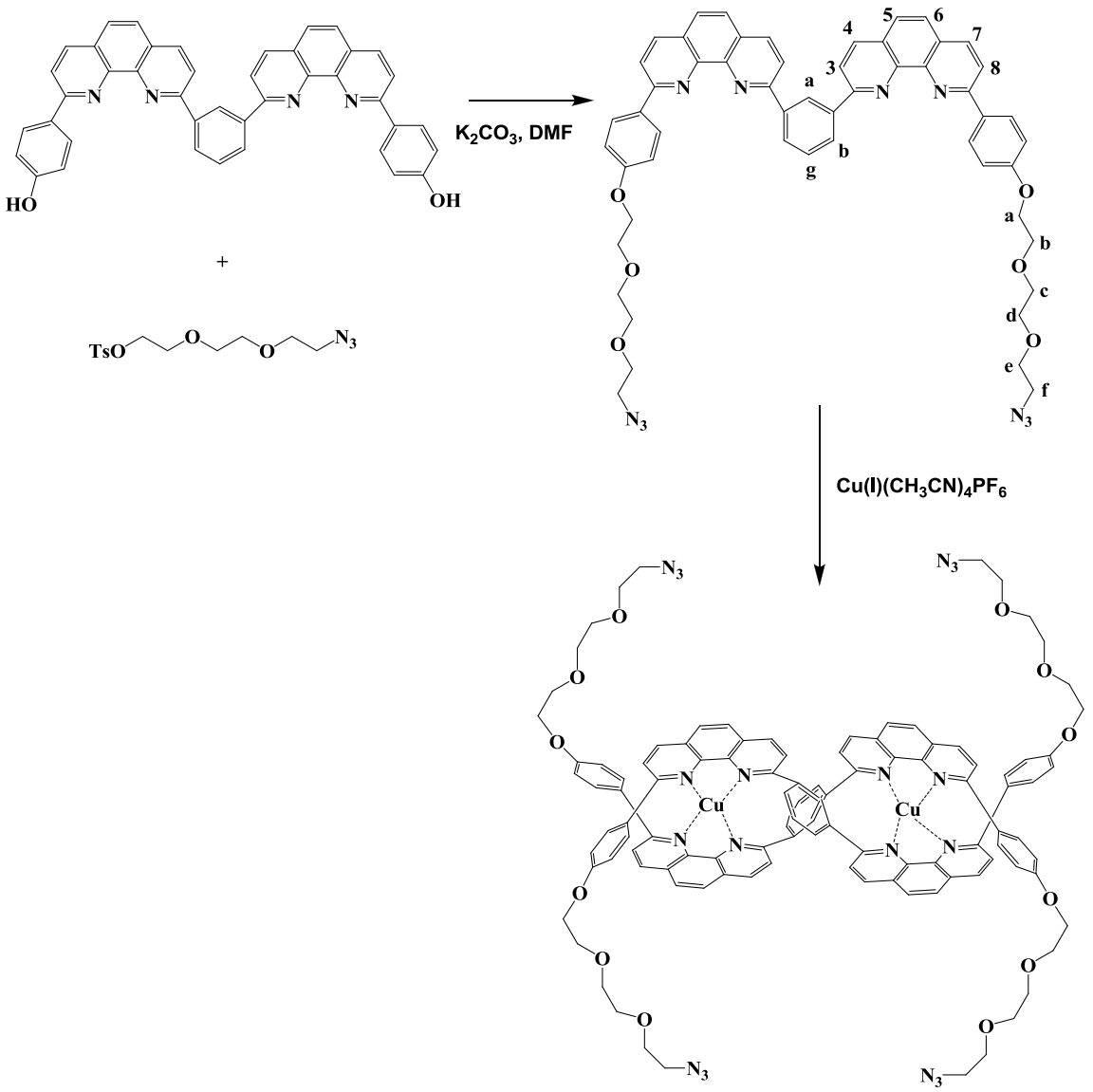

Scheme 6.2. Synthesis route for azide-functionalized double helix metal complex (**2**).

The dark red solid of complex **2** was characterized by UV-Visible analysis **(Figure 6.3)**, which showed intense ligand-centered transition at 325 nm and a weaker absorption peak corresponding to metal-to-ligand charge transfer (MLCT) at ~524 nm.

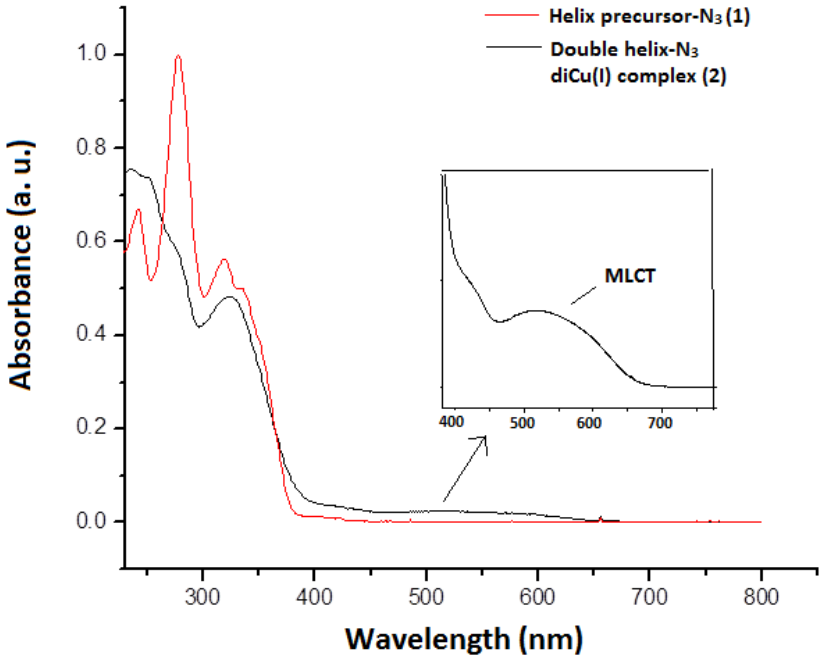

Figure 6.3. UV-visible spectra of helix precursor-N_3 (**1**) and double helix-N_3 diCu(I) complex (**2**) (inset: visible region of the complex (**2**) spectrum).

Further confirmation of the double helical structure of complex **2** was obtained from ^{1}H NMR **(Figure 6.4)**.[26] As compared to the helix precursor-N_3 (**1**), the significant shielding of H_m (-1.3 ppm) and H_o (-1.4 ppm) protons was observed as a result of the magnetic influence of the phenanthroline cores on the phenyl protons.

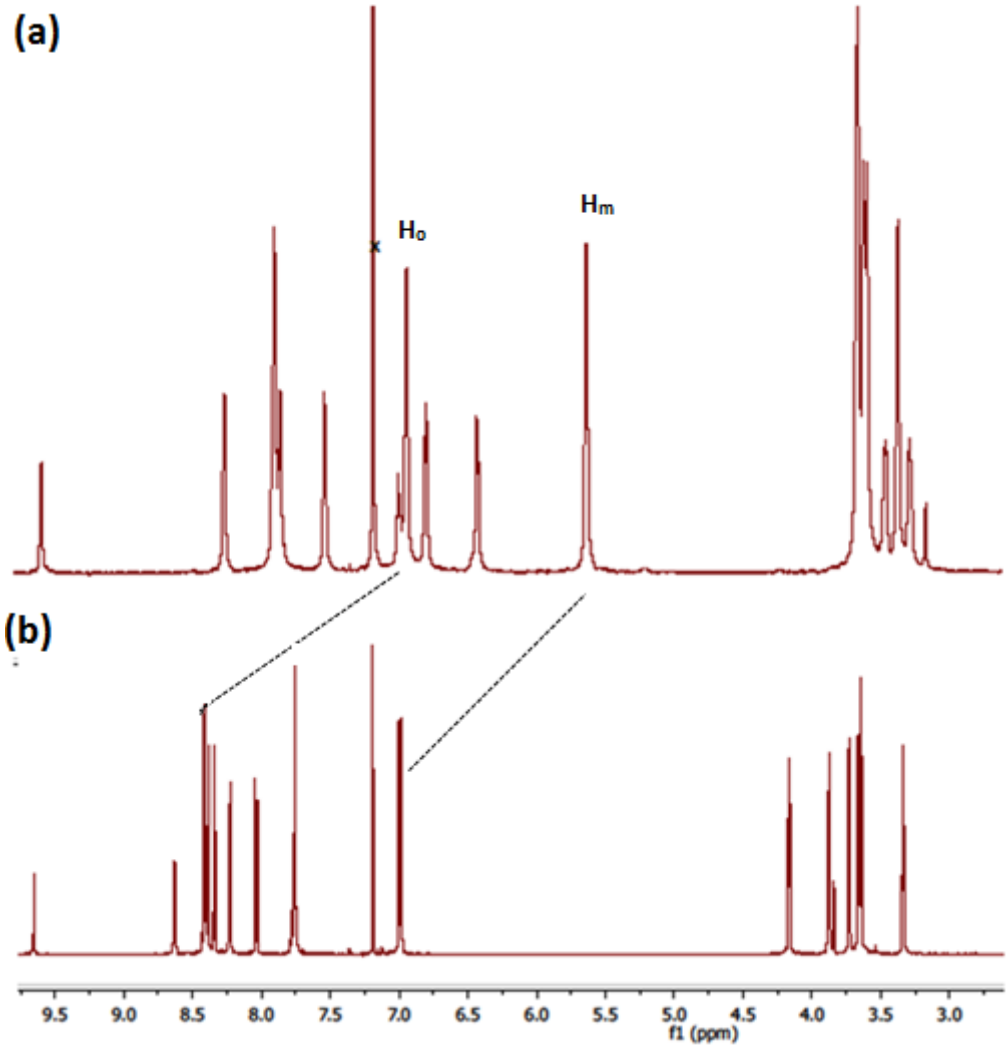

Figure 6.4. ^{1}H NMR spectra of (a) double helix-N_3 diCu(I) complex (**2**), (b) helix precursor-N_3 (**1**).

6.2.2. Synthesis of PS diCu(I) complex *via* "grafting to" click reaction

The stability of a phenanthroline Cu(I) complex under mild reaction conditions has been previously reported in literature. Considering that we will use a copper catalyzed alkyne/azide cycloaddition (CuAAC) click reaction to graft alkyne-functionalized linear polymers onto an azide-functionalized double helix metal complex,

this stability is important. As reported in Chapter 3, a low molecular weight alkyne-functionalized polystyrene (alkyne-PS) (**3**) (M_n: 3,373 g mol^{-1}, PDI: 1.05) was obtained by atom transfer radical polymerization (ATRP) of styrene using an alkyne-functionalized initiator **(Figure 6.5a)**.

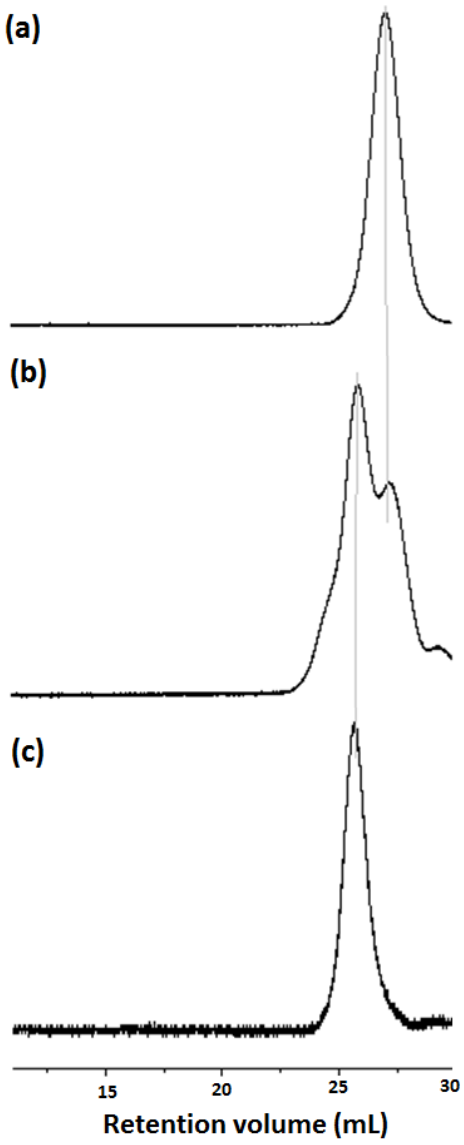

Figure 6.5. GPC traces of a) alkyne-PS (**3**), b) PS diCu(I) complex (**4**), and c) purified PS diCu(I) complex (**4**).

In a next step, click reaction between alkyne-PS (**3**), double helix-N_3 diCu(I) complex (**2**), and using Cu(I)Br/PMDETA as a catalyst afforded four-armed type PS diCu(I) complex (**4**) **(Scheme 6.4**).

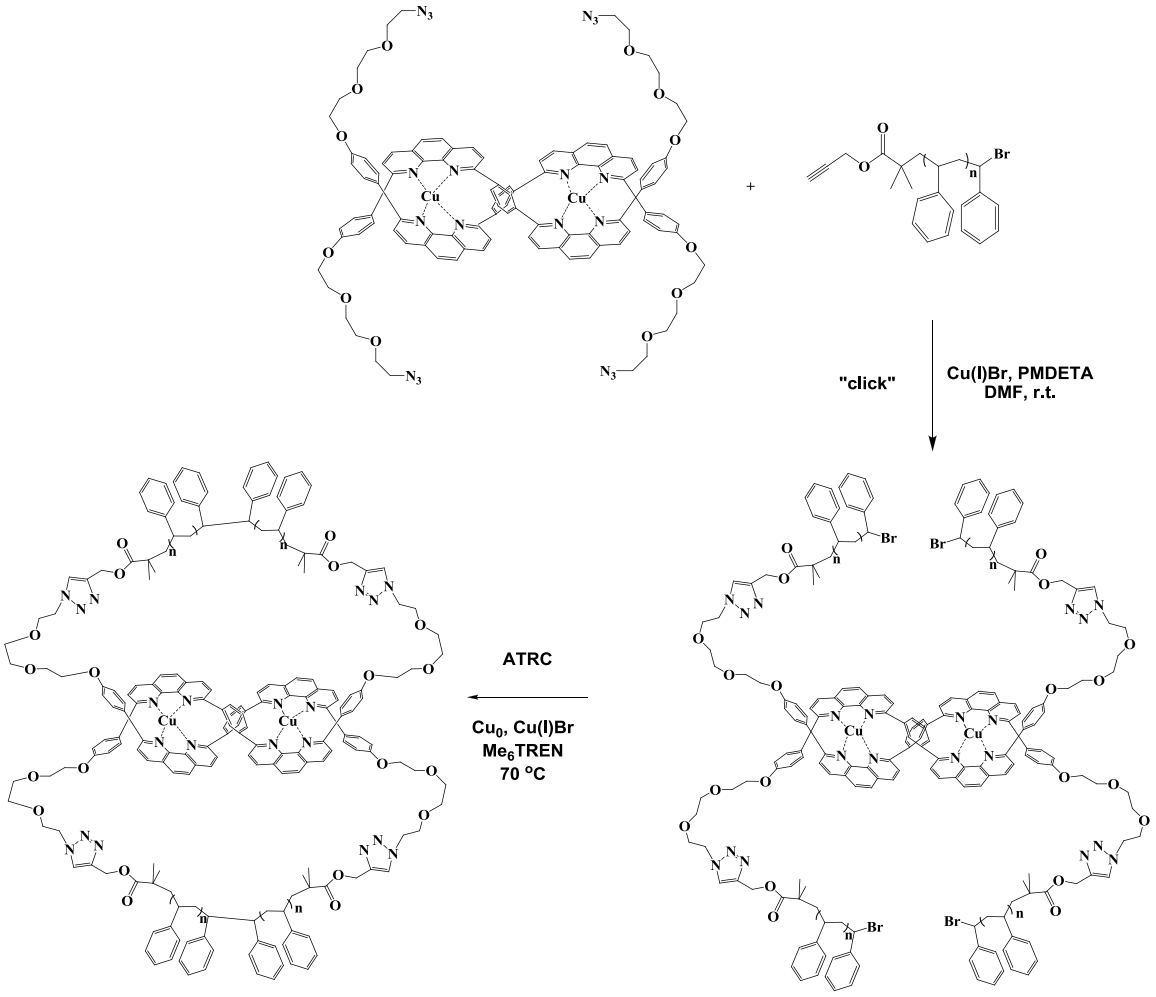

Scheme 6.3. Synthetic route for knotty PS *via* click reaction and ATRC.

The alkyne-PS (**3**) was used in excess to ensure complete conversion of azide-complex (**2**) to polymeric complex (**4**). The progress of the click reaction was monitored by GPC as over time it shows a decrease in intensity of peak corresponding to alkyne-PS (**3**) and the appearance of a new peak in the high molecular weight region. After 48 h, no

further changes in intensity were observed indicating complete conversion of the double helix-N_3 diCu(I) complex (**2**) to PS diCu(I) complex (**4**). The unreacted alkyne-PS was removed by fractional precipitation method using toluene/methanol solvent system. On the basis of GPC data **(Figure 6.5c)**, the apparent molecular weight of PS diCu(I) complex (**4**) was found to be 6,022 Da, which is smaller than expected value (~ 13,000 Da). It is important to note that the GPC system is calibrated with linear polystyrene standard, and since the hydrodynamic volume of four-armed type architecture of PS diCu(I) complex (**4**) is relatively smaller compared to its linear analogue, the observed difference is obvious. ^{1}H NMR of PS diCu(I) complex (**4**) show (**Figure 6.6**) the signals attributed to aromatic protons of styrene at 7.2–6.8 ppm and methylene and methane

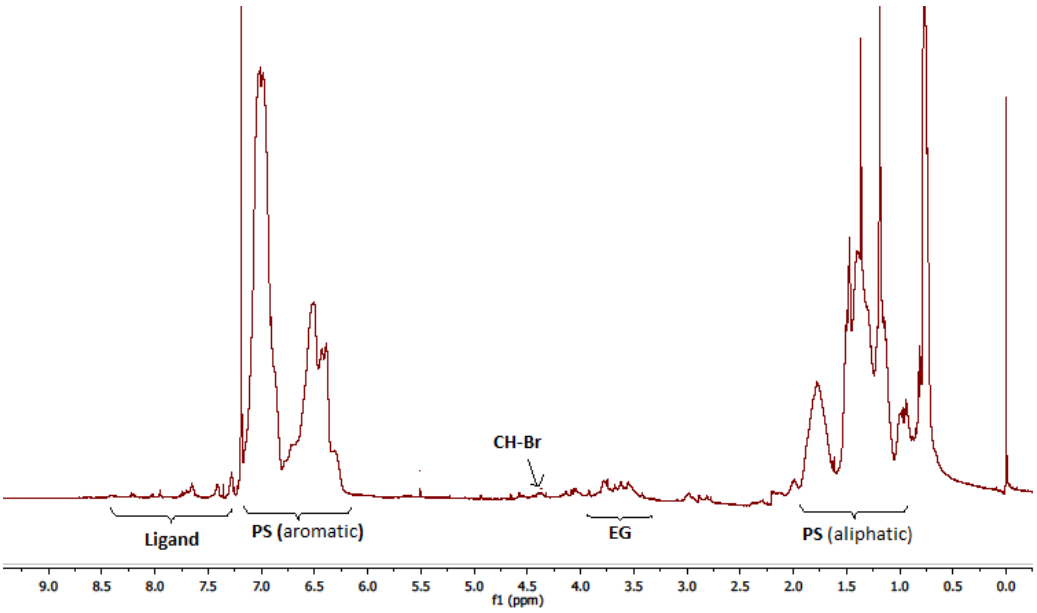

Figure 6.6. ^{1}H NMR of PS diCu(I) complex (**4**).

protons in the main chain at 2.2–1.7 and 1.7–1.2 ppm, respectively. In addition, it also show a peak corresponding to protons of the ligand in metal template at 8.3-7.2 ppm and ethyleneglycol (EG) linker protons 3.8-3.2 ppm. The bromine end-group functionality of PS diCu(I) complex (**4**) was confirmed from C(H)-Br peak at 4.3 ppm. Further evidence of efficient click reaction was obtained from FT-IR analysis **(Figure 6.6)** of PS diCu(I) complex (**4**), which shows the absence of the azide peak at 2090 cm^{-1}.

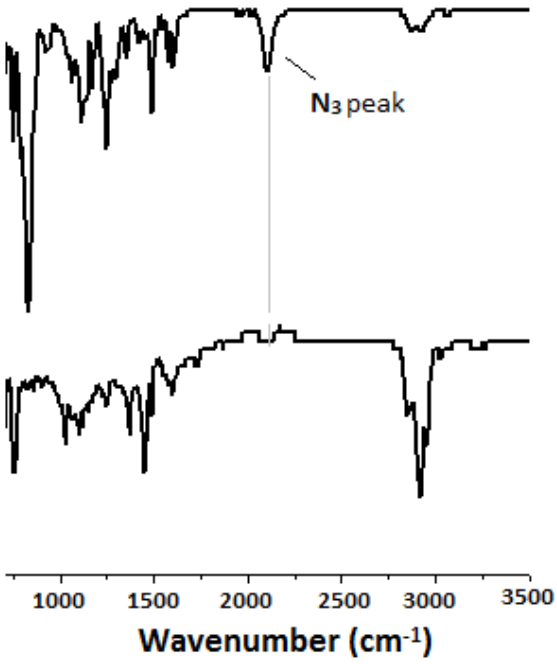

Figure 6.7. FT-IR of (a) double helix-N_3 diCu(I) complex (**2**) (top), (b) PS diCu(I) complex (**4**) (bottom).

6.2.3. Template-closing of PS diCu(I) complex *via* ATRC

The intramolecular ATRC of a linear dibrominated polymer has proven to be an efficient way of preparing macrocycles.[27] Taking advantage of the bromine end-group functionality in PS diCu(I) complex (**4**), template closing was achieved by intra-molecular ATRC under pseudo-high dilution conditions. A solution of the PS diCu(I)

complex (**4**) in THF was added dropwise at a fairly low rate (0.75 mL h^{-1}) to a solution containing CuBr/Me_6TREN and Cu(0) as catalyst. The GPC trace of the resulting closed template, PS diCu(I) knot (**5**) show slight shifting toward higher retention (25.7mL) volume as a result of reduced hydrodynamic radius compare to its precursor (25.6 mL) **(Figure 6.8a)**.

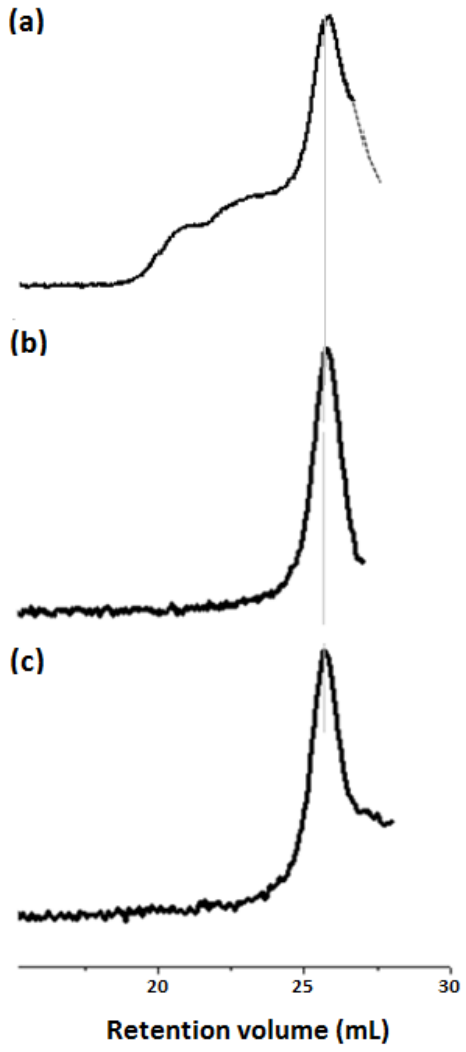

Figure 6.8. GPC traces a) Crude PS diCu(I) knot (**5**), b) purified PS diCu(I) knot (**5**), and c) metal free knotty PS (**6**).

Despite maintaining a high dilute solution condition for cyclization, the inter-molecular coupling was unavoidable as evidenced from the appearance of shoulder at the high molecular weight region in the GPC traces. The PS diCu(I) knot (**5**) was further purified by fractional precipitation **(Figure 6.8b)**. To further elucidate the closing of template chain ends and verify the formation of knotted architecture, the PS diCu(I) knot (**5**) was analyzed by MALDI-TOF mass spectroscopy. The major series of the MALDI-TOF spectrum of the intramolecular ATRC product (**Figure 6.9**) was determined to be consistent with the molecular weight of the expected coupled polymer chains with an

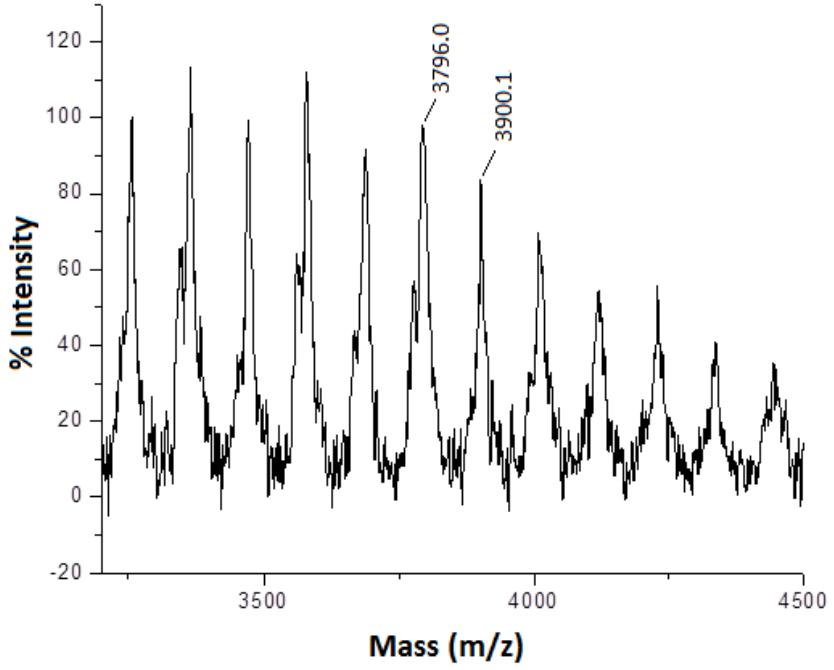

Figure 6.9. MALDI-TOF spectrum of PS diCu(I) Knot (**5**).

associated silver cation. For example, the expected molecular weight of polymer with eight styrene unit together with metal template is 3795.2, and experimental m/z value obtained from MALDI-TOF spectrum was found to be 3796.0. In addition, the mass

differences between the two neighboring peak was found to be 104.1 which correspond to a single styrene unit.

6.2.4. Demetallation of PS diCu(I) knot

A metal-free Knotty PS (**6)** was obtained by refluxing PS diCu(I) knot (**5**) in a saturated solution of KCN in THF: methanol (3:1). The GPC traces of knotty PS **(Figure 6.8c)** confirms its interlocked structure as the retention volume peak has not shifted to a lower molecular weight region after removing the copper from the template. In addition, a small shoulder at a higher retention volume (27.9 mL) can be attributed to the low molecular weight acyclic and/or cyclic polymers generated upon demetallation due to an uncyclized or partially cyclized polymer complex (**4**) during ATRC.

6.2.5 AFM imaging of knotty PS

The direct proof of a trefoil knot formation was obtained by AFM imaging. The samples of knotty PS (**6**) were prepared by spin-coating a very dilute solution of the polymer in $CHCl_3$ onto freshly cleaved mica. As shown in **Figure 6.8**, knotted cyclic structures of a trefoil knot were statistically observed, exhibiting different orientations on the surface. In addition, the line profile analysis of differently oriented structures of trefoil knot on surface further confirms the presence of the cavities inside the entangled topology. Other cyclic structures present indicate the various failed routes for cyclization by ATRC and a more thermodynamic preference for catenated structures or single macrocycles. Nevertheless, the presence of the trefoil knot confirms the bias resulting from a templated helical phenanthroline core.

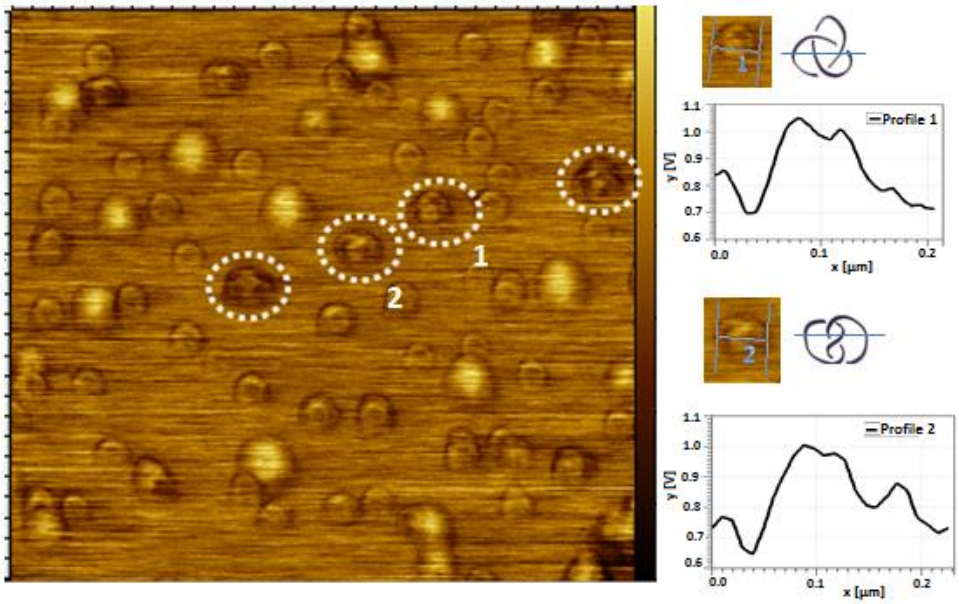

Figure 6.10. AFM image of knotty PS (**6**) on an 8 x 8 µm scale on mica, line profile of the representative structures.

6.3. Conclusions

A well-defined synthesis of a trefoil knot polymer was demonstrated *via* a supramolecular template-directed strategy. The grafting of preformed alkyne-functionalized linear polymer to azide-functionalized template *via* CuAAC click reaction has proven to be an efficient way to obtain trefoil knot polymer precursor. The template-closing *via* intra-molecular ATRC enabled the formation of a trefoil knot polymer without any post functional group modification in the polymer precursor. Characterizations by GPC and AFM confirmed the successful template-closing by ATRC, and thus, the formation of entangled architecture. In the future, this approach can be further explored to obtain structurally different homopolymer and blockcopolymer in a trefoil knot topology.

6.4. Experimental Section

6.4.1. Materials

All chemicals were purchased from Aldrich Chemical Company and were used directly without further purification unless otherwise indicated. All solvents were degassed with nitrogen gas before use.

6.4.2 Instrumentation

^{1}H NMR spectra were recorded on a VARIAN 600 spectrometer (600MHz). GPC was carried out on a Viscotek 270 instrument with a triple detector array (RALS, IV, RI) equipped with 2 GMHHR-M and 1 GMHHR-L mixed bed ViscoGel columns (eluent: THF; flow rate: 1 mL min^{-1}). UV-vis measurements were taken on an Agilent technologies 8453 spectrometer. The FTIR spectra were obtained on a Digilab FTS 7000 equipped with a HgCdTe detector from 4000 to 600 (cm^{-1}) wavenumbers. All atomic force microscopy (AFM) images were recorded in air under ambient conditions on PicoScan 2500 (Agilent Technologies formerly Molecular Imaging, Corp.) equipped with an 8 × 8 μm scanner. The AFM tip used was a silicon-nitride AFM probe from Ted Pella Inc. MALDI-TOF spectra were obtained in a Bruker OmniFLEX MALDI-TOF MS Spectrometer using 10 mg/mL dithranol and 1 mg/mL silver trifluoroacetate, both in THF. The polymer samples were mixed 10:1:1 (matrix:Ag:sample). Samples were analyzed in reflector positive mode, 1000-5000 Da, with a total of 1250 shots collected.

6.4.3. Synthesis of helix precursor-N_3

To a solution of 1,3-bis(2-(4-hydroxyphenyl)-1,10-phenanthrolin-2-yl)benzene (0.15 g, 0.24 mmol) and 2-(2-(2-azidoethoxy)ethoxy)ethyl 4-methylbenzenesulfonate (0.23 g, 0.72 mmol) in DMF (15 mL), K_2CO_3 (0.2 g, 1.5 mmol) was added and the suspension was heated to 80 °C for 18 h. After cooling to room temperature, the reaction mixture was poured into mixture of DCM: water (50 mL). The aqueous layer was extracted with DCM (3 × 50 mL), and the combined organic fractions were washed with brine (50 mL), dried over $MgSO_4$, filtered and concentrated under reduced pressure. The resulting crude oil was then purified by column chromatography (96:4 DCM: methanol) to yield **1** as a pale yellow solid (0.2 g, yield 74%). ^{1}H NMR ($CDCl_3$): 9.65 (s, 1H, H_α), 8.63 (dd, 2H, H_β), 8.42 (d, 4H, H_o), 8.39 (d, 2H, H_3), 8.34 (d, 2H, H_4), 8.23 (d, 2H, H_7), 8.03 (d, 2H, H_8), 7.77 (t, 1H, H_γ), 7.75 (d, 4H, $H_{5\text{-}6}$), ,6.99 (d, 4H, H_m), 4.17 (t, 4H, Ha), 3.88 (t, 4H, H_b), 3.73 (t, 4H, H_c), 3.65 (m, 8H, $H_{d\text{-}e}$), 3.30 (t, 4H, H_f).

6.4.4. Synthesis of double helix-N_3 diCu(I) complex

A degassed CH_3CN solution of 17.5 mg (0.05 mmol) of $Cu(I)(CH_3CN)_4PF_6$ was transferred through a cannula into a stirred degassed solution of **1** (40 mg, 0.04 mmol) in 3 mL DCM under nitrogen at room temperature. The mixture turned dark red instantaneously, indicating the formation of **2**. After the solution was stirred for 1 h under nitrogen at room temperature, the solvents were evaporated to dryness to obtain a dark red solid of crude **2** in quantitative yield. Complex **2** was used without further purification. ^{1}H NMR ($CDCl_3$): 9.58 (s, 2H, Hα), 8.26 (d, 4H, H_7), 7.91 (m, 8H, $H_{5\text{-}6}$),

7.86 (d, 4H, H_4), 7.54 (d, 4H, H_8), 7.0 (t, 2H, H_γ), 6.95 (d, 8H, H_o), 6.81 (d, 4H, H_β), 6.44 (d, 4H, H_3), 5.65 (d, 8H, H_m) 3.8-3.2 (m, 48H, $H_{a\text{-}f}$).

6.4.5. Synthesis of PS diCu(I) complex

In a Schlenk flask, the double helix-N_3 diCu(I) complex (**2**) (1.96 mg, 9.4 μmol), alkyne-functionalized PS (**3**) (80.0 mg, 0.02 mmol), PMDETA (1 mg, 0.02 mmol) and 3 mL DMF were added. The solution was purged with nitrogen and degassed by performing four freeze–pump–thaw cycles and then Cu(I)Br (0.84 mg, 0.02 mmol) was added. The resulting homogeneous reddish brown solution was stirred at room temperature for 48 h. After passing the solution through alumina, the PS diCu(I) complex (**4**) was precipitated from methanol.

6.4.6. Synthesis of PS diCu(I) knot

In a typical ATRC procedure,[27] A 500 mL Schlenk flask containing a 100 mL THF solution of Cu(I)Br (574 mg, 4.0 mmol) and nanosized copper (254 mg, 4.0 mmol) was sealed with a rubber septum, evacuated with four freeze-pump-thaw cycles, backfilled with N_2, and sealed from the Schlenk line. The flask was then placed in an oil bath and stirred at 75 ^oC. After allowing the metal solution to reach the temperature of the bath, Me_6TREN (1.07 mL, 4.0 mmol) was introduced *via* a nitrogen flushed syringe. A syringe pump held a 50 mL syringe containing an 18 mL THF solution of PS diCu(I) complex (**4**) (5 mg), which had separately been subjected to three freeze-pump-thaw cycles and backfilled with N_2. The solution of **4** was slowly dripped through a needle piercing the rubber septum into the stirring THF solution of the metal ligand, over

approximately 24 h (approximate rate = 0.75 mL/h). After the contents of the syringe had been added to the reaction mixture, the reaction mixture was stirred for an additional 1 h. The resulting PS diCu(I) knot (**5**) was passed through an alumina column and precipitated into cold methanol.

6.4.7. Synthesis of knotty PS

A solution of KCN (200 mg, 1.53 mmol) in water (2 mL) was added to PS diCu(I) knot **5** (3.5 mg, 0.88 μmol) in 6 mL mixture of THF: methanol (3:1) and refluxed for 24 h. After reaction completion, the solvent was evaporated under vacuum, and the resulting polymer was extracted twice by DCM: water mixture. The DCM layer containing the polymers were mixed together and dried over anhydrous Na_2SO_4 which upon evaporation under vacuum, yields the knotty PS

6.5. References

1. (a) Thompson, W. *Philos. Mag*. **1867**, *34*, 15. (b) Tait, P. G. in *Scientific Papers* Cambridge University Press, London, 1898.
2. Group, B. *Knot Theory and Statistical Mechanics* edited by C. N. Yang and M. L. Ge, World Scientific, New Jersey, 1989.
3. Sumners, D. W.; Whittington, S. G. *J. Phys.* **1988**, *A 21*, 1689.
4. Rybenkov, V. V.; Cozzarelli, N. R.; Vologodskii, A. V. *Proc. Natl. Acad. Sci. U.S.A.* **1993**, *90*, 5307.

5. Janse van Rensburg, E. J.; Whittington, S.G. *J. Phys. A.* **1991**, *24*, 3935.

6. Yu. A. *Grosberg Phys.-Usp*. **1997**, *40*, 12.

7. (a) Taylor, W. R. *Nature* **2000**, *406*, 916. (b) Krasnow, M. A.; Stasiak, A.; Spengler, F. Dean, S. J.; Koller, T.; Cozzarelli, N. R. *Nature* **1983**, *304*, 559. (c) Liu, Z.; Zechiedrich, E. L.; Chan, H. S. *Biophys. J.* **2006**, *90*, 2344.

8. Wang, J. C. *J. Mol. Bio.* **1971**, *55*, 523.

9. Wasserman, S. A.; Cozzarelli, N. R. *Science* **1986**, 232, 951.

10. Seeman, N. C. *Acc. Chem. Res*. **1997**, *30*, 357.

11. Seeman, N. C.; Chen, J. H.; Du, S. M.; Mueller, J. E.; Zhang, Y. W.; Fu, T. J.; Wang, Y. L.; Wang, H.; Zhang, S. W. *New J. Chem*. **1993**, *17*, 739.

12. (a) Du, S. M.; Stollar, B. D.; Seeman, N. C. *J. Am. Chem. Soc*. **1995**, *117*, 1194. (b) Du, S. M.; Wang, H.; Tsedinh, Y. C.; Seeman, N. C. *Biochemistry* **1995**, *34*, 673.

13. (a) Frank-Kamenetskii, M. D.; Lukashin, A. V.; Vologodskii, A. V. *Nature* **1975**, *258*, 398. (b) van Rensburg, E. J. J.; Sumners, D. A. W.; Wasserman, E.; Whittington, S. *G. J. Phys. A: Math. Gen*. **1992**, *25*, 6557. (c) Frisch, H. L. *New J. Chem*. **1993**, *17*, 697.

14. Schappacher, M.; Deffieux, A. *Angew. Chem., Int. Ed*. **2009**, *48*, 5930.

15. Dietrich-Bucheker, C. O.; Sauvage, J. -P. *Chem. Rev*. **1987**, *87*, 795–810.

16. Ashton, P. R.; Goodnow, T. T.; Kaifer, A. E.; Reddington, M. V.; Slawin, A. M. Z.; Spencer, N.; Stoddart, J. F.; Vicent, C.; Williams, D. J. *Angew. Chem., Int. Ed. Engl*. **1989**, *28*, 1396.

17. (a) Hunter, C. A. *J. Am. Chem. Soc*. *1992*, 114, 5303. (b) Vogtle, F.; Meier, S.; Hoss, R. *Angew. Chem., Int. Ed. Engl*. **1992**, *31*, 1619.

18. Hamilton, D. G.; Davies, J. E.; Prodi, L.; Sanders, J. K. M. *Chem.-Eur. J.* **1998**, *4*, 608.

19. Sambrook, M. R.; Beer, P. D.; Wisner, J. A.; Paul, R. L.; Cowley, A. R. *J. Am. Chem. Soc*. **2004**, *126*, 15364.

20. (a) Zhu, J.; Zhu, X.; Kang, E. T.; Neoh, K. G.; *Polymer* **2007**, *48*, 6992. (b) Tsarevsky, N. V.; Sumerlin, B. S.; Matyjaszewski, K. *Macromolecules* **2005**, *38*, 3558.

21. Agut, W.; Taton, D.; Lecommandoux, S. *Macromolecules* **2007**, *40*, 5653.

22. (a) Antoni, P.; Nystrom, D.; Hawker, C. J.; Hult, A.; Malkoch, M. *Chem. Commun.* **2007**, *22*, 2249. (b) Malkoch, M.; Schleicher, K.; Drockenmuller, E.; Hawker, C. J.; Russell, T. P.; Wu, P.; Fokin, V. V. *Macromolecules* **2005**, *38*, 3663.

23. Laurent, B. A.; Grayson, S. M. *Chem. Soc. Rev.* **2009**, *38*, 2202–2213.

24. Dietrich-Buchecker, C.; Rapenne, G. *J. Chem. Soc., Chem. Commun.* **1997**, 2053–2054.

25. Zhao, Y.; Li, Y.; Huang, C.; Liu, H. Lai, S.; Che, C.; *Zhu, D. Org. Biomol. Chem.* **2010**, *8*, 3923–3927.

26. (a) Dietrich-Buchecker, C. O.; Sauvage, J. P. *Angew. Chem., Int. Ed. Engl.* **1989**, *28*, 189−192. (b) Dietrich-Buchecker, C. O.; Guilhem, J.; Pascard, C.; Sauvage, J. P. *Angew. Chem., Int. Ed. Engl.* **1990**, *29*, 1154−1156.

27. Voter, A. F.; Tillman, E. S. *Macromolecules* **2010**, *43*, 10304–10310.

Chapter 7. Conclusions and Future Work

7.1. Conclusions

This dissertation has focused on the development of novel routes for synthesis of entangled polymer knots and links *via* supramolecular template directive approach and controlled radical polymerization (CRP) methods. The synthesis of novel supramolecular initiators for atom transfer radical polymerization (ATRP) and reversible addition fragmentation chain transfer (RAFT) polymerization was demonstrated and evaluated for its efficiency to generate polymeric template precursor. The efficiency of atom transfer radical coupling (ATRC) to close the polymeric template was also tested.

Chapter 1 gave an overview of the use of various types of supramolecular templates to obtain orderly entangled topology at molecular level. It also outlined the efficient routes for the synthesis of cyclic polymers (topological isomer of catenane and trefoil knot) *via* either end-to-end coupling of linear analogue, or ring-expansion polymerization from cyclic catalyst or initiator.

Chapter 2 demonstrated a new, simple, and versatile method for the synthesis of polymer catenanes *via* polymerization of styrene from supramolecularly assembled ATRP initiators and intra-molecular cyclization of the polymeric template by ATRC. The stability of copper (I) complex during polymerization and the efficiency of ATRC was evaluated by monitoring the change in hydrodynamic volume by Gel Permeation Chromatography (GPC). The interlocked structure of polymer catenanes was also

confirmed by direct visualization through Atomic Force Microscopy (AFM) imaging technique.

Chapter 3 reported the synthesis of polystyrene-b-polymethylmethacrylate copolymers catenanes (PS-b-PMMA catenanes) as an important extension work of Supramolecularly-templated ATRP initiator approach. The chain extension of homopolymeric template was achieved by ATRP of methyl methacrylate (MMA). The styrene assisted low temperature ATRC was able to successfully couple the halide terminated PMMA block, and thus led to the formation of PS-b-PMMA catenanes.

In chapter 4, a novel 'grafting to' approach was demonstrated to synthesize polymer catenanes in good yield. An alkyne-functionalized polystyrene was successfully grafted to azide-functionalized phenanthroline copper (I) complex *via* copper catalyzed alkyne-azide cycloaddition (CuAAC) click reaction. The template-closing *via* intra-molecular ATRC enabled the formation of polymer catenanes without any post end-functional group modification in polymer precursor. In addition to the formation of polymer catenanes, the coexisting of side products of ATRC such as inter-molecular coupling product and other isomer were also confirmed by line profile analysis in AFM image.

Chapter 5 demonstrated synthesis of cyclic polyvinylcarbazole (PVK) *via* thermally initiated ring-expansion RAFT polymerization of N-vinylcarbazole using novel cyclic dixanthate initiator. The living nature of RAFT polymerization was confirmed by the linear growth of molecular weights versus polymerization time. GPC and AFM image analysis revealed the broad distribution of cyclic polymers, which is possibly due to the

chain transfer reaction. This was further confirmed by control experiment of ring opening reaction of cyclic PVK *via* radical induced reduction of xanthate group in polymer.

Chapter 6 demonstrated the feasibility of 'grafting to' approach to synthesize trefoil knot polymer. The alkyne-functionalized linear polymer was successfully attached to azide-functionalized double helical template *via* CuAAC click reaction. In next step, template-closing *via* intra-molecular ATRC led to the formation of trefoil knot polymer. AFM image showed different orientations of trefoil knotty polymers on surface and the line profile analysis of representative structures confirmed the successful formation of entangled architecture.

7.2. Future Work

The work presented in this research dissertation has opened the new area for synthesis of complex macromolecular knots, links, and entanglements. Aside from forming entangled architecture *via* supramolecular template, living nature of controlled radical polymerization offers chain extension by variety of vinyl monomers. Thus, an important future direction of this work is to prepare libraries of diblock or triblock copolymer in catenane or trefoil knot topology and to study for phase separation/micellization behavior. Since the alkyne functionality can be easily introduced in variety of polymers, the applicability of the "grafting to" approach described in this work can be further explored to structurally different homopolymer and block copolymer, which cannot be accessed through CRP method. As an extension of ring-expansion RAFT polymerization from cyclic initiator, a catenane or trefoil knot type RAFT initiator can be synthesized to obtain well-defined polymer catenane or knotty polymer in good

yield thru optimized ring-expansion polymerization conditions. This would further open doors for the investigation of important physicomechanical properties and possible applications of these knotted structures.

7.3. Final Remarks

The combination of controlled radical polymerization method and supramolecular template approach has proven to be simple and efficient way to obtain catenane and trefoil knot topology of high molecular weight polymer. This dissertation has also explored GPC and AFM imaging technique as the primary characterization methods to get detail insight of topological aspect of knotted polymeric structures. Further optimization of reported strategies would lead to high purity materials and practical applications study.

Appendix I: Additional information for Chapter 4

AP.I.1.Synthesis of Propargyl 2-bromoisobutyrate

Propargyl 2-bromoisobutyrate was prepared as per the procedure shown in **Scheme AP.I.1**.

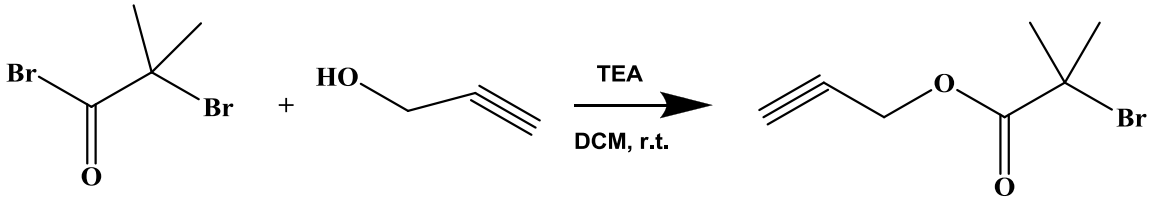

Scheme AP.I.1. Synthesis of propargyl 2-bromoisobutyrate.

Into a 500-mL round-bottom flask equipped with a magnetic stirrer, propargyl alcohol (28 g, 0.5 mol), triethylamine (TEA) (69.4 mL, 0.5 mol), and CH_2Cl_2 (150 mL) were added. When the mixture was cooled to 0 ^oC, 2-bromoisobutyryl bromide (115 g, 0.5 mol) was added dropwise for 1 h. The reaction mixture was stirred at room temperature for 24 h. The salt formed was removed by filtration, and the filtrate was washed with aqueous NaCl solution (3 x 100 mL). The organic layer was dried over $MgSO_4$. After the solvent was removed under reduced pressure, the colorless propargyl 2-bromoisobulyrate was obtained by distillation under reduced pressure.^1H NMR ($CDCl_3$): 4.90 (d, 2H), 2.50 (s, 1H), 1.80 (s, 6H).

Appendix II: Additional Information for Chapter 5

AP.II.1. MALDI-TOF analysis of Cyclic Dixanthate RAFT Initiator

The compound solutions (10^{-3} mol/L) were prepared in THF. The matrix 2-(4'-Hydroxybenzeneazo) benzoic acid (HABA) were also dissolved in THF (10 g/L). 1 μL of compound solution was mixed with 50 μL of matrix solution. The final solution was deposited onto the sample target and allowed to dry in air.

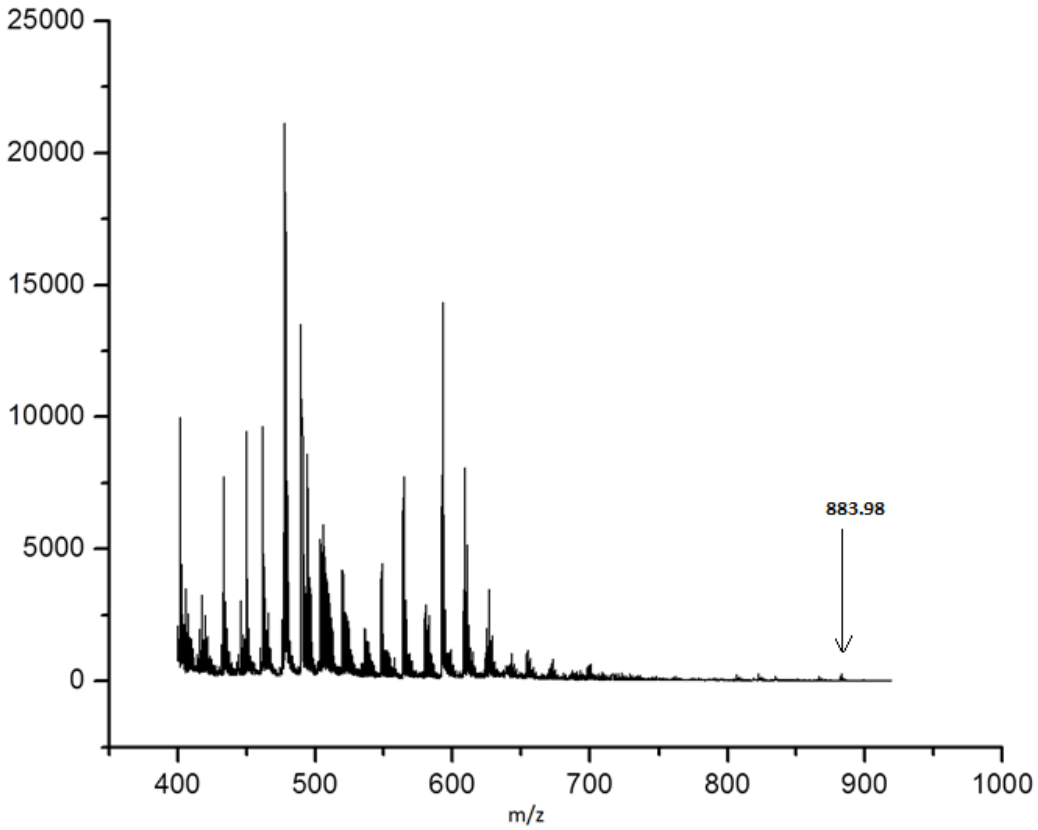

Figure AP.II.1. MALDI-TOF mass-spectrum of cyclic dixanthate initiator in HABA matrix and positive mode.

AP.I.2. AFM Analysis of Linear PVK

The AFM sample of linear PVK resulted from ring-opening reaction of cyclic PVK was prepared by spin-casting dilute solution of polymer in $CHCl_3$ on to freshly cleaved mica substrate.

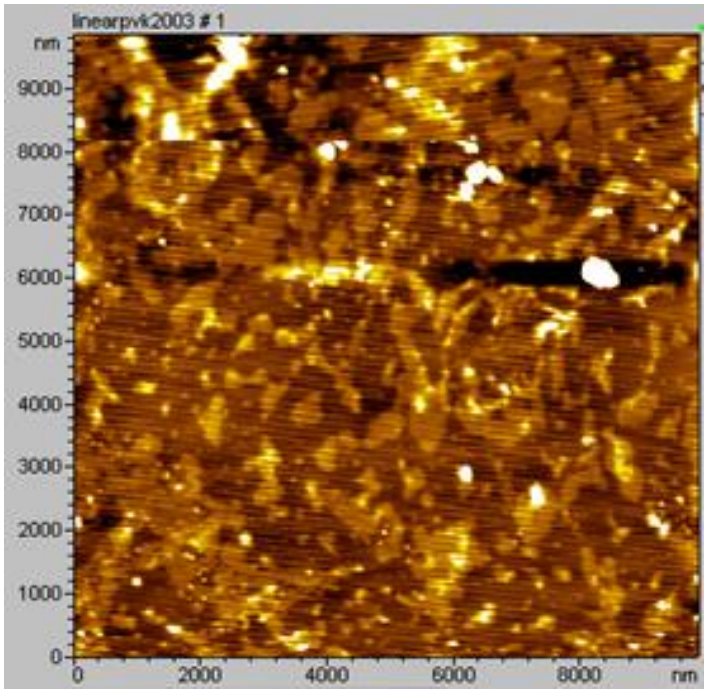

Figure AP.II.2. AFM image of linear PVK on mica substrate.

Appendix III: Additional Information for Chapter 6

AP.III.1. Synthesis of 4,4'-(9,9'-(1,3-phenylene)bis(1,10-phenanthroline-9,2-diyl)) diphenol (Helix precursor-OH)

The synthesis of Helix precursor-OH was performed according to literature procedure as shown in **Scheme AP.III.1**.[1]

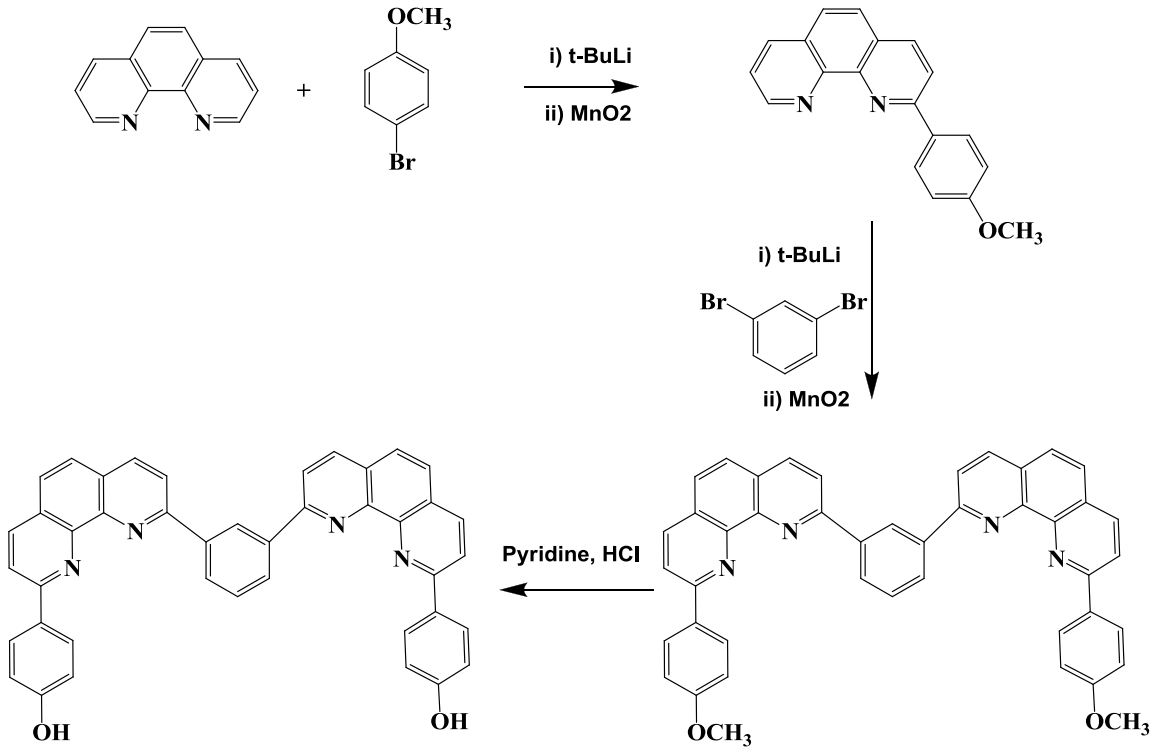

Scheme AP.III.1. Synthesis of helix precursor-OH (**3**).

AP.III.1.1. Synthesis of 2-(4-methoxyphenyl)-1,10-phenanthroline

para-bromoanisole (4.8 mL, 38.6 mmol) was dissolved in 60 mL degassed THF. After cooling down the solution to -30 °C, tert-BuLi (56 mL, 95.2 mmol) was slowly added by cannula under nitrogen atmosphere. After stirring the mixture for another 1.5 h

at 0 °C, it was transferred to the solution of pre-dried 1,10-phenanthroline (5.37 g, 29.8 mmol) in 80 mL degassed toluene. The reaction mixture was stirred under nitrogen for 40 h. After hydrolysis with water at 0 °C, yellow toluene layer was decanted and aqueous layer was extracted three times by DCM. The combined organic layer was re-aromatized by addition of MnO_2 (15 g×3) with efficient stirring. After MnO_2 was filtered and the solvent was removed, the crude product was purified by silica column chromatography using DCM/methanol (100:4) as eluent. Further recrystallization from hot toluene yielded colorless solid (5.12g, 17.9 mmol, yield: 60.1%). ^{1}H NMR ($CDCl_3$): 9.27 (dd, lH), 8.37 (d, 2H), 8.29 (dd, lH), 8.28 (d, lH), 8.08 (d, lH), 7.79 (m, 2H), 7.66 (dd, lH), 7.07 (d, 2H), 3.90 **(**s**,** 3H).

AP.III.1.2. Synthesis of 1,3-bis(9-(4-methoxyphenyl)-1,10-phenanthrolin-2-yl)benzene

In a round bottom flask, 14.5 mL of t-BuLi (1.2M in pentane, 17.4 mmol) was added very slowly to a degassed solution of 1.00 g (4.20 mmo) of 1,3-dibromobenzene in 50 mL of dry THF under N_2 at -78 °C. The solution mixture was stirred at 0°C for 2 h and then it was added very slowly to a degassed solution of 2-(4-methoxyphenyl)-1,10-phenanthroline 2.80 g (9.79 mmol**)** in 120 mL of dry THF, under N_2 at room temperature. The solution was stirred for another 45 h at room temperature before it was hydrolyzed with water. The solvent was removed by rotary evaporation. The crude product was dissolved in DCM and the solution was washed with water. Then the product was re-aromatized with MnO_2 (10 g×3), dried over Na_2SO_4, and then filtered. The product was purified by silica column chromatography using DCM/methanol (100:4) as eluent.

Further purification by recrystallization from hot toluene afforded colorless solid 1.48 g (2.29 mmol, 54.5%).^{1}H NMR ($CDCl_3$): 9.75 (s, 1H), 8.71 (d, 2H), 8.45 (m, 8H), 8.40 (d, 2H), 8.32 (d, 2H), 8.10 (d, 2H), 7.85 (m, 5H), 7.10 (d, 4H), 3.87 (s, 6H).

AP.III.1.3. Synthesis of Helix precursor-OH (3)

In a round bottom flask, 1,3-bis(9-(4-methoxyphenyl)-1,10-phenanthrolin-2-yl)benzene 0.65 g (1.0 mmol) was added to 50 mL of anhydrous pyridinium hydrochloride at 130 °C. After the mixture was refluxed at 200-210 °C for 4 h, it was hydrolyzed with 30 mL of water. The yellow crude acidic product was suspended in 80 mL of hot water and the mixture was neutralized to pH=7.3 by sodium hydroxide solution. Filtration and drying afforded reddish product (0.53 g, 0.86 mmol, yield: 86%). ^{1}H NMR (DMSO-d): 9.87 (s, 2H), 9.74 (s, 1H), 8.72 (d, 2H), 8.66 (m, 4H), 8.50 (d, 2H), 8.40 (d, 4H), 8.27 (d, 2H), 8.00 (s, 4H), 7.91 (t, 1H), 6.88 (d, 4H).

AP.III.1.3. Synthesis of 2-(2-(2-azidoethoxy)ethoxy)ethyl 4-methylbenzenesulfonate

As per literature procedure,[2] a solution of 2-(2-azidoethoxy) ethoxy) ethanol (1.31 g, 10 mmol) and TEA (2.0 mL, 14.4 mmol) in CH_2Cl_2 (50 mL) was cooled to 0°C. p-toluenesulfonyl chloride (2.17 g, 11.4 mmol) was added and the solution was stirred at room temperature for 18 h. The reaction was quenched with water (20 mL). The organic layer was separated, dried over $MgSO_4$, filtered, concentrated under reduced pressure and the resulting crude oil was purified by column chromatography (petroleum ether:CH_2Cl_2 9:1 then 1:1 as eluent) to yield 2-(2-azidoethoxy)ethoxy)ethyl 4-methylbenzenesulfonate

as a colorless oil (2.31 g, yield = 75%). ^{1}H NMR ($CDCl_3$): 7.81 (d, 2H), 7.35 (d, 2H), 4.25 (t, 2H), 3.70 (t, 2H), 3.61 (m, 6H), 3.35 (t, 2H), 2.45 (s, 3H).

AP.III.2. References

1. Dietrich-Buchecker, C.; Rapenne, G. *J. Chem. Soc., Chem. Commun.* **1997**, 2053–2054.
2. Zhao, Y.; Li, Y.; Huang, C.; Liu, H. Lai, S.; Che, C.; *Zhu, D. Org. Biomol. Chem.* **2010**, *8*, 3923–3927